EDITORIAL BOARD OF THE JOURNAL OF AGRICULTURE AND DEVELOPMENT

EDITORIAL SECRETARIAT

Contact information:
Nong Lam University
Room 404, Thien Ly Building
Linh Trung Ward, Thu Duc City, Ho Chi Minh City, Vietnam
Tel: (84-28)37245670
Email: jad@hcmuaf.edu.vn

The Journal of Agriculture and Development
Volume 22 - Issue 6 (2023)
pISSN 2615-9503
eISSN 2615-949x

CONTENT

Effects of different doses of micro-organic and phosphorus fertilizers on growth and yield of red turmeric (*Curcuma longa* L.)

Trang T. H. Nguyen[1]*, Thinh V. Tran[1], Binh V. Tran[1], Tri D. Q. Phan[1], Linh D. Dinh[1], Son T. T. Le[1], Quang T. Le[1], & Truong V. Nguyen[2]

[1]Faculty of Agronomy, Nong Lam University, Ho Chi Minh City, Vietnam

[2]Department of Plant Bioscience, Life and Industry Convergence Research IDACitute, Pusan National University, Miryang, South Korea

ARTICLE INFO

Research Paper

Received: February 28, 2022
Revised: June 24, 2022
Accepted: June 28, 2022

Keywords

Growth
Micro-organic fertilizer
Phosphorus
Red turmeric
Yield

***Corresponding author**

Nguyen Thi Huyen Trang
Email:
nthtrang@hcmuaf.edu.vn

ABSTRACT

The objective of the study was to determine the appropriate doses of micro-organic and phosphorus fertilizers for good growth, high rhizomes yield and enhancing the economic efficiency of red turmeric cultivated in gray soil in Thu Duc city. The two-factor experiment was laid out in a split-plot design with three replications. The main plots consisted of four doses of phosphorus fertilizer as 30, 60 (control), 90, & 120 kg P_2O_5/ha. The sub-plots included three doses of micro-organic fertilizer (2, 4, & 6 tons/ha) and a control with cow dung of 10 tons/ha. A common dose of 500 kg lime, 90 kg N, 120 kg K_2O/ha was applied in all treatments The results showed that red turmeric was applied at the dose of 120 kg P_2O_5 combined with 6 tons of micro-organic fertilizer/ha exhibited the highest growth, yield and economic outcomes including a plant height of 41.2 cm, stem diameter of 16.2 mm, leaf length of 24.4 cm, leaf width of 8.5 cm, leaf count of 7.0, soil-plant analysis development index of 35.6, the profit of VND 386.32 million/ha, and the benefit cost ratio of 2.4.

Cited as: Nguyen, T. T. H., Tran, T. V., Tran, B. V., Phan, T. D. Q., Dinh, L. D., Le, S. T. T., Le, Q. T., & Nguyen, T. V. (2023). Effects of different doses of micro-organic and phosphorus fertilizers on growth and yield of red turmeric (*Curcuma longa* L.). *The Journal of Agriculture and Development* 22(6), 1-11.

1. Introduction

Turmeric (*Curcuma* sp.) is a large genus in the Ginger family (Zingiberaceae) and an annual plant with tuberous roots that can regenerate new shoots for many years. Turmeric has been widely used as a spice, fabric dye as well as medicine (Ravindran et al., 2007). In Vietnam, red turmeric (Curcuma longa L.) is commonly grown on different soils mainly for its tuberous roots and used in food processing and treated of some diseases according to traditional experience (Do, 2004).

In intensive farming of red turmeric, fertilization is an important technique that not only affects growth and yield but also determines economic efficiency, especially when cultivated on nutrient-poor soils. Therefore, in order to improve the efficiency of red turmeric yield and quality when cultivating this plant on infertile gray soil, the combination of organic and inorganic fertilizers to enhance water retention, porosity, quality, and soil nutrients is necessary.

In addition, the application of organic fertilizer before planting offers a great effect on plant growth (Kamal & Yousuf, 2012) because it helps the soil increasing the ability of the soil to retain macro-minerals from chemical fertilizers, prevent fertilizer loss, creating aeration for roots to thrive, supporting the soil retain moisture better and create a living environment for beneficial microorganisms. Thus, applying organic fertilizers when growing red turmeric is crucial to foster the absorption efficiency of inorganic fertilizers such as N, P and K during the period of plant growth and development.

Stemming from the practical requirements of local production, the study was carried out to determine the appropriate combination rates between two organic fertilizers (cow manure fertilizer and micro-organic fertilizer) and phosphorus fertilizer, which would have the most positive effect on growth, rhizomes yield, and quality, and economic efficiency of red turmeric.

2. Materials and Methods

2.1. Materials

The red turmeric tuberous roots were collected from a farm in Bu Gia Map district, Binh Phuoc province, Vietnam. Red turmeric rhizomes were then treated with 0.5% chlorine for 30 min before dried and incubated for 2 weeks. When the red turmeric seedlings reached 10 - 15 cm in height and were produced with 1 - 3 leaves, each plant was separated before growing (Mai et al., 2000).

Fertilizers used in the experiment included cow manure fertilizer (1% N, 2% P_2O_5, 1% K_2O); La Nga micro-organic fertilizer (hereafter referred to as MOF) (2% N; 1.67% P_2O_5; 1.12% K_2O_{hh}; macro and micro element: 1.63% Ca, 20.2% SiO_2, 67.7 mg/kg Cu; 0.39% Mg; 1070 mg/kg Mn; 211 mg/kg Zn; 7660 mg/kg Fe; 3.7 x 10^8 CFU/g bacterial cellulose; 6.3 x 10^8 CFU/g bacterial phosphorus; 35.3% organic content; 5.72% acid humid; humidity 28.6%); Phu My urea fertilizer (46.3% N); Lam Thao superphosphate fertilizer (16% P_2O_5, 10% S, 12 mg Cd/kg); Canadian potassium chloride fertilizer (61% K_2O, 16% S).

Soil sample was analysed by Forestry Science Institute of Southern Vietnam, 2021.

Table 1. Physical and chemical properties of soil sample used in the experiment

Texture (%)			pH_{KCl}	Organic matter (%)	Total N (%)	Total P_2O_5 (%)	Total K_2O (%)
Clay	Silt	Sand					
68	28	4	5.9	3.71	0.1	0.417	3.5

The main characteristics of soil sample were presented in Table 1. The data showed that the soil is classified as clay texture, moderately acidic, high in soil organic matter, and low in total nitrogen but high in total phophorus and potassium.

2.2. Experimental design

The experiment was carried out at the Agronomy Research Station in Nong Lam University, Ho Chi Minh City, Vietnam from December 2020 to October 2021.

Two-factor experiment was arranged in a split-plot design (SPD) with three replicates. The main-plots were four doses of phosphorus fertilizer as 30, 60 (control), 90, & 120 kg P_2O_5/ha. The sub-plots were three doses of MOF (2, 4, & 6 tons/ha) and a cow dung of 10 tons/ha as control. All treatments were fertilized with the same dose of 500 kg lime, 90 kg N, 120 kg K_2O/ha. Entire amount of cow dung and MOF were applied in respective plots as per treatment during the final land preparation. The amount of nitrogen and potassium was split into three installments: 2/4 N + 1/4 K_2O (30 DAP), 1/4 N + 1/4 K_2O (90 DAP), 1/4 N +2/4 K_2O (150 DAP).

The plot size was 6.3 m^2 (4.5 m in length, 1.4 m in width). The health primary rhizomes of red turmeric were planted at the distance of 35 cm x 25 cm. The spacing between blocks and plots was 1.0 and 0.5, respectively.

2.3. Data collection and analysis

The data on growth parameters were recorded from 10 randomly selected plants per plot. The plant height, the main stem diameter per plant, the leaf length and the leaf width were recorded at 180 days after planting (DAP). The average chlorophyll content was determined before harvest using the Top IDAC ruments SPAD-502PLUS handheld chlorophyll meter at 60 and 120 DAP. The fresh and dry weight of rhizome and roots per plant was recorded at harvest (270 DAP). Regarding the fresh weight of rhizomes per plant, the theoretical fresh rhizomes yield and the actual fresh rhizomes yield of red turmeric were collected at the time of harvest. Fresh rhizomes yield was calculated based on per plant yield and per net plot yield and then converted onto an ha basis, and the data expressed as tons per ha. Economic efficiency included total expenditure, total revenue, profit and benefit cost ratio were computed.

All variables were subjected to analysis of variance (SPD) using mixed models of SAS version 9.1 (SAS Institute Inc., Cary, NC, USA, SAS Institute, 2004).

3. Results and Discussion

3.1. Effects of micro-organic and phosphorus fertilizers on growth and yield of red turmeric

At 180 DAP, the amounts of phosphate fertilizers had a statistically significant effect on the plant height and diameter of the red turmeric. Detailedly, the height of the red turmeric plants at 90 & 120 kg P2O5/ha of phosphorus fertilizer obtained the high stem height, and there were statistically significant differences as compared to 30 & 60 kg/ha treatments. In terms of different MOF levels, applied 4 and 6 tons/ha obtained the highest (37.4 and 38.8 cm, respectively) and significantly different from the others. The interaction between mirco-organic and phosphorus fertilizers has not prevailed (Table 2).

The diameter of the red turmeric stem was highest (14.7 and 15.2 mm), when fertilized with 90 & 120 kg P_2O_5/ha, respectively, there were statistically significant differences compared

Table 2. Effects of micro-organic and phosphorus fertilizers on plant height and diameter of red turmeric at 180 days after planting

Parameters	MOF dose (tons/ha) (O)	Phosphorus dose (kg P_2O_5/ha) (P)				Average (O)
		30	60[(2)]	90	120	
Stem height (cm)	Cow dung [(1)]	34.0	34.7	35.5	35.5	34.9^{b}
	2	34.3	35.0	35.5	38.0	35.7^{b}
	4	35.0	35.5	39.5	39.5	37.4^{a}
	6	36.5	38.0	39.5	41.2	38.8^{a}
	Average (P)	35.0^{b}	35.8^{b}	37.5^{a}	38.6^{a}	
	CV (%) = 4.6		$F_P = 32,6^{**}$	$F_O = 18,7^{**}$	$F_{P*O} = 1,7^{ns}$	
Stem diameter (mm)	Cow dung [(1)]	12.8^{e}	13.0^{de}	13.0^{de}	14.1^{cde}	13.2^{b}
	2	13.2^{cde}	13.4^{cde}	14.7^{a-d}	14.3^{b-e}	13.9^{b}
	4	13.5de	14.1^{cde}	15.0^{abc}	16.1^{ab}	14.7^{a}
	6	14.4^{b-e}	14.1^{cde}	16.0^{ab}	16.3^{a}	15.2^{a}
	Average (P)	13.5^{b}	13.7^{b}	14.7^{a}	15.2^{a}	
	CV (%) = 7.1		$F_P = 27.4^{*}$	$F_O = 28.4^{*}$	$F_{P*O} = 3.6^{**}$	

Within a group of means, values followed by the same letter are not significantly different at 5% level. **: significant at 1% level; *: significant at 5% level; [ns]: non significant; [(1)] 10 tons/ha (control); [(2)] 60 kg P_2O_5/ha (control); MOF: micro-organic fertilizer.

with those in 30 & 60 kg/ha. Regarding the effect of different MOF applications, the red turmeric plants applied with 4 & 6 tons/ha achieved the largest plant diameter and there were statistically significant differences compared with other treatments (Table 2). There was an interaction between the applied rates of MOF and phosphate fertilizer on the stem diameter of red turmeric at 180 DAP. Red turmeric plants were applied 6 tons of MOF and 120 kg of P_2O_5/ha produced the largest stem diameter (16.3 cm), however, there was not significantly different from those fertilized with 6 tons of MOF + 90 kg P_2O_5/ha and 4 tons of MOF at 90 and 120 kg P_2O_5/ha. The results were consistent with the study of Hossain & Ishimine (2007) that there were differences in growth parameters when growing red turmeric in different types of soil such as plant height, the number of leaves, leaf biomass, and especially using on gray soil and red-brown soil achieved the best results compared to the remaining soil types. In addition, by reporting of Chanchan et al. (2018) also concluded that when the applied rates of organic fertilizers, nitrogen, and phosphorus could affect the growth of leaves of red turmeric.

At 180 DAP, red turmeric plants at most applied rates of microbial organic and phosphate fertilizers did not significantly affect the length and width of red turmeric leaves. It can be figured out that did not interact between the doses of phophorus and MOF (Table 3).

Table 3. Effects of micro-organic and phosphorus fertilizers on the length and width of red turmeric leaves at 180 days after planting

Parameters	MOF dose (tons/ha) (O)	Phosphorus dose (kg P_2O_5/ha) (P)				Average (O)
		30	60[(2)]	90	120	
Leaf length (cm)	Cow dung [(1)]	20.1	20.3	21.1	21.5	20.8[d]
	2	21.3	21.8	21.9	22.0	21.8[c]
	4	21.7	22.3	22.4	23.9	22.6[b]
	6	22.5	22.9	23.8	24.4	23.4[a]
	Average (P)	21.4	21.8	22.3	23.0	
	CV (%) = 7.1		$F_P = 8.4^{ns}$	$F_O = 0.8^*$	$F_{P*O} = 1.3^{ns}$	
Leaf width (cm)	Cow dung [(1)]	7.4	7.9	8.0	8.1	7.9
	2	8.0	8.1	8.1	8.1	8.1
	4	8.0	8.1	8.2	8.2	8.1
	6	8.1	8.2	8.4	8.4	8.3
	Average (P)	7.9	8.1	8.2	8.2	
	CV (%) = 4.8		$F_P = 1.7^{ns}$	$F_O = 0.7^{ns}$	$F_{P*O} = 1.0^{ns}$	

Within a group of means, values followed by the same letter are not significantly different at 5% level. *: significant at 5% level; [ns]: non significant; [(1)] 10 tons/ha (control); [(2)] 60 kg P_2O_5/ha (control); MOF: micro-organic fertilizer.

However, red turmeric at the treatment with 6 tons per ha of microbial organic fertilizer recorded the longest leaves (23.4 cm), and there statistically varied those in the other treatments (Table 3). According to MOF, amount of nitrogen helped leaf of red turmeric became generative growth during the period of plant (180 DAP), this appropriate statement also proved by Barker & Pilbeam (2007), mineral element plays important role to growth and development that enhance the yield of crops dramatically. Mazid (1993) also indicated that the combination of organic and in-organic fertilizers or the substances of N, P, K mixed enables turmeric enormously improve growth capacity.

Amount of phosphorus fertilizers affected to soil-plant analysis development (SPAD) index, its gradually increased from 60 to 120 DAP at all treatments, however, there were no statistically significant differences among levels of P application (Table 4). In the comparison with micro-organic and phosphorus fertilizer applications, the recorded data figured out that did not interact SPAD index during the red turmeric growth period. However, the difference of cow dung fertilizer statical significantly improved the SPAD index. In which, the treatment with 6 tons of MOF per ha had the highest average SPAD index of 31.7 and 34.4 at the time of 60 and 120 DAP, respectively. Trinh (2015) assumed that macro and micro elements had tremendously contributed to the material transformation in the plant, and that includes chlorophyll content. The main reason that leads to this significance could be that MOF was added NPK nutrient and other elements which enables red turmeric to reinforce chlorophyll content what could accumulate matters for plants.

Table 4. Effects of micro-organic and phosphorus fertilizers on soil-plant analysis development index of red turmeric leaves

Observed time	MOF dose (tons/ha) (O)	Phosphorus dose (kg P_2O_5/ha) (P)				Average (O)
		30	60[(2)]	90	120	
60 DAP	Cow dung [(1)]	30.1	30.3	30.3	31.3	30.5[c]
	2	30.4	30.6	31.2	31.4	30.9[b]
	4	30.6	31.0	31.0	31.4	31.0[b]
	6	31.2	31.6	31.9	31.9	31.7[a]
	Average (P)	30.6	30.9	31.1	31.5	
	CV (%) = 1.9		$F_P = 5.5^{ns}$	$F_O = 0.7^*$	$F_{P*O} = 1.1^{ns}$	
120 DAP	Cow dung [(1)]	32.7	32.9	33.5	33.6	33.2[d]
	2	33.5	33.9	34.0	34.2	33.9[c]
	4	33.6	34.0	34.3	34.7	34.2[b]
	6	33.8	34.1	34.6	34.9	34.4[a]
	Average (P)	33.4	33.7	34.1	34.4	
	CV (%) = 2.5		$F_P = 20.1^{ns}$	$F_O = 0.3^*$	$F_{P*O} = 1.3^{ns}$	

Within a group of means, values followed by the same letter are not significantly different at 5% level. *: significant at 5% level; [ns]: non significant; [(1)] 10 tons/ha (control); [(2)] 60 kg P_2O_5/ha (control); MOF: micro-organic fertilizer; DAP: days after planting.

At the period of 180 DAP, in term of stem fresh weight, the phosphate fertilizer factor did not significantly affect the criteria of the fresh stems, rhizomes, and roots of red turmeric in the experiment, and no significant interaction between the applied rates of microbial organic and phosphate fertilizer was observed.

However, applying different amounts of MOF, a statistical difference in the fresh weight of stems, rhizomes and roots were recorded. Particularly, the red turmeric plants applied 6 tons/ha indicated the highest fresh stem weight (1908.3 g), rhizomes (293.8 g), and roots (255.2 mg) (Table 5).

At the different applied rates of phosphate fertilizer, the dry weight of red turmeric stems, rhizomes and roots were not a statistically significant difference, and the combination of different applied rates of microbial organic and phosphorus fertilizers recorded no significant effect on these parameters in the experiment. The resemblance of the fresh weight indicators, the experiment prevailed that there was a statistically significant difference in the stem dry weight (308.4 g) when applying 6 tons of MOF per ha as compared with the other treatments (Table 6).

Table 5. Effects of micro-organic and phosphorus fertilizers on the fresh weight of red turmeric stems, rhizomes and roots at 180 days after planting

Parameters	MOF dose (tons/ha) (O)	Phosphorus dose (kg P_2O_5/ha) (P)				Average (O)
		30	60[(2)]	90	120	
Stem fresh weight (g)	Cow dung [(1)]	1166.7	1233.3	1333.3	1366.7	1275.0[c]
	2	1233.3	1333.3	1466.7	1533.3	1391.7[b]
	4	1333.3	1333.3	1433.3	1600.0	1425.0[b]
	6	1733.3	1900.0	1866.7	2133.3	1908.3[a]
	Average (P)	1366.7	1450.0	1525.0	1658.3	
	CV (%) = 17.0		$F_P = 0.1^{ns}$	$F_O = 9.2^*$	$F_{P*O} = 0.7^{ns}$	
Rhizomes fresh weight (g)	Cow dung [(1)]	195.9	236.4	236.4	256.7	231.4[c]
	2	236.4	243.2	263.4	276.9	255.0[b]
	4	270.2	290.4	303.9	310.7	287.1[a]
	6	256.7	263.4	297.2	331.0	293.8[a]
	Average (P)	239.8[c]	258.4[b]	275.3[b]	293.8[a]	
	CV (%) = 13.7		$F_P = 2.3^*$	$F_O = 2.6^*$	$F_{P*O} = 0.5^{ns}$	
Root fresh weight (mg)	Cow dung [(1)]	128.0	136.7	149.3	165.3	144.8[b]
	2	172.7	196.7	222.3	231.0	205.7[a]
	4	199.3	210.7	354.0	256.7	246.7[a]
	6	214.7	225.3	229.0	317.7	255.2[a]
	Average (P)	178.7	192.4	238.7	242.7	
	CV (%) = 15.4		$F_P = 1.3^{ns}$	$F_O = 3.7^*$	$F_{P*O} = 0.9^{ns}$	

Within a group of means, values followed by the same letter are not significantly different at 5% level. *: significant at 5% level; [ns]: non significant; [(1)] 10 tons/ha (control), [(2)] 60 kg P_2O_5/ha (control); MOF: micro-organic fertilizer.

Table 6. Effects of micro-organic and phosphorus fertilizers on the dried weight of stems, rhizomes, and roots of red turmeric at 180 days after planting

Parameters	MOF dose (tons/ha) (O)	Phosphorus dose (kg P_2O_5/ha) (P)				Average (O)
		30	60[(2)]	90	120	
Stem dry weight (g)	Cow dung [(1)]	166.7	200.0	200.0	233.3	200.0[c]
	2	200.0	200.0	200.0	233.3	208.3[c]
	4	233.3	233.3	233.3	266.7	241.7[b]
	6	266.7	300.0	300.0	366.7	308.4[a]
	TB (P)	216.7	233.3	233.3	275.0	
	CV (%) = 15.5		$F_P = 0.1^{ns}$	$F_O = 10.8^{*}$	$F_{P*O} = 1.0^{ns}$	
Rhizomes dry weight (g)	Cow dung [(1)]	31.4	35.9	37.4	41.5	36.6
	2	36.5	40.0	42.0	47.9	41.6
	4	38.2	40.9	43.9	48.4	42.9
	6	39.9	41.5	46.0	51.2	44.7
	Average (P)	36.5	39.6	42.3	47.3	
	CV (%) = 17.2		$F_P = 2.4^{ns}$	$F_O = 2.5^{ns}$	$F_{P*O} = 0.7^{ns}$	
Root dry weight (mg)	Cow dung [(1)]	19.3	20.7	24.0	26.7	22.7[c]
	2	27.3	31.0	33.7	37.3	32.3[b]
	4	28.3	35.0	38.7	39.0	35.3[ab]
	6	34.0	34.0	35.0	45.7	37.2[a]
	Average (P)	27.2	30.2	32.9	37.2	
	CV (%) = 12.1		$F_P = 1.2^{ns}$	$F_O = 3.3^{*}$	$F_{P*O} = 0.5^{ns}$	

Within a group of means, values followed by a same letter are not significantly different at 5% level. *: significant at 5% level; [ns]: non significant; [(1)] 10 tons/ha (control), [(2)] 60 kg P_2O_5/ha (control); MOF: micro-organic fertilizer.

3.2. Effects of micro-organic and phosphorus fertilizers on yield of red turmeric

In terms of the correlation between the microbial organic and phosphorus fertilizers, a statistically nonsignificant difference in the theoretical fresh yield of red turmeric was recorded when applied these fertilizers at different rates (Table 7). Particularly, the treatment with 120 kg P_2O_5/ha achieved the highest average theoretical fresh yield of 34.3 tons per ha, whereas the treatment with 30 kg of P_2O_5 per ha had the lowest average theoretical fresh yield of 27.6 tons/ha. The treatment with 6 tons of MOF per ha produced the highest average theoretical fresh yield of 32.7 tons/ha.

The effect of phosphorus fertilizer on the actual fresh yield of red turmeric was also statistically significant between different treatments at the time of harvest. The experimental application of 120 kg P_2O_5/ha obtained the highest actual fresh yield of 24.3 tons/ha, a statistically significant difference compared with the other treatments.

Table 7. Effects of micro-organic and phosphorus fertilizers on theoretical and actual fresh yield of red turmeric

Parameters	MOF dose (tons/ha) (O)	Phosphorus dose (kg P_2O_5/ha) (P)				Average (O)
		30	60[(2)]	90	120	
Theortical fresh rhizomes yield (tons/ha)	Cow dung [(1)]	26.3	27.0	27.0	29.3	27.4[b]
	2	27.7	30.0	31.6	34.7	31.0[a]
	4	27.0	30.8	33.1	35.4	31.6[a]
	6	29.3	30.0	33.9	37.7	32.7[a]
	Average (P)	27.6[c]	29.5b[c]	31.4[b]	34.3[a]	
	CV (%) = 13.7		F_P = 2.3*	F_O = 2.6*	F_{P*O} = 0.5[ns]	
Actual fresh rhizomes yield (tons/ha)	Cow dung [(1)]	15.3	18.9	19.7	20.7	18.7[b]
	2	19.4	21.3	21.5	25.1	21.8[a]
	4	18.4	21.7	22.9	24.0	21.8[a]
	6	20.7	21.1	23.9	27.5	23.3[a]
	Average (P)	18.5[c]	20.8[b]	22.0[b]	24.3[a]	
	CV (%) = 15.5		F_P = 2.7*	F_O = 2.8*	F_{P*O} = 0.6[ns]	

Within a group of means, values followed by a same letter are not significantly different at 5% level. *: significant at 5% level; [ns]: non significant; [(1)] 10 tons/ha (control), [(2)] 60 kg P_2O_5/ha (control); MOF: micro-organic fertilizer.

In terms of the amount of MOF, the collected data showed that the treatment with 6 tons MOF achieved the highest average actual fresh yield of 23.3 tons/ha, which was statistically significant for the control treatment. These result was in concordance with the study of Banwasi & Singh (2010) that the application of 100 and 150 kg P_2O_5/ha recorded the highest red turmeric yield growing in light clay soil, with the increasing level of phosphorus up to 200 kg/ha, the yield of red turmeric was tended to decrease. Besides, the study results of Padmapriya & Chezhiyan (2009) prevailed the effect of fertilizers (organic, inorganic) on the yield and quality of red turmeric concluded that applying microbial organic fertilizers and NPK significantly increased the yield of red turmeric, and relatively consistented with the contemporary study.

The results showed that red turmeric plants were treated at 120 kg P_2O_5/ha combined with 6 tons of MOF per ha achieved the highest revenue of VND 550 million/ha, the highest cost of VND 163.68 million per ha, the highest profit of VND 386.32 million/ha, and highest benefit-cost ratio of 2.4 (Table 8).

Table 8. Effects of micro-organic and phosphorus fertilizers on economic efficiency of red turmeric

Phosphorus dose (kg P_2O_5/ha)	MOF dose (tons/ha)	AFY (ton/ha)	Total revenue	Total costs	Profit	BCR
			(million VND/ha)			
30	Cow dung [(1)]	15.3	306	155.42	150.58	1.0
	2	18.9	378	144.42	233.58	1.6
	4	19.7	394	153.42	240.58	1.6
	6	20.7	414	162.42	251.58	1.5
60[(2)]	Cow dung [(1)]	19.4	388	155.84	232.16	1.5
	2	21.3	426	144.84	281.16	1.9
	4	21.5	430	153.84	276.16	1.8
	6	25.1	502	162.84	339.16	2.1
90	Cow dung [(1)]	18.4	368	156.26	211.74	1.4
	2	21.7	434	145.26	288.74	2.0
	4	22.9	458	154.26	303.74	2.0
	6	24.0	480	163.26	316.74	1.9
120	Cow dung [(1)]	20.7	414	156.68	257.32	1.6
	2	21.1	422	145.68	276.32	1.9
	4	23.9	478	154.68	323.32	2.1
	6	27.5	550	163.68	386.32	2.4

AFY: Actual fresh yield; BCR: Benefit-Cost ratio, [(1)] 10 tons/ha (control), [(2)] 60 kg P_2O_5/ha (control); MOF: micro-organic fertilizer.

4. Conclusions

The experiment clearly indicated that on the gray infertile soil at Thu Duc city, red turmeric applied with 120 kg P_2O_5/ha combined with 6 tons of MOF/ha (a common dose of 500 kg lime, 90 kg N, 120 kg K_2O/ha) obtained the outstanding results in the growth, development and yield. The yield and yield components of red turmeric were also highest in this treatment with weight of fresh rhizomes (331.0 g), fresh root weight (317.7 mg), theoretical fresh yield (37.7 tons/ha), and actual fresh yield (27.5 tons/ha). Red turmeric was applied at the dose of 120 kg P_2O_5/ha combined with 6 tons of MOF/ha achieving the highest revenue of VND 550 million/ha and highest cost-benefit ratio of 2.4.

Conflict of interest

The authors declare no conflict of interest.

Acknowledgements

The authors would like to express their deep gratitude to Nong Lam University, Ho Chi Minh City, Vietnam for funding this study. These works were supported by the students and staff of Faculty of Agronomy.

References

Banwasi, R., & Singh, A. K. (2010). Effect of phosphorus levels on growth and yield of turmeric (*Curcuma longa* L.). *Journal of Spices and Aromatic Crops* 19(1,2), 76-86.

Barker, A. V., & Pilbeam, D. J. (2007). *Handbook of plant nutrition* (2nd ed.). London, UK: CRC Press.

Chanchan, M., Ghosh, D. K., & Hore, J. K. (2018). Influence of manures, biofertilizers along with grade levels of inorganic nitrogen and phosphorus on growth, yield and qualoty of turmetric (*Curcuma longa* L.). *Journal of Crop and Weed* 14(3), 113-118.

Do, L. T. (2004). *Medical plants and medical drug in Vietnam*. Ha Noi, Vietnam: Ha Noi Medicine Publisher.

Hossain, A., & Ishimine, Y. (2007). Effects of farmyard manure on growth and yield of turmeric (*Curcuma longa* L.) cultivated in dark-red soil, red soil and gray soil in Okinawa, Japan. *Plant Production Science* 10(1), 146-150. https://doi.org/10.1626/pps.10.146.

Kamal, M. Z. U., & Yousuf, M. N. (2012). Effect of organic manures on growth, rhizome yield and quality attributes of turmeric (*Curcuma longa* L.). *The Agriculturists* 10(1), 16-22. https://doi.org/10.3329/agric.v10i1.11060.

Mai, Q. V., Le, N. T. V., Ngo, V. Q., Nguyen, H. T., & Nguyen, K. T. (2000). *Popular herbs and spices in Vietnam*. Ho Chi Minh City, Vietnam: Agricultural Publishing House.

Mazid, M. A. (1993). Sulfur and nitrogen for sustainable rainfed lowland rice (Unpublished doctoral dissertation). University of the Philippines, Los Banos, Laguna, Philippines.

Padmapriya, S., & Chezhiyan, N. (2009). Effect of shade, organic, inorganic and bioferlitizers on morphology, yield and quaity of turmeric. *Indian Journal of Horticulture* 66(33), 333-339.

Ravindran, P. N., Babu, K. N, & Sivaraman, K. (Eds.). (2007). *Turmeric: The genus Curcuma* (1st ed.). Florida, USA: CRC Press. https://doi.org/10.1201/9781420006322.

Trinh, V. H. (2015). Effect of five mixed-fertilizers and propagation techniques using rhizome and in vitro on yield and curcumin content of red turmeric. *Agricultural Sciences, Fisheries and Biotechnology* 7(1), 84-93.

Treatment of sludge from intensive whiteleg shrimp farming using a sequencing batch reactor

Tran T. Q. Cao[1], Ha N. Nguyen[2], & Tu P. C. Nguyen[1*]

[1]Faculty of Fisheries, Nong Lam University, Ho Chi Minh City, Vietnam

[2]Research Institute of Biotechnology and Environment, Nong Lam University, Ho Chi Minh City, Vietnam

ARTICLE INFO

Research Paper

Received: April 17, 2023

Revised: April 29, 2023

Accepted: May 10, 2023

Keywords

Intensive shrimp farming

Nutrient mineralizatio

Sequencing batch reactor

Sludge

Treatment efficiency

Corresponding author

Nguyen Phuc Cam Tu

Email:

npctu@hcmuaf.edu.vn

ABSTRACT

The wastewater/sludge generated from the shrimp aquaculture industry contains high levels of nitrogen (N), phosphorous (P), and carbon (C). This study aimed to evaluate the efficacy of N, P, and C removal and recovery from sludge obtained during the siphoning process of intensive white leg shrimp farming by using a sequencing batch reactor (SBR) with two trials. In the first trial, reactors were operated aerobically (3 - 5 days) and anaerobically (4 - 6 days) in sequence, resulting in a total cycle time of 9 days. In trial 2, the reactors were run aerobically for the first 3, 4, & 5 days, respectively, succeeded by anoxic conditions until the end of the experiment on day 14. The results showed that the removal of total ammonia nitrogen and chemical oxygen demand was about 60 - 70%, but the treatment efficiencies of total N and P were extremely low. Moreover, the anaerobic mode improved the mineralization of P, while aerobic condition promoted nitrate production. Further studies are needed to improve the nutrient and organic removal performance of the SBR.

Cited as: Cao, T. T. Q., Nguyen, H. N., & Nguyen, T. P. C. (2023). Treatment of sludge from intensive whiteleg shrimp farming using a sequencing batch reactor. *The Journal of Agriculture and Development* 22(6), 12-21.

1. Introduction

Vietnam has many advantages to develop brackish-water shrimp farming, especially in provinces of Mekong delta (MK). Particularly, brackish-water shrimp farming area is about 740,000 ha with shrimp production volume reaching over 900,000 tons (DOF, 2021). Shrimp farming contributes to income rising, employment generating, and poverty alleviation for people. However, the high development of shrimp farming, especially intensive shrimp farming (ISF) models, has led to the problem of environmental pollution.

Activities of ISF have generated wastewater, particularly sludge from siphon process (sludge), containing a wide range of organic and inorganic

nutrients. Investigating 20 typical ISF ponds in the MK, Tran et al. (2022) reported that average levels (mg/L) of total suspended solid (TSS), chemical oxygen demand (COD), total ammonia nitrogen (TAN), total Kjeldahl nitrogen (TKN), total phosphorous (TP) in sludge were 3.423, 1.854, 101, 161, and 92, respectively. Compared to the QCVN 02-19:2014/BNNPTNT (MARD, 2014), concentrations of TSS and COD exceeded the permitted standards by over 34 and 12 times, respectively.

Conventional wastewater treatment methods can treat wastewater and sludge from the ISF ponds. Aerobic (activated sludge) and anaerobic (up-flow anaerobic sludge blanket, UASB) biological treatment process helps to reduce nitrogen and carbon concentration in the ISF effluents; however, these systems are costly to construct, operate and generate secondary waste (solid waste) requiring an area for disposal (Timmons et al., 1998; Boopathy et al., 2005).

Sequencing batch reactor (SBR), a variant of activated sludge, is seen as a potential solution to reduce nutrient concentrations in sludge from the ISF ponds (Boopathy, 2018). Unlike conventional activated sludge treatment technology that requires many reaction tanks, the SBR is a type of wastewater treatment facility based on suspended growth of microorganisms, in which there are two phases: an aerobic phase, where carbon oxidation (COD removal) and nitrification are combined into a single process, and an anaerobic phase where denitrification is accomplished (Boopathy et al., 2005; Boopathy et al., 2007; Boopathy, 2018). Therefore, the SBR can overcome most of the disadvantages of conventional aerobic - anoxic methods and biological filtration such as: no need for a settling tank after biological treatment; combine aerobic and anoxic processes in the same tank, thereby increasing nitrogen and carbon treatment efficiency (Boopathy et al., 2005; Boopathy et al., 2007; Boopathy, 2018). Moreover, anaerobic and aerobic sludge reactors can apply microbe to decompose the sludge into bioavailable nutrients and facilitates the nutrients recovery that can subsequently be used as algae/plant nutrition (Goddek et al., 2015; Goddek et al., 2016). The SBR systems have been used to treat many types of wastewater containing high nutrient and organic content such as slaughterhouse, swine manure, dairy, sewage, especially sludge from the ISF (Boopathy et al., 2005; Boopathy et al., 2007; Kundu et al., 2013). Regarding to the treatment of sludge from the ISF (raceway) by SBR, Boopathy et al. (2005) found that the treatment efficiencies of organic carbon and nitrogen compounds reached nearly 100% with the operating mode: aerobic phase for 3 days and anaerobic phase for 6 days.

The application of SBR in the treatment and nutrient recovery of sludge from the ISF can be a potential technical alternative to current technologies in the management of sludge. The objective of this study was to evaluate the removal efficiencies and recovery performance of nitrogen, carbon, and phosphorus (P) in sludge from the intensive whiteleg shrimp ponds under different sequences of react periods (aerobic/anoxic).

2. Materials and Methods

2.1. Collecting sludge

Sludge was collected from the intensive whiteleg shrimp ponds at Phuoc An shrimp farm, Nhon Trach district, Dong Nai province (10,648 N; 106,941 E). Shrimps were intensively cultured according to a three-stage process with an initial stocking density of 1,000 fish/m^2 and gradually decreasing stocking density to about 400 - 500 shrimp/m^2 in stage 2 and about 150 - 200 shrimp/

m2 in stage 3 until harvesting. The sludge samples were collected through the siphon discharge pipe and put into a large plastic tank, then let it settle for 1 h, decant the clear water above to take only the settled sludge. When sampling, the samples were stirred well and sieved through a 2 mm sieve to remove peeled shrimp shells, dead shrimp, and large-sized matter. After screening through a sieve, the samples were kept in PE nylon bags (30 cm x 50 cm) and stored in a foam box with ice. The samples were then transported to the Toxicology Laboratory, Research Institute of Biotechnology and Environment, Nong Lam University, Ho Chi Minh City within 1 h. Salinity and pH in samples were in the range of 4 - 5‰ & 6.2 - 6.7, respectively.

2.2. Experimental procedure

2.2.1. Reactor configuration

In this experiment, a lab scale reactor was cylindrical in shape with 27 cm in diameter and 35 cm in height and made from plastic buckets. The reactor was painted black outside and equipped with an aeration system and stirring motor. Total working volume of the reactor was 20 L that just 5 L were used. Air was injected into the reactor by dispersing air bubbles through 2-mm holes in copper pipe (spacing 10 cm) placed on the reactor floor. An impeller positioned 10 cm from the bottom of the reactor (Figure 1). During aerobic phase, the reactors were continuously aerated and stirred at 100 rpm. In anaerobic phase, aeration and stirring were turned off (Boopathy et al., 2005).

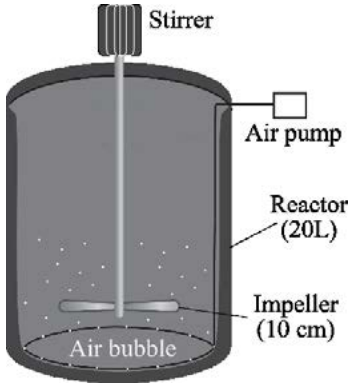

Figure 1. Reactor configuration.

2.2.2. Sequencing batch reactor operational conditions

The experiment consisted of two trials. The trial 1 was to evaluate the effectiveness of the SBR with the operating mode as reported by Boopathy et al. (2005) with slight modifications.

The trial 1 was carried out in three SBR reactors: reactor 1, 2 and 3 operating aerobically (DO > 3 mg/L) for the first 3, 4 and 5 days, respectively (Figure 2). In anaerobic phase, reactor 1, 2 and 3 were operated anaerobically

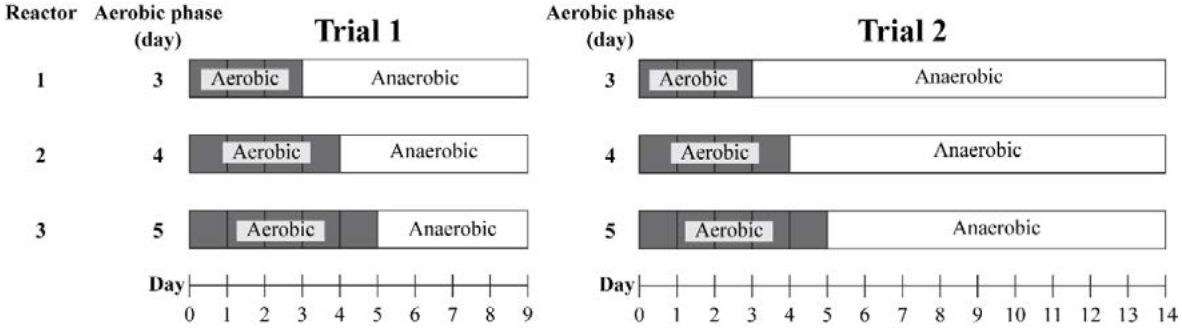

Figure 2. Sequencing batch reactor operational conditions for two trials.

(DO < 0.5 mg/L) since day 4, 5 and 6 until the end of the trial on day 9. The experiment was repeated three times using a different initial sludge sample.

Sludge samples were collected in the beginning (day 0) and at the end of the aerobic (days 3, 4, & 5) and anaerobic phase (day 9) and were analyzed for parameters including nitrogenous compounds (TKN, TAN, nitrite, and nitrate), phosphorous (TP and soluble - PO_4^{3-}), and COD (total and soluble). Moreover, total solid (TS) and total volatile solid (TVS) were determined in the beginning and at the end of the experiment.

For trial 2, based on the performance of the reactors from the trial 1, the reactors 1, 2 and 3 were operated aerobically for the first 3, 4 and 5 days, respectively, and then operated anoxically until the end of the experiment on day 14 (Figure 2). The experiment was conducted without replication. Samples were collected daily and were analyzed for COD, TAN, and nitrate.

2.3. Analytical methods

Sludge from each reactor was sampled and centrifuged at 5,000 rpm for 10 min and the supernatant used for chemical analyses of TAN, nitrite, nitrate, PO_4^{3-} and soluble COD (sCOD). For the other parameters, sludge is used without centrifuge. All parameters were analyzed using standard methods (Baird et al., 2017).

2.4. Statistical analysis

All data were presented on mean ± standard deviation (SD). Levels of parameters in sludge were compared to the QCVN 02-19:2014/BNNPTNT standards (MARD, 2014). A Tukey test, along with one-way blocked analysis of variance (ANOVA) with replication as blocks was used to assess differences in levels of parameters in sludge during trial 1. Statistical analysis was done using the IBM SPSS Statistics for Windows, version 22 (Armonk, NY: IBM Corp). Significant level was evaluated as $P < 0.05$. Because of no replication in trial 2, data were shown in figures without statistical analysis.

The removal efficiency of the SBR was estimated using the equation:

$$Removal\ efficiency\ (\%) = (\Delta C_{in\text{-}out}/C_{in}) \times 100$$

where, ΔC_{in-out}: inflow-outflow concentrations of parameters (mg/L); C_{in}: inflow concentrations of parameters (mg/L). For trial one, carbon and nitrogen removal was reported as the average of triplicate SBRs.

3. Results

For trial 1, average levels of parameters in sludge in the beginning and at the end of the aerobic and anaerobic phase were presented in Table 1. Initial sludge from siphon process contains very high concentrations of organic compounds (COD and TVS) and nutrients (TKN, TAN, nitrate, TP, and PO_4^{3-}). Particularly, COD levels exceeded the permitted standards of the QCVN 02-19:2014/BNNPTNT (COD ≤ 150 mg/L) (MARD, 2014) by 250-fold. But nitrite level in the initial sludge was very low (Table 1).

In general, the concentrations of organic compounds and nutrients during the experimental period tended to decline (Table 1). The initial TKN content of 1,803 ± 453 mg/L was reduced to 1,695 ± 430 mg/L (a decrease of about 100 mg/L) at the end of experiment with a removal efficiency of only 6%. Meanwhile, nitrification during the aerobic stage of SBR resulted in the decrease of TAN from 172 ± 41 mg/L to 68 ± 14 mg/L at day 5 with a relatively high treatment efficiency (60%) but increased in the anaerobic phase (86 mg/L ± 23 mg/L at the end of the experiment) (Table 1). Nitrate

Table 1. Concentrations (mean ± SD, n = 3) of parameters in sludge in the beginning and treatment phases in the trial 1

Day	Phase	TKN (mg/L)	TAN (mg/L)	Nitrite (mg/L)	Nitrate (mg/L)	TP (mg/L)
0		1,803 ± 453^{a}	172 ± 41^{a}	0.033 ± 0.011^{a}	86 ± 10^{ab}	651 ± 210^{a}
3	Aerobic	1,788 ± 450^{a}	138 ± 41^{a}	0.209 ± 0.297^{a}	151 ± 20^{a}	641 ± 217^{ab}
4	Aerobic	1,755 ± 431^{ab}	100 ± 37^{b}	0.044 ± 0.035^{a}	180 ± 64^{a}	634 ± 213^{ab}
5	Aerobic	1,721 ± 480^{ab}	68 ± 14^{b}	0.036 ± 0.007^{a}	183 ± 53^{a}	628 ± 208^{ab}
9	Anaerobic	1,695 ± 430^{b}	86 ± 23^{b}	0.062 ± 0.024^{a}	49 ± 12^{b}	589 ± 163^{b}

Day	Phase	PO_4^{3-} (mg/L)	COD (g/L)	sCOD (g/L)	TS (g/L)	TVS (g/L)
0		10.3 ± 13.2^{a}	37.5 ± 11.3^{a}	6.14 ± 1.67^{a}	135 ± 47^{a}	34.1 ± 0.^{5}a
3	Aerobic	6.07 ± 3.31^{a}	34.3 ± 8.8^{ab}	4.75 ± 1.99^{ab}	-	-
4	Aerobic	4.01 ± 4.77^{a}	31.0 ± 7.0^{b}	3.75 ± 1.82^{bc}	-	-
5	Aerobic	3.87 ± 2.41^{a}	29.7 ± 8.3^{b}	3.18 ± 1.39^{bc}	-	-
9	Anaerobic	16.1 ± 14.9^{a}	24.2 ± 7.4^{c}	2.33 ± 0.94^{c}	125 ± 40^{a}	29.3 ± 4.0^{a}

Mean values in the same column with different superscript letters differ significantly (One-way ANOVA, Tukey test, $P < 0.05$).

TKN: total Kjeldahl nitrogen; TAN: total ammonia nitrogen ; TP: total phosphorus; COD: chemical oxygen demand; sCOD: soluble chemical oxygen demand; TS: total solid; TVS: total volatile solid.

concentrations increased with time in the aerobic phase, from an initial concentration of 86 ± 10 mg/L to 183 ± 53 mg/L on day 5 and decreased in the anoxic phase (49 mg/L ± 12 mg/L at the end of the experiment) (Table 1). The concentrations of TKN and TAN after the SBR treatment were statistically significantly lower than those of the initial ($P < 0.05$); but there was no statistically significant difference in the content of nitrite and nitrate between day 0 and 9 ($P > 0.05$) (Table 1).

It seems there was a steady decline in TP during the experimental period, from an initial concentration of 651 ± 210 mg/L to 589 ± 163 mg/L on day 9 with a removal efficiency of about 10% (Table 1). Concentrations of PO_4^{3-} were decreased with time in the aerobic phase, from the initial concentration of 10.3 ± 13.2 mg/L to 3.87 ± 2.41 mg/L at day 5 (removal efficiency of 62%) and increased in the anaerobic phase (concentration reached 16.1 ± 14.9 mg/L at the end of the experiment), attributing to the release of soluble P from the sludge. Differences in TP concentrations between sampling days were statistically significant ($P < 0.05$), whereas differences in PO_4^{3-} levels among sampling days were not statistically significant ($P > 0.05$) (Table 1).

The initial COD and sCOD concentrations of 37.5 ± 11.3 g/L and 6.14 ± 1.67 g/L, respectively, were decreased slowly in both aerobic and anaerobic phases. Levels of these COD were

removed more in the oxic phase than in the anoxic phase. Levels of COD and sCOD at day 9 dropped to 24.2 ± 7.4 g/L and 2.33 ± 0.94 mg/L, respectively. The removal efficiencies of COD and sCOD were 36 and 62%, respectively. Significant differences in COD and sCOD concentrations between day 0 and day 9 were found ($P < 0.05$) (Table 1).

During the SBR treatment, the initial contents of TS (135 ± 47 g/L) and TVS (34.1 ± 0.5 g/L) were dropped to 125 ± 40 g/L and 29.3 ± 4.0 g/L at the end of the trial with relatively low removal efficiencies of 7.3 and 14%, respectively. Differences in TS and TVS levels in the beginning and at the end of the experiment were not significant ($P > 0.05$) (Table 1).

Figure 3 presented changes in concentrations of TAN, nitrate, and COD during the trial 2. From this figure, the initial TAN level of 130 mg/L were gradually decreased to 58.5 mg/L, 37.0 mg/L, and 16.4 on days 3, 4, and 5, respectively, during the aerobic phase of operation (Figure 3). At the same time, the nitrate concentrations were increased correspondingly with a decline in TAN in the reactors implying nitrification. Particularly nitrate levels increased from 281 mg/L at the beginning of the trial to a maximum of 523 mg/L in reactor 3 on day 5. When the reactor 1 was operated anoxically the nitrate level decreased slowly and finally reached 218 mg/L on day 14. While the SBR also treated the COD during both aerobic and anaerobic steps of the reactor operation (Figure 3), which slowly dropped from 45.8 g/L at the beginning of SBR operation to 12 g/L at the end of the trial on day 14, leading to 73% removal of COD in the SBR. More organic compounds were eliminated in the aerobic mode than the anaerobic mode.

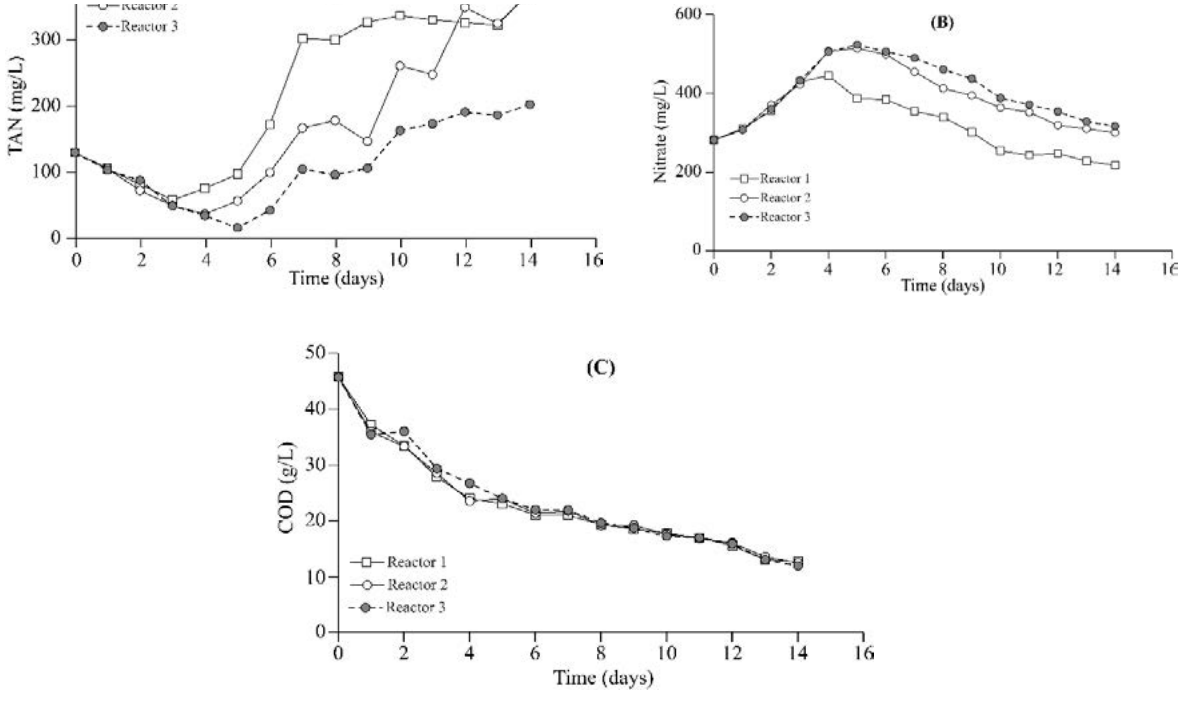

Figure 3. Changes in concentrations of total ammonia nitrogen (TAN; A), nitrate (B), and chemical oxygen demand (COD; C) during the trial 2.

4. Discussion

Previous publications have revealed that the ISF wastewater (including wastewater from water exchange and sludge from siphoning) from intensive and super-intensive shrimp farming often contains high levels of biodegradable organic compounds and dissolve nutrients (Boopathy, 2018; Nguyen et al., 2022; Tran et al., 2022). Average COD levels were in the 466 - 1,854 mg/L range; while concentrations of TAN, TKN, and TP were in a typical range of 29.8 - 101 mg/L, 9.63 - 161 mg/L, & 17.3 - 92 mg/L, respectively (Boopathy, 2018; Tran et al., 2022; Nguyen et al., 2022). The sludge characteristics in this study were much higher than the results of previous studies. It could be due to the difference in sludge sampling methods. In this study, the sludge from siphoning process was settled for 1 hour and the clear water decanted, thus the sludge sample would be denser. Meanwhile, the studies of the above-mentioned authors sampled sludge without settling.

According to the literature, wastewater and sludge from the ISF might be treated by activated sludge method, UASB, filtration system and sludge management; yet, these treatment methods can be costly to construct and operate (Timmons et al., 1998; Boopathy et al., 2005). On the contrary, the SBR reactors are very simple in design and operation, using only one reactor for many treatment phases. The SBR effectively removed organic matters and nutrients in sludge come from intensive shrimp recirculating aquaculture systems in the US (Boopathy et al., 2005; Boopathy, 2009; Boopathy, 2018). Regarding to the treatment of sludge from an intensive shrimp raceway system by the SBR (3 days aerobic phase, 6 days anaerobic phase), Boopathy et al. (2005) found that the initial TAN concentration in sludge of 91 mg/L was decreased to 5.3 mg/L on the third day of the oxic phase. While, in the aerobic phase, the nitrite concentrations were increased from 237 to 403 mg/L on the second day and decreased sharply in the anaerobic phase (to 3.0 mg/L on day 9). At the same time, the levels of nitrate increased, and the highest nitrate level was 91.8 mg/L on day 3. Then in the anoxic phase, the nitrate content declined steadily and dropped to 1 mg/L at the end of the trial. The initial COD content of 1,602 mg/L was slowly decreased in both aerobic and anaerobic phases and the removal of organic matter in oxic condition was higher than in anoxic condition. Level of COD decreased to 69 mg/L on day 9 (Boopathy et al., 2005). Remarkably, the addition of Bacillus consortium in the SBR can be effective in controlling the growth of shrimp pathogen, *Vibrio harveyi* in the sludge (Boopathy, 2018). According to these authors, the sludge of the ISF already contained many different groups of bacteria that perform nitrification and denitrification reactions as well as carbon metabolism (Boopathy et al., 2005; Boopathy et al., 2007; Boopathy et al., 2018). The results of this study showed that nitrate levels increased due to nitrification in oxic stages and reduced due to denitrification in anoxic stages. While carbon removal occurred in both aerobic and anaerobic phases (Table 1).

No study has evaluated the potential of treating P in sludge/wastewater from the ISF by the SBR. But the SBR has proven to be able to remove P from slaughterhouse wastewater with a removal efficiency of 85 - 89% (Fongsatitkul et al., 2011). According to Dutta & Sarkar (2015), P was removed by a special group of bacteria known as polyphosphate accumulating organisms (PAO). Under anoxic phase, PAOs utilize carbon source, mostly volatile fatty acids and change them to polyhydroxyalkanoates (PHAs). The energy for this process was taken chiefly through the intracellular hydrolysis of poly-P compounds,

leading to the regeneration of ortho-phosphate into the water. Under oxic phase, PAOs can uptake surplus P and convert into intracellular poly-P, biomass growth, and glycogen replenishment by oxidizing stored PHAs (Dutta & Sarkar, 2015). In this study, the increased ortho-phosphate content in the anaerobic phase could be due to the mineralization of the precipitated P compounds (such as calcium phosphate, calcium sulphate, calcium carbonate, etc.) in the SBR when the pH dropped under 6 as stated by Delaide et al. (2019). Goddek et al. (2018) also reported that the UASB worked best at mineralizing and mobilizing P (7 - 26%) from fish sludge, whereas the aerobic reactor showed the least mineralization performance (-5%). Levels of P from these UASB effluents were close to the lettuce hydroponic solution (Goddek et al., 2018).

The removal efficiencies of nutrient and organic matter (in range of 60 - 70% at the highest) in this work were lower than those of reported by the aforesaid authors (nearly 100%) (Boopathy et al., 2005; Boopathy, 2009; Boopathy et al., 2018). It could be due to the concentrations of nutrients and organic matter in the sludge of this experiment was higher, so the treatment time of 9 or 14 days might be not enough. In addition, the C/N ratio in this study (20/1) was higher than the optimal C/N ratio for SBR tanks of 10/1 (Fontenot et al., 2007; Roy et al., 2010). Moreover, addition of Bacillus consortium could be to enhance the performance of SBR for the treatment of sludge (Boopathy et al., 2015).

5. Conclusions

The SBR was relatively effective in treating TAN and COD in the sludge from three-stage ISF. However, the removal efficiencies of TN, TP, TS, and TVS were very low. Our findings obviously imply that anaerobic mode improves the mineralization performance of P, but aerobic condition enhances nitrate production. Further studies are needed to improve the treatment efficiencies of nutrients and organic matter in sludge/wastewater from the ISF and other aquaculture species: prolonging the treatment time in aerobic and anaerobic phases, optimizing the C/N ratio, adding microorganisms, etc. Generally, the use of SBR in wastewater/sludge treatment from aquaculture can be a simple, low-cost technical solution that supports current technologies in waste management from aquaculture.

Conflict of interest

The authors declare that there is no conflict of interest regarding the publication of this paper.

Acknowledgements

This study was funded by the Nong Lam University, Ho Chi Minh City under grant number CS-SV22-TS-01.

References

Baird, R. B., Eaton, A. D., & Rice, E. W. (2017). Standard methods for the examination of water and wastewater (23rd ed.). Washington DC, USA: American Public Health Association.

Boopathy, R. (2018). Waste treatment in recirculating shrimp culture systems. In Hai, F. I., Visvanathan, C., & Boopathy, R. (Eds.). *Sustainable aquaculture* (301-322). New York, USA: Springer International Publishing. https://doi.org/10.1007/978-3-319-73257-2_10.

Boopathy, R. (2009). Biological treatment of shrimp production wastewater. *Journal of Industrial Microbiology and Biotechnology* 36(7), 989-992. https://doi.org/10.1007/s10295-009-0577-0.

Boopathy, R., Bonvillain, C., Fontenot, Q., & Kilgen, M. (2007). Biological treatment of

low-salinity shrimp aquaculture wastewater using sequencing batch reactor. *International Biodeterioration and Biodegradation* 59(1), 16-19. https://doi.org/10.1016/j.ibiod.2006.05.003.

Boopathy, R., Fontenot, Q., & Kilgen, M. B. (2005). Biological treatment of sludge from a recirculating aquaculture system using a sequencing batch reactor. *Journal of the World Aquaculture Society* 36(4), 542-545. https://doi.org/10.1111/j.1749-7345.2005.tb00403.x.

Boopathy, R., Kern, C., & Corbin, A. (2015). Use of Bacillus consortium in waste digestion and pathogen control in shrimp aquaculture. *International Biodeterioration and Biodegradation* 102, 159-164. https://doi.org/10.1016/j.ibiod.2015.02.001.

Delaide, B., Monsees, H., Gross, A., & Goddek, S. (2019). Aerobic and anaerobic treatments for aquaponic sludge reduction and mineralisation. In Goddek, S., Joyce, A., Kotzen, B., & Burnell, G. M. (Eds.). *Aquaponics food production systems: Combined aquaculture and hydroponic production technologies for the future* (247-266). Cham, Switzerland: Springer International Publishing. https://doi.org/10.1007/978-3-030-15943-6_10.

DOF (Directorate of Fisheries). (2021). Vietnam shrimp 2021: Farming production increases, export value is estimated at 3.8 billion USD. Retrieved March 17, 2023, from https://tongcucthuysan.gov.vn/vi-vn/Tin-t%E1%BB%A9c/-Tin-v%E1%BA%AFn/doc-tin/016572/2021-12-13/tom-viet-nam-2021-san-luong-nuoi-tang-xuat-khau-uoc-dat-38-ty-usd.

Dutta, A., & Sarkar, S. (2015). Sequencing batch reactor for wastewater treatment: recent advances. *Current Pollution Reports* 1(3), 177-190. https://doi.org/10.1007/s40726-015-0016-y.

Fongsatitkul, P., Wareham, D. G., Elefsiniotis, P., & Charoensuk, P. (2011). Treatment of a slaughterhouse wastewater: effect of internal recycle rate on chemical oxygen demand, total Kjeldahl nitrogen and total phosphorus removal. *Environmental Technology* 32(15), 1755-1759. https://doi.org/10.1080/09593330.2011.555421.

Fontenot, Q., Bonvillain, C., Kilgen, M., & Boopathy, R. (2007). Effects of temperature, salinity, and carbon: nitrogen ratio on sequencing batch reactor treating shrimp aquaculture wastewater. *Bioresource Technology* 98(9), 1700-1703. https://doi.org/10.1016/j.biortech.2006.07.031.

Goddek, S., Delaide, B., Mankasingh, U., Ragnarsdottir, K. V., Jijakli, H., & Thorarinsdottir, R. (2015). Challenges of sustainable and commercial aquaponics. *Sustainability* 7(4), 4199-4224. https://doi.org/10.3390/su7044199.

Goddek, S., Delaide, B. P. L., Joyce, A., Wuertz, S., Jijakli, M. H., Gross, A., Eding, E. H., Bläser, I., Reuter, M., Keizer, L. C. P., Morgenstern, R., Körner, O., Verreth, J., & Keesman, K. J. (2018). Nutrient mineralization and organic matter reduction performance of RAS-based sludge in sequential UASB-EGSB reactors. *Aquacultural Engineering* 83, 10-19. https://doi.org/10.1016/j.aquaeng.2018.07.003.

Goddek, S., Schmautz, Z., Scott, B., Delaide, B., Keesman, K. J., Wuertz, S., & Junge, R. (2016). The effect of anaerobic and aerobic fish sludge supernatant on hydroponic lettuce. *Agronomy* 6(2), 37. https://doi.org/10.3390/agronomy6020037.

Kundu, P., Debsarkar, A., & Mukherjee, S. (2013). Treatment of slaughter house wastewater in a sequencing batch reactor: performance evaluation and biodegradation kinetics. *BioMed Research International* 2013, 134872. https://doi.org/10.1155/2013/134872.

MARD (Ministry of Agriculture and Rural Development). (2014). *National technical regulation No. QCVN 02-19:2014/BNNPTNT*

date on July 29, 2014. National technical regulation on brackish water shrimp culture farm - conditions for veterinary hygiene, environmental protection and food safety. Retrieved February 20, 2022, from https://luatvietnam.vn/nong-nghiep/quy-chuan-viet-nam-qcvn-02-19-2014-bnnptnt-bo-nong-nghiep-va-phat-trien-nong-thon-157372-d3.html.

Nguyen, T. L. M., Tran, H. T., Tran, K. T., Nguyen, T. V., Nguyen T. T. P., & Nguyen, S. V. (2022). Assessment of the current status of wastewater and sewage sludge generated from intensive and super-intensive shrimp farms in Bac Lieu province and proposal of wastewater treatment and sludge management methods. *Environment Magazine* 3, 98-104.

Roy, D., Hassan, K., & Boopathy, R. (2010). Effect of carbon to nitrogen (C:N) ratio on nitrogen removal from shrimp production waste water using sequencing batch reactor. *Journal of Industrial Microbiology and Biotechnology* 37(10), 1105-1110. https://doi.org/10.1007/s10295-010-0869-4.

Timmons, M. B., Summerfelt, S. T., & Vinci, B. J. (1998). Review of circular tank technology and management. *Aquacultural Engineering* 18(1), 51-69. https://doi.org/10.1016/S0144-8609(98)00023-5.

Tran, N. S., Huynh, T. V., Nguyen, L. T., Nguyen, P. D., & Nguyen, C. V. (2022). Optimizing hydraulic retention time and area of biological settling ponds for super-intensive shrimp wastewater treatment systems. *Water* 14(6), 932. https://doi.org/10.3390/w14060932.

Sex reversal using 17 α-methyltestosterone immersion and its effect on sex reversal and growth performance of Nile tilapia (*Oreochromis niloticus* L., 1758)

Dang H. Nguyen[1], Nhung T. H. Nguyen[2], Hien T. Nguyen[2], Nam V. Nguyen[1], & Tuan V. Vo[1*]

[1]Faculty of Fisheries, Nong Lam University, Ho Chi Minh City, Vietnam

[2]Plant and Livestock Hatcheries, Agricultural Service Center of Binh Phuoc Province, Binh Phuoc, Vietnam

ARTICLE INFO

Research Paper

Received: March 28, 2023

Revised: April 28, 2023

Accepted: May 08, 2023

Keywords

Immersion method

Nile tilapia

17 α-methyltestosterone

Sex-reversal

Corresponding author

Vo Van Tuan

Email:

vovantuan@hcmuaf.edu.vn

ABSTRACT

The study aimed to evaluate the optimal dose of 17 α-methyltestosterone (MT) and stocking density using immersion method for maximum survival, masculinization rates and growth performance of Nile tilapia (*Oreochromis niloticus*). The experimental design employed complete randomization including three concentrations of 17 α-methyltestosterone (1.5, 2.0, and 2.5 mg/L) and three stocking densities of 500, 750, and 1000 fish/L and a control group, arranged in three replicates. The control groups consisted of 3 stocking densities of 500, 750, & 1000 fish/L and fish were kept in glass aquaria containing MT-free water. Fish were exposed to MT solution for 2 h, and the fish were then transferred to nursery in hapas in earthen ponds at a density of 1,000 fish/m^2 for 60 days. After the hormone treatment and 60 days of rearing, the highest survival rate was found in the control group. The male ratios in the MT treatments ranged from 78.9 to 91.1% and were statistically higher than that in the control (55.1%) ($P < 0.05$). The most effective doses and stocking density in sex-reversal of the tilapia fry using immersion method were 2.0 mg 17 α-MT/L and 750 fish/L, respectively. The mean weight and length of fish in the MT treatments were greater than those in the control treatment, although the difference was not statistically significant ($P > 0.05$). The results also showed that the average weight of experimental fish was directly proportional to the hormone concentration but inversely proportional to the stocking density. Based on the study findings, the recommended dose for producing maximum mono-sex male tilapia is 2.0 mg 17 α-MT /L, and the most suitable stocking density is 750 fish/L.

Cited as: Nguyen, D. H., Nguyen, N. T. H., Nguyen, H. T., Nguyen, N. V., & Vo, T. V. (2023). Sex reversal using 17 α-methyltestosterone immersion and its effect on sex reversal and growth performance of Nile tilapia (*Oreochromis niloticus* L., 1758). *The Journal of Agriculture and Development* 22(6), 22-31.

1. Introduction

Tilapia is an economically important fish species that is widely cultured in the world with the second highest total global production next to carps (Ridha, 2006). The reasons are due to its fast growth rate, high tolerance to low water quality and adverse environmental conditions, efficient use of a variety of available feeds, good disease resistance, easy reproduction, and good meat quality and acceptable by different groups of consumers (El-Saidy & Gaber, 2005). To promote tilapia production, studies on nutritional requirements, farming systems, as well as post-harvest handling/storage processes, and market development have been carried out worldwide. However, the advantage of easy reproduction in captivity has become the biggest obstacle to intensive farming of tilapia on a commercial scale. Usually tilapias are very early reproductive maturity species (4 - 5 months old) at a fairly small average weight (20 - 30 g/individual) and spawning continuously every month. This leads to the increasing density of pond culture, which reduces the efficient use of feed and growth rate, thereby reducing the economic efficiency of the culture model (Varadaraj & Pandian, 1987). In addition, male tilapia has a faster growth rate than female tilapia of the same age (Hossain et al., 2022), which make a lot of fish that are smaller than commercial size when harvested, so it is difficult to apply industrial farming scale with a mixed sex of tilapia.

To avoid these undesirable obstacles in intensive culture, farmers have adopted an all-male tilapia culture (Sultana et al., 2020). There are many ways to produce the male monogamous tilapia (Hossain et al., 2022). The first method is manual sexing based on the difference in secondary sexual characteristics, external genitalia morphology, eliminating the females and keeping the males. The main disadvantages of this method are human errors and the waste of females. The second method is hybridization method including: i) using interspecific hybridization with different sex-determining chromosomal mechanisms (XY & ZW) (Lovshin, 1982); ii) using cross breeding between normal female and super male (YY) (Mair et al., 1995). According to Pruginin et al. (1975), the main advantage of the crossbreeding method is that it can produce 100% males; however the biggest drawbacks of this method are the cost and technique to maintain the purebred brood stock. The third method is sex-reversal using male sex hormones to masculinize tilapia (Le, 2008; El-Zaeem, 2013). According to Andersen et al. (2003), tilapia fry are sexually underdeveloped at the hatching time. Thus, changes in sex hormone levels in their bodies may have an impact on genetic sex during early gonadal development. Sex-reversal by feeding fish with food containing 17 α-methyltestosterone is one of the most effective and commonly used methods because of its low investment cost and short processing time (Prabu et al., 2019). Moreover, the obtained male ratio is always high and stable compared to other methods. Recently, the immersion method that exposing Tilapia fry before gonadal differentiation in water containing 17 α-methyltestosterone showed more advantages such as high male and survival rate, simplicity, short implementation time, lower MT dose and workers are not directly exposed to the hormone so it is safe for both consumers and producers. However, the MT concentration and treatment density in the immersion method have not been fully studied on Nile tilapia in Vietnam. Therefore, this study was conducted to determine the optimal dose of 17 α-methyltestosterone hormone and effective treatment density to improve the survival rate, sex conversion rate and growth performances of tilapia treated by immersion method.

2. Material and methods

Broodstock development

The brood fishes (200 - 250 g) were purchased from National Breeding Centre for Southern Freshwater Aquaculture, Research Institute for Aquaculture No. 2, Vietnam. The fish were acclimatized for 15 days and raised to reproductive maturity in 60 days in hapa (12 m x 5 m x 1.5 m) suspended in the earthen ponds (15 m x 30 m) in the Plants and Livestock Hatcheries, Agricultural Service Center of Binh Phuoc province. The ready spawning brood fishes were then paired for spawning in six matting hapas (12 m x 5 m x 1.5 m) with a ratio of 3 females: 1 male/m^2 in the earthen ponds (30 m x 50 m). The brood fishes were fed twice in a day at 3% body weight on a commercial floating pelleted feed (Brand Tilapia feed, Cargill company), with approximately 27% of crude protein.

Fry collection

After 15 days of pairing, fry were collected every seven days. The fry were collected using a soft net in the early morning to avoid stress and mortality. The fish were acclimated in the one m^3 composite tanks for one day, then removing weak/dead fish and sorting out fish by mesh size.

Preparation of hormone treated solutions

The 17 α-methyltestosterone hormone used in the present study was obtained from the Sigma Aldrich Ltd., Germany. A stock solution was made by dissolving 400 mg of hormone in 1 L of 95% ethanol to achieve the stock solution with the nominal concentration of 400 mg. Treatment concentrations were prepared by dissolving the accurate amount of the hormone from stock solution in 20 L glass tanks containing 10 L of water and with vigorously aerating to allow the alcohol to evaporate.

Experimental design

The experiment was carried out in 20 L glass tanks using completely randomized design. The experiment included three 17 α-methyltestosterone (MT) concentrations of 1.5, 2.0, & 2.5 mg/L and three stocking densities of 500, 750, & 1000 fish/L and a control in triplicates (Table 1). The control groups consisted of three stocking densities of 500, 750, & 1000 fish/L and fish were kept in glass aquaria containing MT-free water. One day after acclimatization in the composite tank that is continuously aerated, tilapia fry (0.24 g ± 0.06) were randomly stocked into the glass aquaria according to the treatments of stocking densities, MT concentrations and control experiment. Fish were exposed to MT solution for two hours, and the fry were then transferred to nursery in hapas (4 m x 2 m x 1.6 m) suspended in earthen ponds at a density of 1,000 fish/m^2 for 60 days. The fishes were fed twice a day on a commercial floating pelleted feed (Brand Tilapia feed, Cargill company)with approximately 40% of crude protein, at a feeding rate of 5% of body weight.

Sex reversal

At the end of experiment, 50 fish were randomly collected in each experimental replicate to identify the sex of the fishes. Morphology of the gonads were examined and recorded. Sexing determination was done by standard aceto-carmine gonad squashing technique and hematoxylen & eosin staining (Guerrero & Shelton, 1974).

Table 1. Treatment combination details of the experiment

Treatment	Stoking density (fish/L)	17 α-methyltestosterone concentration (mg/L)
C1	500	0
C2	750	0
C3	1000	0
T1	500	1.5
T2	750	1.5
T3	1000	1.5
T4	500	2.0
T5	750	2.0
T6	1000	2.0
T7	500	2.5
T8	750	2.5
T9	1000	2.5

Growth performance

Every 30 days, 10 fish were randomly collected in each experimental replica te to measure the mean growth (average weight and total length), then released the fish back into experimental hapa. Survival rates were recorded at 2 h after immersion of fish in MT solutions and at the end of the growth experiment (day 60).

Statistical analysis

The data were statistically analyzed by statistical package SPSS version 16.0 in which data were subjected to one-way ANOVA and Duncan's multiple range test (DMRT) was used to determine the significant differences between the means at 5% level of significance.

3. Results and Discussion

Survival

Survival rate of fish after 2 h of treatment with MT and at the end of the experiment (60 days) was presented in Figure 1.

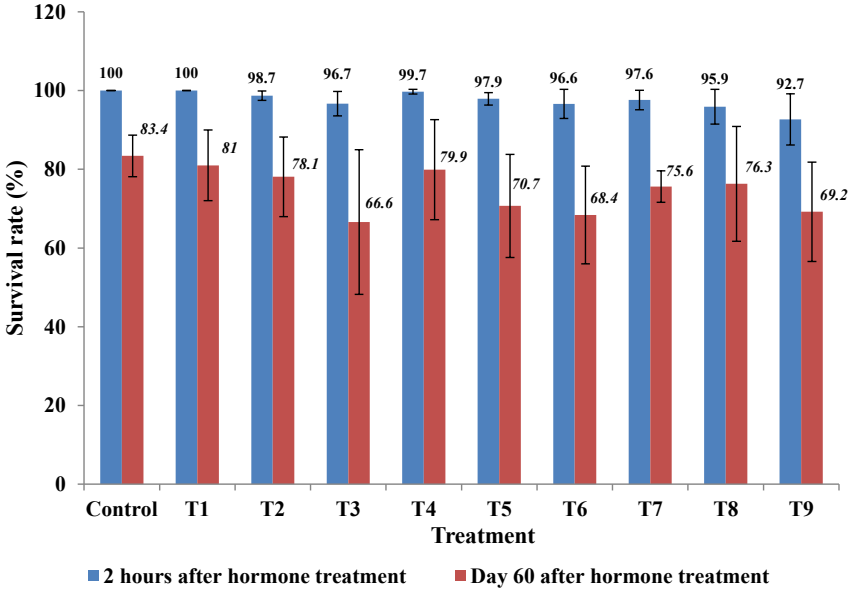

Figure 1. The survival rate of tested fish after 2 h of hormone treatment.

The results showed that the survival rate of tilapia fry after 2 h of hormone treatment ranged from 92.7 to 100%, in which the fish in the control and T1 (1.5 mg MT/L + stocking density of 500 fish/L) had the highest survival rates of 100%, followed by treatments T4 (2.0 mg MT/L + stocking density of 500 fish/L), T2 (1.5 mg MT/L + stocking density of 750 fish/L), T5 (2.0 mg MT/L + stocking density of 750 fish/L) and T7 (2.5 mg MT/L + stocking density of 500 fish/L), respectively. However, there was no statistically significant difference in survival rate among treatments ($P > 0.05$).

At the end of 60 day of nursing period, the maximum survival rate (83.4%) was found in control group, while the lowest survival rate (66.6%) was found in T3 group. Experimental results showed that the survival rates of fish in the control treatment at all experimental stages were higher than the survival rates in all MT treatments, but the difference was not statistically significant ($P > 0.05$). The result also indicated that the survival rate was inversely proportional to the MT concentrations and stocking densities. In general, the MT hormone immersing method is not significantly affect the survival rate of tilapia fry during treatment and rearing periods.

The survival rate of tilapia in this experiment is consistent to that of tilapia treated with oral administration method for 21 days of authors such as Tu (2006) (69.5 - 83.4%), Jensi et al. (2016) (87.33 - 95.00%) and Alam et al. (2023) (81.3 - 92.0%). In addition, this result is similar to the survival rate of other fish when treated with feeding methods such as Aulonocara nyassae (62.2 - 93.3%) (Karslı, 2021) and Clarias gariepinus (81.1 - 92.2%) (Alam et al., 2023).

Sex reversal

The effectiveness of sex reversal treatments is greatly depended on the amount of hormone, the duration of use, the administration method that the fish can absorb hormone during its labile period of sexual differentiation. The rate of masculinization is considered one of the important indicators to help evaluate the quality

and effectiveness of the hormone used as well as the efficiency of the all-male tilapia production process. Therefore, in this study, different concentrations of MT were used to observe the effects of these different doses on sex-reversal of tilapia fry after exposed to MT in 2 h.

From the histological analysis of gonadal tissues (Figure 2), there was no intersex individuals found in all MT treatments as well as in control groups (Table 2). The control group showed the normal sex ratio of 1 male: 0.81 female. The male ratios in the MT treatments ranged from 78.9 to 91.1% and were statistically significant higher than that in the control treatment (55.1%) ($P < 0.05$). Experimental results showed that the highest rates of masculinization of 91.1%, 90.0% and 87.8% were found in treatment T8 (MT concentration of 2.5 mg/L and stocking density of 750 fish/L), treatment T7 (MT concentration of 2.5 mg/L and density 500 fish/L) and treatment T5 (MT concentration of 2.0 mg/L and density of 750 fish/L), respectively, and the difference was not statistically significant among these treatments ($P > 0.05$). It indicated that MT at concentrations of 2 and 2.5 mg/L are effective doses for the masculinization of tilapia using immersion method. The finding showed that treatment T8 (MT concentration of 2.0 mg/L and density of 750 fish/L) is the most appropriate concentration and stocking density in sex-reversal of the tilapia fry using immersion method.

The results of this experiment are consistent with the research results of tilapia sex-reversal using the MT immersion method of other authors. Wassermann & Afonso (2003) masculinized the 14 days post hatching (DPH) tilapia fry by MT immersion method with the rate of masculinization ranging from 86.0 to 91.6%; Male proportion (68.5 - 83.3%) was observed when Duong & Pham (2006) treated tilapia fry (15 - 17 DPH) with the MT immersion method. Le (2008) reported the higher sex reversal rate (88.89 - 98.89%) when exposing tilapia fry (13 - 15 DPH) to MT solution. The results of this study are also consistent with the results of sex-

Table 2. Sex ratio of *O. niloticus* in different 17 α-methyltestosterone immersion treatments and stocking density treatments

Treatment	Number of analyzed fish	Male (%)	Female (%)	Sex ratio male:female
Control	100	55.1a	44.9	1:0.81
T1	100	81.1b	18.9	1:0.23
T2	100	81.1b	18.9	1:0.23
T3	100	84.5b	15.5	1:0.18
T4	100	78.9b	21.1	1:0.27
T5	100	87.8bc	12.2	1:0.14
T6	100	80.0b	20.0	1:0.25
T7	100	90.0bc	10.0	1:0.11
T8	100	91.1c	8.9	1:0.10
T9	100	80.0b	20.0	1:0.25

Values (mean ± standard deviation of data for triplicate groups) with different superscripts in the same column are significantly different (one-way ANOVA and Tukey test, $P < 0.05$).

reversal studies using feeding method. Jensi et al. (2016) reported that the male populations (83.3 to 93.3%) were obtained when feed new hatching tilapia fry with feed containing MT at doses of 50, 60 and 100 mg/kg feed in 21 days. The results show that the masculinization rate in this study is slightly lower than that of male proportions of other studies. However, the optimal MT concentration in this study was 2.0 mg/L, which was 33.33% lower than the dose used by Wassermann & Afonso (2003) and 4.17 times lower than that used by Duong & Pham (2006). In addition, the optimal stocking density of this study was 750 fish/L, which was much higher than the stocking densities in Wassermann & Afonso (2003) and Le (2008) studies of 60 fish/L, and Karaket et al. (2023) study of 100 fish/L.

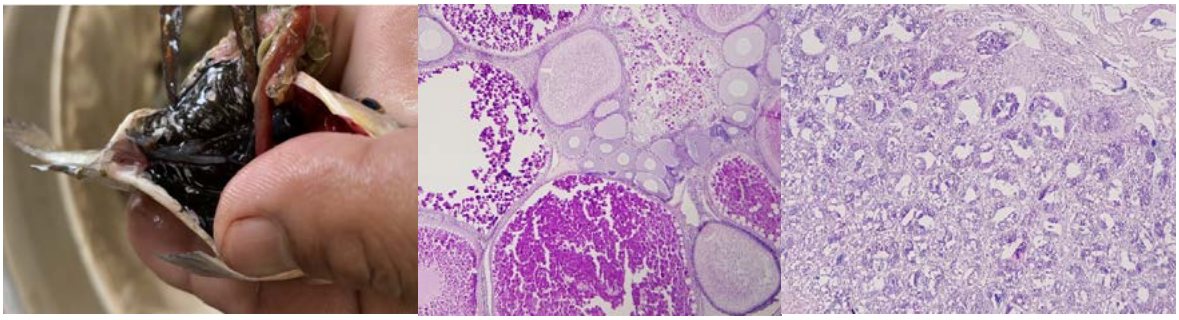

Figure 2. The observed gonad of male and female tilapia after 2 h of 17 α-methyltestosterone treatment. (A) Gonad removal (B) Eggs, and (C) Spermatozoa under light microscope.

Growth Performance

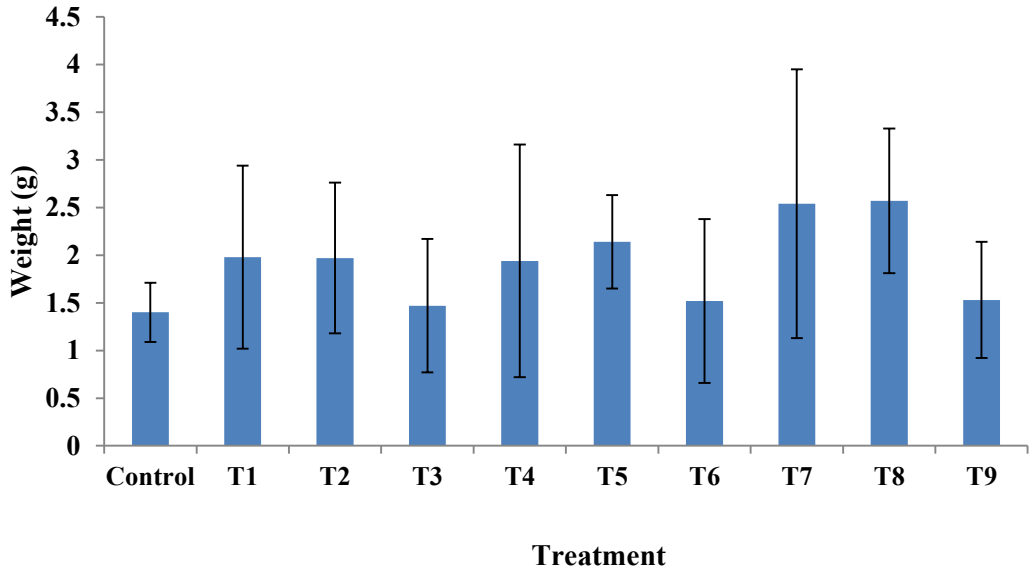

Figure 3. Effects of hormone sex-reversal on the weight of *O. niloticus*.

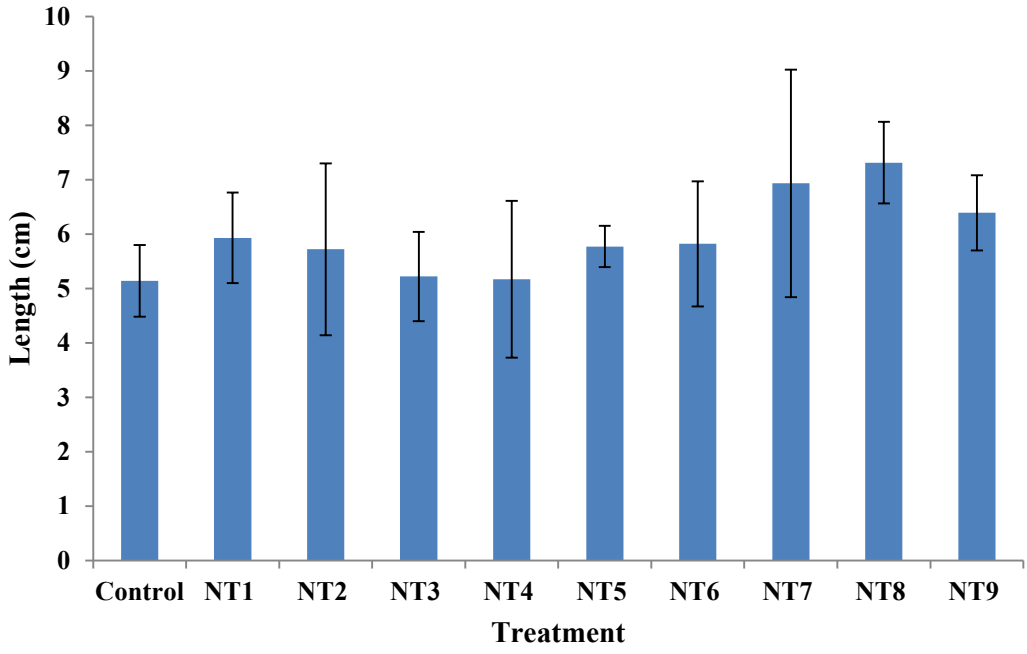

Figure 4. Effects of hormone sex-reversal on the length of *O. niloticus*.

Experimental results indicated that the average weight and total length of tested fish ranged from 1.40 to 2.57 g and from 5.14 to 7.13 cm, respectively (Figures 3 & 4). The mean weight and length of fish in the MT treatments were greater than that of the fish in the control treatment, although the difference was not statistically significant ($P > 0.05$). The results showed that the mean growth of experimental fish was not affected by hormonal masculinization over a period of 60 days after exposure to MT. In addition, the study results also showed that the average weight of experimental fish was directly proportional to the hormone concentration but inversely proportional to the stocking density.

4. Conclusions

According to the research findings, tilapia sex reversal using 17 α-methyltestosterone immersion method gives the same rate of masculinization as the feeding method, but the processing time is much shorter, only 2h compared to 21 days of oral administration method. The most effective 17 α-methyltestosterone concentration in tilapia sex-reversal of the immersion method is 2 mg/L and the most appropriate stocking density is 750 fish/L. In addition, the mean growth of experimental fish was not affected by hormonal masculinization over a period of 60 days after exposure to 17 α-methyltestosterone.

Conflict of interest

The authors have no conflicts of interest to declare.

Acknowledgements

This study was made with financial support from Nong Lam University (Ref. no. CS-SV22-TS-03) and from Department of Science and Technology, Binh Phuoc province.

References

Alam, M. S., Roy, A., Shathi, S. B., Deb, S., Alam, M. S., & Mondal, M. N. (2023). Dose optimization of 17 α-methyltestosterone to maximize sex reversal of Nile tilapia (*Oreochromis niloticus*). *Research in Agriculture Livestock and Fisheries* 9(3), 377-384.

Andersen, L., Holbech, H., Gessbo, A., Norrgren, L., & Petersen, G. I. (2003). Effects of exposure to 17alpha-ethinylestradiol during early development on sexual differentiation and induction of vitellogenin in zebrafish (*Danio rerio*). *Comparative Biochemistry and Physiology C Toxicology Pharmacology* 134(3), 365-374. https://doi.org/10.1016/s1532-0456(03)00006-1.

Duong, B. V., & Pham, T. A. (2006). *Study on the effects of temperature and age on sex change results of Oreochromis niloticus tilapia by soaking 17α-methyltestosterone hormone* (Unpublished master's thesis). Vietnam Academy of Agriculture, Ha Noi, Vietnam.

El-Saidy, D. M. S. D., & Gaber, M. M. A. (2005). Effect of dietary protein levels and feeding rates on growth performance, production traits and body composition of Nile tilapia, *Oreochromis niloticus* (L.) cultured in concrete tanks. *Aquaculture Research* 36(2), 163-171. https://doi.org/10.1111/j.1365-2109.2004.01201.x.

El-Zaeem, S. Y., & Salam, G. M. (2013). Production of genetically male tilapia through interspecific hybridization between oreochromis niloticus and *O. aureus*. *Iranian Journal of Fisheries Sciences* 12(4), 802-812. https://doi.org/20.1001.1.15622916.2013.12.4.8.7.

Guerrero III, R. D., & Shelton, W. (1974). An aceto-carmine squash method for sexing juvenile fishes. *The Progressive Fish-Culturist* 36(1). https://doi.org/10.1577/1548-8659(1974)36[56:AASMFS]2.0.CO;2.

Hossain, M. A., Sutradhar, L., Sarker, T. R., Saha, S., & Iqbal, M. M. (2022). Toxic effects of chlorpyrifos on the growth, hematology, and different organs histopathology of Nile tilapia, *Oreochromis niloticus*. *Saudi Journal of Biological Sciences* 29(7), 103316. https://doi.org/10.1016/j.sjbs.2022.103316.

Jensi, A., Marx, K. K., Rajkumar, M., Shakila, R. J., & Chidambaram, P. (2016). Effect of 17 α-methyl testosterone on sex reversal and growth of Nile tilapia (*Oreochromis niloticus* L., 1758). *Ecology, Environment and Conservation* 22(3), 1493-1498. http://eprints.cmfri.org.in/id/eprint/13846.

Karaket, T., Reungkhajorn, A., & Ponza, P. (2023). The optimum dose and period of 17 α-methyl testosterone immersion on masculinization of red tilapia (*Oreochromis* spp.). *Aquaculture and Fisheries* 8(2), 174-179. https://doi.org/10.1016/j.aaf.2021.09.001.

Karslı, Z. (2021). Effects of synthetic androgen (17α-methyltestosterone) and estrogen (17β-estradiol) on growth and skin coloration in emperor red cichlid, aulonocara nyassae (Actinopterygii: cichliformes: Cichlidae). *Acta Ichthyologica et Piscatoria* 51(4), 357-363. https://doi.org/10.3897/aiep.51.70223.

Le, T. N. (2008). *Evaluation of the masculinization efficiency of tilapia oreochromis niloticus Linnaeus by soaking in water mixed with 17 α methyltestosterone in Quang Nam* (Unpublished master's thesis). Nong Lam University, Ho Chi Minh City, Vietnam.

Lovshin, L. L. (1982). Tilapia hybridization. In Pullin, R. S. V., & Lowe McConnell, R. H. (Eds). *The biology and culture of Tilapias* (279-308). Manila, Philippines: ICLARM Conference Proceedings & International Center for Living Resources Management.

Mair, G. C., Abucay, J. S., Beardmore, J. A., & Skibinski, D. O. F. (1995). Growth performance

trials of genetically male tilapia (GMT) derived from YY-males in *Oreochromis niloticus* L.: On station comparisons with mixed sex and sex reversed male populations. *Aquaculture* 137(1-4), 313-323. https://doi.org/10.1016/0044-8486(95)01110-2.

Prabu, E., Rajagopalsamy, C. B. T., Ahilan, B., Jeevagan, I. J. M. A., & Renuhadevi, M. (2019). Tilapia-An excellence candidate species for world aquaculture: A review. *Annual Research & Review in Biology* 31(3), 1-14. https://doi.org/10.9734/arrb/2019/v31i330052.

Pruginin, Y., Rothbard, S., Wohlfarth, G., Halevy, A., Moav, R., & Hulata, G. (1975). All-male broods of *Tilapia nilotica* × *T. aurea hybrids*. *Aquaculture* 6(1), 11-21. https://doi.org/10.1016/0044-8486(75)90086-1.

Ridha, M. T. (2006). Comparative study of growth performance of three strains of Nile tilapia, *Oreochromis niloticus*, L. at two stocking densities. *Aquaculture Research* 37(2), 172-179. https://doi.org/10.1111/j.1365-2109.2005.01415.x.

Sultana, N., Khan, M. G. Q., Alam, M. S., & Hossain, M. A. R. (2020). Allelic segregation of sex-linked microsatellite markers in Nile tilapia (*Oreochromis niloticus*) and validation of inheritance in YY population. *Aquaculture Research* 51(5), 1923-1932. https://doi.org/10.1111/are.14543.

Varadaraj, K., & Pandian, T. J. (1987). Masculinization of oreochromis niloticus by administration of 17 α-methyl -5 and rosten 3β-diol through rearing water. *Current Science* 56, 412-413.

Wassermann, G. J., & Afonso, L. O. B. (2003). Sex reversal in Nile tilapia (*Oreochromis niloticus* Linnaeus) by androgen immersion. *Aquaculture Research* 34(1), 65-71. 65-71. https://doi.org/10.1046/j.1365-2109.2003.00795.x.

Sequencing *p72* gene of field strain of African swine fever virus (ASFV) in Vietnam and generation of enhanced immunogenic fusion protein G-p72 potentially expressed as a recombinant antigen in ASFV subunit vaccine

Mai N. Tran[1], Hoang M. Nguyen[1], Loc T. Le[1], Hue T. Doan[1], Mi M. T. Nguyen[1], Binh T. Nguyen[2], & Phat X. Dinh[1*]

[1]Faculty of Biological Sciences, Nong Lam University, Ho Chi Minh City, Vietnam

[2]Biotechnology Center of Ho Chi Minh City, Ho Chi Minh City, Vietnam

ARTICLE INFO

Research Paper

Received: May 30, 2023
Revised: June 06, 2023
Accepted: June 17, 2023

Keywords

Gene fusion
G-VSV
Protein expression
p72-ASFV

***Corresponding author**

Dinh Xuan Phat
Email:
dinhxuanphat@hcmuaf.edu.vn

ABSTRACT

Protein *p72* is the major surface protein of African swine fever virus (ASFV), which is immunogenic and can prime the host to elicit a protective immune response, while G protein is the surface glycoprotein of vesicular stomatitis virus (VSV), which is well-known to be a strong antigen to stimulate an effective humoral immunity. The aim of this study was to sequence full-length *p72* gene of a field strain of ASFV causing typical ASF in Dong Nai province in 2020 and fuse this *p72* gene with VSV *G* gene to generate a recombinant fusion gene G-p72 that could simultaneously express both proteins and stimulate a better host immune response than *p72* expression alone. The sequence of the gene showed 99.59% nucleotide sequence similarity to an ASFV isolate from China. The PCR was employed to produce the recombinant G-p72 gene, which was cloned into plasmid pET28a, followed by transformation into *E. coli* BL21 (DE3) for protein expression. The G-p72 expression was induced at 37°C and 28°C for 6 and 16 h, respectively. The expression showed that G-p72 was observed at 28°C for 16 h. In summary, the full length *p72* gene of a field strain of ASFV was successfully sequenced and expressed as the recombinant G-p72 protein in *E. coli* BL21 (DE3). The expression level of the G-p72 fusion should be optimized and the immunogenicity of the recombinant protein should be examined in futher studies.

Cited as: Tran, M. N., Nguyen, H. M., Le, L. T., Doan, H. T., Nguyen, M. M. T., Nguyen, B. T., & Dinh, P. X. (2023). Sequencing *p72* gene of field strain of African swine fever virus (ASFV) in Vietnam and generation of enhanced immunogenic fusion protein G-p72 potentially expressed as a recombinant antigen in ASFV subunit vaccine. *The Journal of Agriculture and Development* 22(6), 32-41.

1. Introduction

African swine fever (ASF) is a lethal viral disease of swine that leads to a very high mortality in domestic and wild pigs. ASF cases were first recorded in Kenya in 1921 and then spread to some sub-Saharan African countries, Central and Eastern Europe, and Asia which were causing significant damage in global economic losses (Costard et al., 2009; Urbano & Ferreira, 2020). In Vietnam, the ASF outbreak started in February 2019 (Nguyen et al., 2022). There have been many efforts to develop vaccines against this disease so far. Unfortunately, the current vaccines have not been successful (Ramirez-Medina et al., 2022). Presently, early detection and depopulation of pig farms are the primary methods for decreasing the virus' spread.

The ASF is caused by the African swine fever virus (ASFV), a large-double strand DNA virus genome is 170-190 kbp in length and also the only member of the Asfarviridae family, genus Asfivirus (Alonso et al., 2018; Miao et al., 2023). The most important structural element of the virion is the protein *p72*, which is the primary capsid protein and accounts for approximately 31 - 33% of the total mass of the virion (Alonso et al., 2018; Revilla et al., 2018; Miao et al., 2023). The protein *p72* is considered to be the primary and highly immunogenic antigen in infected pigs (Kollnberger et al., 2002; Miao et al., 2023). Additionally, studies using monoclonal antibodies demonstrated that *p72* contains a variety of neutralizing epitopes that could be utilized to develop vaccines or other control strategies against virulent ASFV isolates (Yin et al., 2022; Miao et al., 2023).

Vesicular stomatitis virus (VSV) belongs to the Vesiculovirus genus of the family Rhabdoviridae and order of Mononegavirales, and is a zoonotic pathogen (Liu et al., 2021). This virus is an unsegmented, negative-stranded RNA virus, 180 nm long and 65 nm wide, with a single-stranded approximately 11 kb in size (Rozo-Lopez et al., 2018; Velazquez-Salinas et al., 2020). The VSV genome encoded five structural proteins: nucleoprotein (N), phosphoprotein (P), matrix protein (M), large protein polymerase (L), and glycoprotein (G). These proteins were structural protein and constituted the bullet-shaped virions of the rhabdovirus (Liu et al., 2021). Glycoprotein G was the first component of the virus to attach to the host cells and was the major immunogen of VSV. Multiple research demonstrated that the recombinant G protein effectively stimulated immune responses (Falkensammer et al., 2009; Brakel et al., 2022). Additionally, Cobleigh et al. (2010) demonstrated that VSV virus vector was able to induce strong protective cell-mediated and humoral responses. Nowadays, the applications of G glycoprotein from VSV are diverse. It could be used for the creation of prosthetic vesicles that transport several therapeutic agents, such as antibodies and DNA directly into cells, as well as being used for anti-cancer treatments (Scher & Schnell, 2020). As a foreign protein in various constructs of recombinant antigens for vaccine development, VSV G has been successfully applied for a number of pathogens including Influenza virus, Hepatitis B virus (HBV), Ebola virus, Hepatitis C virus, etc. (Ezelle et al., 2002; Schwartz et al., 2007; Crozier et al., 2022). Our long-term research was to examine the potential of producing a recombinant antigen that could effectively trigger an immune response against ASFV. In this initial study, we focused on sequencing the entire *p72* gene from an ASFV field strain and fusing this *p72* gene with VSV *G* gene to create a recombinant gene that could express ASFV-*p72* and VSV-G proteins together in one frame. The successfully expressed recombinant protein G-p72 was expected to have

better immunogenicity and could be applied in vaccine development against ASFV compared to *p72* expression alone.

2. Materials and methods

2.1. Sequences of ASFV-p72 and VSV-G

For sequences of ASFV-*p72*, the positive blood samples for ASFV were collected from a field sample of infected ASFV in Dong Nai province in 2020 and confirmed by Realtime PCR. WizPrepTM Viral DNA/RNA Mini Kit was used to collect the pathogen's viral DNA. The *p72* gene of the ASFV was intended to be amplified with a product size of 1,941 bp using the primers GAAGTGCCTTTTGTACTTAGCCTTT-3', Tm = 61.61°C" and p72-R primer TTACTTTCCAAGTCGGTTCATCTCTATG-3', Tm = 61.05°C". This amplicon was sequenced and used for subsequent works. The sequences of VSV-*G* gene used for PCR amplification was obtained from a plasmid containing full-length genome of a wild type VSV Indiana strain which was published previously (Dinh et al., 2012).

2.2. Primers for PCR

The specific primers were designed for fusion of the two genes. The primer sequences of ASFV *p72* gene and VSV *G* gene were based on reference sequences MN793051.1 and J02428.1, respectively (Figure 1). EcoRI and NotI were added for cloning purpose (underlined) and the stop codon of VSV-*G* gene was removed (Table 1).

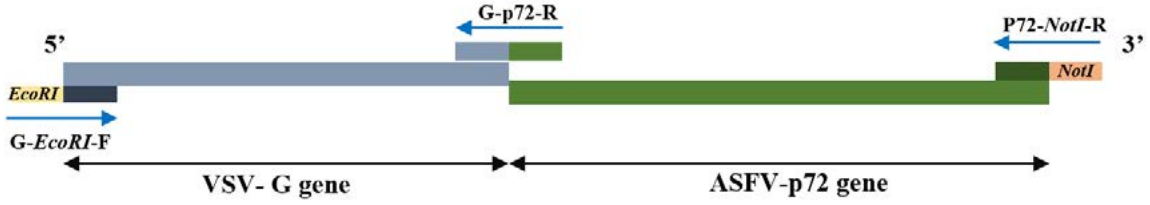

Figure 1. Diagram of designed primers to fuse VSV-*G* gene and ASFV-*p72* gene.

Table 1. Primers were used for PCR

Primer's name	Sequence 5' --> 3'	Tm
G-EcoRI-F	atatatGAATTCATGAAGTGCCTTTTGTACTTAGCCTTT	61.61
G-p72-R	CAAAAAGCTCCTCCTGATGCCATCTTTCCAAGTCG-GTTCATCTCTATGT	61.44
P72-NotI-R	atatatGCGGCCGCTTAGGTACTGTAACGCAGCACAG	60.61

2.3. PCR condition

In order to fuse the two genes, the PCR was performed in two steps. The PCR-1 using G-EcoRI-F and G-p72-R amplified *G*-gene of VSV. In PCR-2, the products in PCR-1 were used as the forward primer, in combination with p72-NotI-R primer as the reverse primer to amplify the *p72* gene. As a result, VSV-G and ASFV- *p72* gene were linked together in one open reading frame with EcoRI and NotI restriction sites at 5' and 3' ends of the fused gene, respectively.

The PCRs were performed with 10 µL of DreamTaq Mastermix 2X (Cat# K1081, ThermoFisher), 1 µL of each primer pair (with the initial concentration of primers being 10 µM), 1 µL template, and DEPC (Cat# K1081, ThermoFisher) - treated water was added to a total volume of 20 µL. The PCR conditions for both two-steps were established with initial denaturation at 96°C for 4 min and followed by 35 cycles with denaturation at 96°C for 1 min, annealing at 60°C for 60 sec, and extension at 72°C for 2 min, and final extension at 72°C for 7 min. After that, the amplicons were analyzed by electrophoresis in a 1% (w/v) agarose gel in 0.5X Tris-Acetate-EDTA (TAE) (Cat#B49, ThermoFisher) containing Midori Green Advance DNA stain (Cat#MG04, Nippon Genetics). The DNA marker 1Kb plus (Cat#10787018, Invitrogen) was included in each DNA gel electrophoresis to indicate the PCR product size and analyzed for experiments under UV light.

2.4. Cloning and transformation

After electrophoresis, the fused gene G-p72 was recovered from low-temperature agarose gel following manufacturer's procedure of WizPrep™ Viral DNA/RNA Mini Kit (V2) (Cat#NAPK059388WIZ, Wizbio solutions, Korea). The recovered fused gene was then inserted vector pET28a (Novagen, Germany). The successful insertion was examined by PCR using primers binding to T7 promoter and T7 terminator flanking the inserted gene. The pET28a containing the G-p72 gene was then transformed into *E. coli* DH10β-capable cells (NEB, England) by heat shock method. The transformed *E. coli* DH10β cells were spread onto LB agar plates at 37°C containing 50 ng/mL kanamycin, then incubated for 16 - 18 h at 37°C. Plasmid DNA from transformed cells was purified using GeneJET Plasmid Miniprep Kit (Cat#K0503, Thermo Scientific) according to the manufacturer's protocol. The plasmid DNA constructs were sequenced to reconfirm the fidelity of the fused G-p72 gene. The sequence data were analyzed by Bioedit (version 7.2), MEGA software (version 11), and BLAST tools before gene expression experiments.

2.5. Recombinant protein expression

In the next step, the purified plasmid pET28a containing the G-p72 gene was transformed into *E. coli* BL21 (DE3) cells by heat shock method. The pure selected colony was grown in LB broth medium until the OD reached 0.6 - 0.8. Then, 0.4 mM IPTG (Cat#15529019) was added for inducing protein expression. The expression experiments were carried out at two conditions: 37°C for 6 h and 28°C for 16 h. *E. coli* BL21 containing empty vector of pET28a was used as the negative control. The recombinant protein expression was analyzed by 12.5% SDS-PAGE gel containing Coomassie Brilliant Blue G-250 staining (Cat#20279, Thermo Scientific).

3. Results

3.1. PCR generating G-p72 gene

The amplicon of 1,981 bp (including 1,941 bp of *p72* gene together with restriction sites

and extra nucleotide designed for cloning) was successfully amplified (Figure 2A) and the nucleotide sequence was determined via Sanger sequencing method. Alignment of the sequencing result of the *p72* gene shared 99.59% and 98.7% identity of nucleotide and amino acid sequence compared to the the Chinese reference strain (MN793051.1) and it belonged to genotype II of ASFV. Similarly, the *G* gene of VSV was also amplified successfully from DNA plasmid to produce a product of 1,568 bp (Figure 2B).

To generate fused gene *G-p72* encoding two proteins (*G* and *p72*) simultaneously, primers G-EcoRI-F and G-p72-R were used in PCR-1 to amplify *G* gene, followed by PCR-2 using the product of PCR-1 as forward primer together with *P72-NotI-R* as reverse primer. The product of the fusion *G-p72* gene was 3,481 bp in size (Figure 2C).

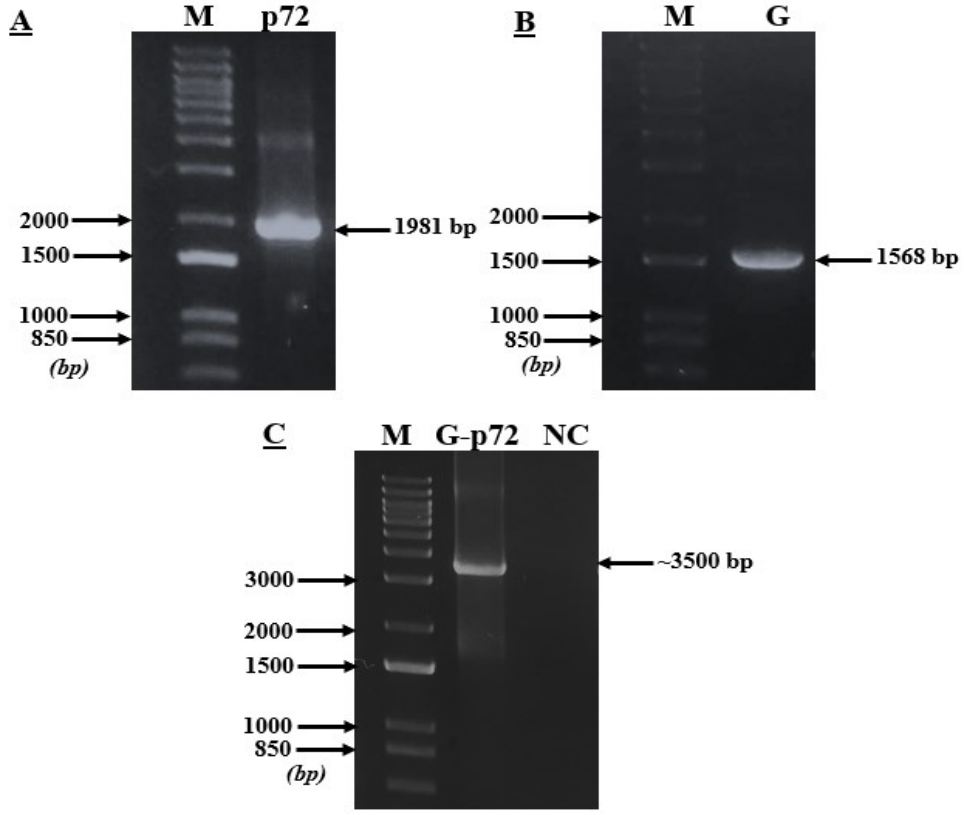

Figure 2. PCR amplification. Lane M: DNA ladder 1Kb plus; (A). *p72* gene of African swine fever virus; (B). G gene of vesicular stomatitis virus; (C). Fused product of *G-p72* gene. NC: Negative control with pure water.

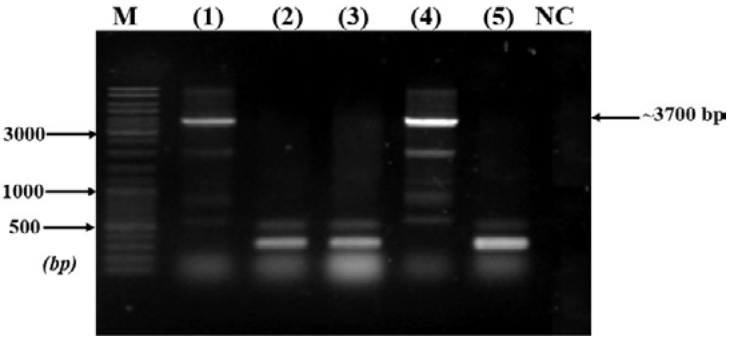

Figure 3. Colony-PCR results of colonies with primer pair T7: Lane M: DNA ladder 1Kb plus; Lane 1-5: Pure white colonies; Lane (NC) Negative control with pure water.

3.2. Expression of the recombinant protein G-p72

The PCR product of G-p72 was purified, inserted in plasmid pET28a, and transformed into *E. coli* DH10β. The *E. coli* cells that received the plasmid were selected by white-blue system. The pure white colonies were collected and examined by PCR using primers specific for T7 promoter and T7 terminator in pET28a plasmid, with the amplicon of approximately 3,700 bp to determine the successfully transformed colonies (Figure 3). The fusion gene G-p72 in the plasmid pET28a was successfully sequenced to reconfirm the nucleotide fidety and the correct direction of the inserted gene compared to the promoter direction in the pET28a which is critical for successful expression (Figure 4).

The recombinant pET28a containing G-p72 was transformed into BL21 (DE3) for evaluating the protein expression under two conditions: 37°C for 6 h and 28°C for 16 h. The results showed that the G-p72 protein (130 kDa) was detected at 28°C for 16 h (Figure 4). Further experiments should be done to improve the expression level of recombinant G-p72 protein from *E. coli* BL21 and the expressed protein should be confirmed specifically by Western blotting.

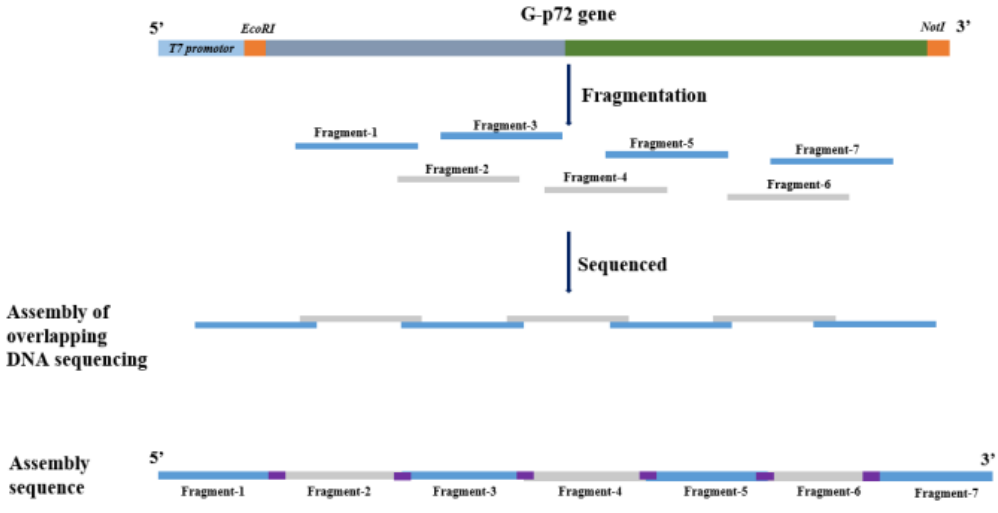

Figure 4. Principle for sequencing G-p72 gene.

4. Discussions

African swine fever (ASF) is a viral disease with a high fatality in domestic pigs and wild boars. The ASF has greatly challenged pig-raising countries and negatively impacted the regional and national trade of pork products. The development of safe and effective ASF vaccines is urgently required for the control of ASF outbreaks. So far, the viral surface protein *p72* is known to be responsible for membrane fusion and viral entry as well as being the primary target for a protective immune response. Therefore, in order to create a possibly better immunogen, we combined the G gene from VSV with the *p72* gene from ASFV, expressed the recombinant protein, and utilized it as an antigen for a subunit vaccination against ASFV.

Nowadays, developing vaccines against ASFV is urgently necessary and thus different types of vaccines have been evaluated including live-attenuated vaccines, subunit vaccines, and DNA vaccines. Live attenuated vaccines harbor some limitations such as safety concerns and side effects in the vaccinated animals (Revilla et al., 2018). Besides, Blome et al. (2014) demonstrated that inactivated ASFV did not provide the protective ability, even when various adjuvants were used. The subunit vaccines have been considered as alternative ways to set the light to vaccine development for ASFV. Andrés et al. (2001) demonstrated the possible combination of pE120R and *p72* which could be incorporated into the virus particle when expressed in cells. The viral proteins p30, p54, p72, A104R, B602L, NP419L, and K205R have also been studied regarding their immunogenicity and vaccine application. Neutralizing epitopes found inside p72, p54, and p30 have been reported and designed for the development of ASFV vaccines and diagnostic techniques (Gaudreault & Richt, 2019; Cadenas-Fernández et al., 2020; Goatley et al., 2020).

Previously, Cobleigh et al. (2010) showed that using VSV was as a vector vaccine, it could induce strong protective T cell and antibody responses. Attenuated VSV vector or VSV G protein were widely applied in vaccine research (Chattopadhyay et al., 2013; van den Pol et al., 2017; Crozier et al., 2022). With the aim of developing a subunit vaccine that could mount a better immunity against field strain of ASFV, full-length *p72* gene from a virulent ASFV infected pig was isolated and used to design a contruct that could express *p72* protein of ASFV together with G protein of VSV in a monocistronic mRNA in hope that G protein of VSV could serve as a natural adjuvant to stimulate a bettern immune response compared to expression of *p72* protein alone. Eventually, the G-p72 coding gene was sucessfully constructed and expressed the recombinant protein from *E. coli* BL21 (DE3) at 28°C for 16 h. The expressive condition was consistent to the report by Sidoruk et al. (2011) in which the 1 kb gene was expressed well at 28°C compared to 37°C after 17 h.

5. Conclusions

In summary, the full-length *p72* gene of a field strain of ASFV circulating in Vietnam was sucessfully sequenced and generated G-p72 fusion gene that was carried by pET28a plasmid in *E. coli* BL21 (DE3). The G-p72 was expressed at 28°C for 16 h. Further research should be done to increase expression level and examine the potential use of the fused protein G-p72 as an immunogenic antigen.

Conflict of interest

The authors have no conflicts of interest to declare.

Acknowledgements

The authors would like to thank Nong Lam University Ho Chi Minh City for funding this study under the project CS-SV22-KHSH-01.

References

Alonso, C., Borca, M., Dixon, L., Revilla, Y., Rodriguez, F., Escribano, J. M., & ICTV Report Consortium. (2018). ICTV virus taxonomy profile: Asfarviridae. *Journal of General Virology* 99(5), 613-614. https://doi.org/10.1099/jgv.0.001049.

Andrés, G., García-Escudero, R., Viñuela, E., Salas, M. L., & Rodríguez, J. M. (2001). African swine fever virus structural protein pE120R is essential for virus transport from assembly sites to plasma membrane but not for infectivity. *Journal of Virology* 75(15), 6758-6768. https://doi.org/10.1128/jvi.75.15.6758-6768.2001.

Blome, S., Gabriel, C., & Beer, M. (2014). Modern adjuvants do not enhance the efficacy of an inactivated African swine fever virus vaccine preparation. *Vaccine* 32(31), 3879-3882. https://doi.org/10.1016/j.vaccine.2014.05.051.

Brakel, K. A., Ma, Y., Binjawadagi, R., Harder, O., Watts, M., Li, J., Binjawadagi, B., & Niewiesk, S. (2022). Codon-optimization of the respiratory syncytial virus (RSV) G protein expressed in a vesicular stomatitis virus (VSV) vector improves immune responses in a cotton rat model. *Virology* 575, 101-110. https://doi.org/10.1016/j.virol.2022.08.017.

Cadenas-Fernández, E., Sánchez-Vizcaíno, J. M., Kosowska, A., Rivera, B., Mayoral-Alegre, F., Rodríguez-Bertos, A., Yao, J., Bray, J. B., Lokhandwala, S., Mwangi, W., & Barasona, J. A. (2020). Adenovirus-vectored African swine fever virus antigens cocktail is not protective against virulent Arm07 isolate in Eurasian wild boar. *Pathogens* 9(3), 171. https://doi.org/10.3390/pathogens9030171.

Chattopadhyay, A., Wang, E., Seymour, R., Weaver, S. C., & Rose, J. K. (2013). A chimeric vesiculo/alphavirus is an effective alphavirus vaccine. *Journal of Virology* 87(1), 395-402. https://doi.org/10.1128/jvi.01860-12.

Cobleigh, M. A., Buonocore, L., Uprichard, S. L., Rose, J. K., & Robek, M. D. (2010). A vesicular stomatitis virus-based hepatitis B virus vaccine vector provides protection against challenge in a single dose. *Journal of Virology* 84(15), 7513-7522. https://doi.org/10.1128/jvi.00200-10.

Costard, S., Wieland, B., De Glanville, W., Jori, F., Rowlands, R., Vosloo, W., Roger, F., Rfeiffer, D. U., & Dixon, L. K. (2009). African swine fever: how can global spread be prevented?. *Philosophical Transactions of the Royal Society B: Biological Sciences* 364(1530), 2683-2696. https://doi.org/10.1098/rstb.2009.0098.

Crozier, I., Britson, K. A., Wolfe, D. N., Klena, J. D., Hensley, L. E., Lee, J. S., Wolfraim, L. A., Taylor, K. L. Higgs, E. S., Montgomery, J. M., & Martins, K. A. (2022). The evolution of medical countermeasures for Ebola virus disease: lessons learned and next steps. *Vaccines* 10(8), 1213.

Dinh, P. X., Panda, D., Das, P. B., Das, S. C., Das, A., & Pattnaik, A. K. (2012). A single amino acid change resulting in loss of fluorescence of eGFP in a viral fusion protein confers fitness and growth advantage to the recombinant vesicular stomatitis virus. *Virology* 432(2), 460-469. https://doi.org/10.1016/j.virol.2012.07.004.

Ezelle, H. J., Markovic, D., & Barber, G. N. (2002). Generation of hepatitis C virus-like particles by use of a recombinant vesicular stomatitis virus vector. *Journal of Virology* 76(23), 12325-12334. https://doi.org/10.1128/JVI.76.23.12325-12334.2002.

Falkensammer, B., Rubner, B., Hiltgartner, A., Wilflingseder, D., Hennig, C. S., Kuate, S., Überla, K., Norley, S., Strasak, A., & Stoiber, H. (2009). Role of complement and antibodies in controlling infection with pathogenic simian immunodeficiency virus (SIV) in macaques vaccinated with replication-deficient viral vectors. *Retrovirology* 6, 1-12. https://doi.org/10.1186/1742-4690-6-60.

Gaudreault, N. N., & Richt, J. A. (2019). Subunit vaccine approaches for African swine fever virus. *Vaccines* 7(2), 56. https://doi.org/10.3390/vaccines7020056.

Goatley, L. C., Reis, A. L., Portugal, R., Goldswain, H., Shimmon, G. L., Hargreaves, Z., Ho, C., Montoya, M., Sánchez-Cordón, P. J., Taylor, G., Dixon, L. K., & Netherton, C. L. (2020). A pool of eight virally vectored African swine fever antigens protect pigs against fatal disease. *Vaccines* 8(2) 234. https://doi.org/10.3390/vaccines8020234.

Kollnberger, S. D., Gutierrez-Castañeda, B., Foster-Cuevas, M., Corteyn, A., & Parkhouse, R. M. E. (2002). Identification of the principal serological immunodeterminants of African swine fever virus by screening a virus cDNA library with antibody. *Journal of General Virology* 83(6), 1331-1342. https://doi.org/10.1099/0022-1317-83-6-1331.

Liu, G., Cao, W., Salawudeen, A., Zhu, W., Emeterio, K., Safronetz, D., & Banadyga, L. (2021). Vesicular stomatitis virus: from agricultural pathogen to vaccine vector. *Pathogens* 10(9), 1092. https://doi.org/10.3390/pathogens10091092.

Miao, C., Yang, S., Shao, J., Zhou, G., Ma, Y., Wen, S., Hou, Z., Peng, D., Guo, H., Liu, Wei., & Chang, H. (2023). Identification of *p72* epitopes of African swine fever virus and preliminary application. *Frontiers in Microbiology* 14, 1126794. https://doi.org/10.3389/fmicb.2023.1126794.

Nguyen, V. T., Cho, K. H., Mai, N. T. A., Park, J. Y., Trinh, T. B. N., Jang, M. K., Nguyen, T. T. H., Vu, X. D., Nguyen, V. D.., Ambagala, A., Kim, Y., & Le, V. P. (2022). Multiple variants of African swine fever virus circulating in Vietnam. *Archives of Virology* 167(4), 1137-1140. https://doi.org/10.1007/s00705-022-05363-4.

Ramirez-Medina, E., Vuono, E., Silva, E., Rai, A., Valladares, A., Pruitt, S., Espinoza, N., Velazquez-Salinas, L., Borca, M., Gladue, D. P., Borca, M. V., & Gladue, D. P. (2022). Evaluation of the deletion of MGF110-5L-6L on swine virulence from the pandemic strain of African swine fever virus and use as a DIVA marker in vaccine candidate ASFV-G-ΔI177L. *Journal of Virology* 96(14), e00597-22. https://doi.org/10.1128/jvi.00597-22.

Revilla, Y., Pérez-Núñez, D., & Richt, J. A. (2018). African swine fever virus biology and vaccine approaches. *Advances in Virus Research* 100, 41-74. https://doi.org/10.1016/bs.aivir.2017.10.002.

Rozo-Lopez, P., Drolet, B. S., & Londoño-Renteria, B. (2018). Vesicular stomatitis virus transmission: a comparison of incriminated vectors. *Insects* 9(4). 190. https://doi.org/10.3390/insects9040190.

Scher, G., & Schnell, M. J. (2020). Rhabdoviruses as vectors for vaccines and therapeutics. *Current Opinion in Virology* 44, 169-182. https://doi.org/10.1016/j.coviro.2020.09.003.

Schwartz, J. A., Buonocore, L., Roberts, A., Suguitan Jr, A., Kobasa, D., Kobinger, G., Feldmann, H., Subbarao, K., & Rose, J. K. (2007). Vesicular stomatitis virus vectors expressing avian influenza H5 HA induce cross-neutralizing antibodies and long-term protection. *Virology* 366(1), 166-173. https://doi.org/10.1016/j.virol.2007.04.021.

Sidoruk, K. V., Pokrovsky, V. S., Borisova, A. A., Omeljanuk, N. M., Aleksandrova, S. S., Pokrovskaya, M. V., Gladilina, J. A., Bogush,

V. G., & Sokolov, N. N. (2011). Creation of a producent, optimization of expression, and purification of recombinant Yersinia pseudotuberculosis L-asparaginase. *Bulletin of Experimental Biology and Medicine* 152, 219-223. https://doi.org/10.1007/s10517-011-1493-7.

Urbano, A. C., & Ferreira, F. (2020). Role of the DNA-binding protein pA104R in ASFV genome packaging and as a novel target for vaccine and drug development. *Vaccines* 8(4), 585. https://doi.org/10.3390/vaccines8040585.

van den Pol, A. N., Mao, G., Chattopadhyay, A., Rose, J. K., & Davis, J. N. (2017). Chikungunya, influenza, Nipah, and Semliki Forest chimeric viruses with vesicular stomatitis virus: actions in the brain. *Journal of Virology* 91(6), 10-1128. https://doi.org/10.1128/jvi.02154-16.

Velazquez-Salinas, L., Pauszek, S. J., Holinka, L. G., Gladue, D. P., Rekant, S. I., Bishop, E. A., Stenfeldt, C., Verdugo-Rodriguez,. A., Borca, M. V., Arzt, J., & Rodriguez, L. L. (2020). A single amino acid substitution in the matrix protein (M51R) of vesicular stomatitis New Jersey virus impairs replication in cultured porcine macrophages and results in significant attenuation in pigs. *Frontiers in Microbiology* 11, 1123. https://doi.org/10.3389/fmicb.2020.01123.

Yin, D., Geng, R., Shao, H., Ye, J., Qian, K., Chen, H., & Qin, A. (2022). Identification of novel linear epitopes in *p72* protein of African swine fever virus recognized by monoclonal antibodies. *Frontiers in Microbiology* 13, 1055820. https://doi.org/10.3389/fmicb.2022.1055820.

Prevalence of dermatophytosis and *Malassezia* infection in dogs and cats in Thonglor Bangkok Pet Hospital in Ho Chi Minh City, Vietnam

Trung T. Nguyen[1], Khanh N. Dinh[2], & Thuong T. Nguyen[1*]

[1]Faculty of Animal Science and Veterinary Medicine, Nong Lam University, Ho Chi Minh City, Vietnam

[2]Nong Lam University Veterinary Hospital, Ho Chi Minh City, Vietnam

ARTICLE INFO

Research Paper

Received: September 04, 2023

Revised: September 25, 2023

Accepted: October 03, 2023

Keywords

ATI methods

Dermatitis

Dermatophytosis

Malassezia

***Corresponding author**

Nguyen Thi Thuong

Email:

thuong.nguyenthi@hcmuaf.edu.vn

ABSTRACT

Malassezia yeasts are occasional human and animal skin organisms that commensally act as pathogens, while dermatophytes are common fungi in many clinics and hospitals. The aim of this study was to evaluate the prevalence of dermatophytosis and *Malassezia* infections in dogs and cats, and the effect of treatments. The study was carried out from December 2022 to May 2023 in Thonglor Bangkok Pet Hospital, Ho Chi Minh City, Vietnam. Total 208 cases visited the hospital, in which 32 cases of otitis and 53 dermatitis were recorded. Sterile cotton swabs were used to collect the aural samples from 32 cases, then observed under the microscope to detect the presence and population of *Malassezia* yeasts. In 53 dermatitis cases, adhesive tape impressions (ATI) methods and fungal culture were used to identify the species of dermatophytes and *Malassezia* dermatitis. The results showed that *Malassezia* was isolated from 24 cases, including 23 *Malassezia otitis* and 1 *Malassezia* dermatitis. However, there was only one positive case with dermatophyte by two methods. Therefore, dermatophytosis could not be concluded due to the small number of positive cases. Meanwhile, *Malassezia* infection occurred mainly in dogs rather than cats at every age, and the infected rates were found more in exotic animals than in domestic animals and usually in males than females. The effect of treatments illustrated the significant improvement in *Malassezia* otitis by using Epiotic solution combined with Oridemyl ear drop. Moreover, great improvement was evident in dermatophytosis therapy with Itraconazole.

Cited as: Nguyen, T. T., Dinh, K. N., & Nguyen, T. T. (2023). Prevalence of dermatophytosis and *Malassezia* infection in dogs and cats in Thonglor Bangkok Pet Hospital in Ho Chi Minh City, Vietnam. *The Journal of Agriculture and Development* 22(6), 42-54.

I. Introduction

Malassezia yeasts had been known common commensal organisms on the skin of humans and animals that could be secondary infections under various influences of predisposing factors (Cafarchia et al., 2005). In comparison, dermatophyte was a pathogenic keratinolytic fungus in animals and humans. The common *Malassezia* in companion animals was *Malassezia pachydermatitis*, and the common dermatophyte species were *Microsporum* and *Trichophyton* spp. (Begum & Kumar, 2021). Both diseases were recorded as highly risks of skin diseases in dogs and cats, which were commonly found in veterinary clinic. The diseases gradually became a special attention in public health, particularly in dogs and cats. Various diagnostic methods could be used in *Malassezia* infection and dermatophytosis, including cytological examination and fungal culture, such as cotton swab methods, adhesive tape impressions (ATI), and dermatophyte test medium (DTM) culture (Bouza-Rapti et al., 2023). *Malassezia* otitis could be detected through cotton swab methods and microscopic examination. While dermatophytosis could be suspected through different methods, such as Wood's lamp, ATI, and DTM culture (Moriello, 2019). Topical treatment, including Epiotic cleanser and Oridermyl ear drop, could be applied for *Malassezia* otitis, while systemic therapy with Itraconazole was used for *Malassezia* dermatitis and dermatophytosis. Therefore, the objective of this study was to determine the prevalence of dermatophytosis and *Malassezia* infections in dogs and cats, and evaluate the effect of treatments.

2. Materials and Methods

2.1. Determination of *Malassezia* infection and dermatophytosis cases in Thonglor Bangkok Pet Hospital

2.1.1. Clinical examination

In total of 208 cases visited the Thonglor Bangkok Pet Hospital from December 2022 to May 2023, 85 cases including dermatitis and otitis externa were collected through clinical examination. In which, 32 cases were detected with otitis externa, and 53 cases were detected with different kinds of dermatitis through clinical examination. Otitis external cases were collected based on the changes in ear pinna, including alopecia, excoriation, crusting, erythema, and hyperpigmentation. Other signs can be observed in the external ear canal, consisting of hyperemia, ulceration, discharge, masses, and stenosis (Bajwa, 2019). Otherwise, dermatitis cases were collected according to general clinical signs, such as pruritis, alopecia, erythema, crust, hyperpigmentation, and many other dermatological lesions in various areas, including lip margins, axilla, groin, ventral neck, interdigital skin, facial or tail folds, and other signs.

2.1.2. Cytological examination

Malassezia dermatitis and *Malassezia* otitis could be detected by using skin cytological examinations, including sterile cotton swabs and adhesive tape impression (ATI). With *Malassezia* otitis, a sterile cotton swab was rolled on a clean slide and stained with Diff-Quik solution for microscopic examination. While ATI was applied for *Malassezia* dermatitis by using transparent tapes to collect samples at the skin lesions suspected of fungi infection (Sudipa et al., 2021). Afterward, the samples were stuck on the slides, stained with a few drops of Giemsa or Diff-Quik solution, and observed under the microscope. *Malassezia* spp. could be identified through microscopic examination with the characteristic of a round to oval or classical peanut form with monopolar budding (Sudipa et al., 2021). The

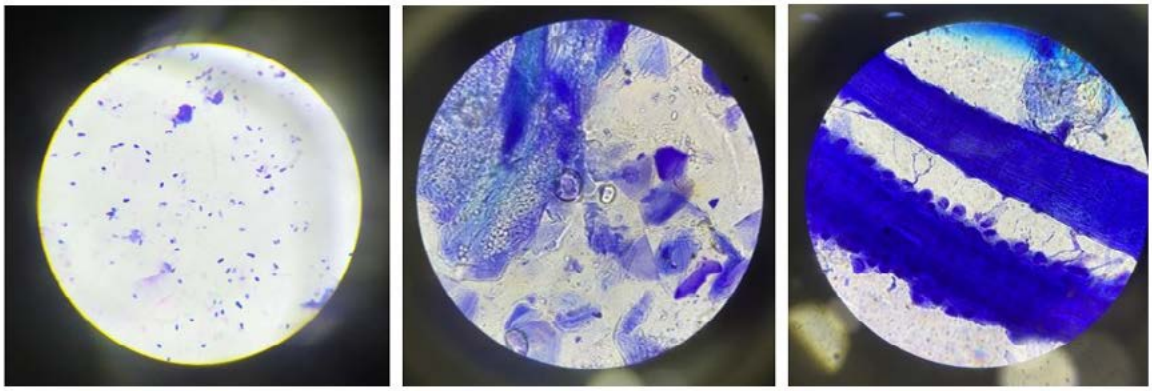

Figure 1. *Malassezia* and *Arthroconidia* were observed under the microscope.

result was identified to be positive if more than 5 *Malassezia* cells in one random field at 100x magnification; and the number of less than 2 *Malassezia* cells in one random field was detected in the negative result (Sudipa et al., 2021).

Dermatophytosis should be identified by rapid diagnostic tests for early treatment and prevention. At least two diagnostic tests were essential for dermatophyte detection, as no single test could be considered the "gold standard" (Bouza-Rapti et al., 2023). So the most common techniques used for dermatophyte identification were the hair plucking and fungal culture. And another method was ATI that was the valuable and sensitive diagnosis to detect dermatophytes in dogs and in cats with kerion for quick test (Bouza-Rapti et al., 2023). After collecting samples by impressing three times on the suspected lesions, then the slide was stained with a few drops of Giemsa or Blue Diff-Quik and observed under the microscope with 40x or 100x magnification to identify the presence of fungal hyphae, macroconidia, or arthrospores (Figure 1) (Begum & Kumar, 2021). Therefore, in Thonglor Bangkok Pet Hospital, both ATI technique and fungal culture have been applied to detect dermatophytosis in dogs and cats.

2.1.3. Fungal culture

The indirect examination for identification of dermatophytosis was fungal culture, which commonly used Sabouraud dextrose agar (SDA) or Dermatophyte test media (DTM) (Bouza-Rapti et al., 2023). The DTM was an innovative SDA adding cycloheximide, gentamycin, and chlortetracycline to prevent fungal and bacterial contamination (Kaufmann et al., 2016). At Thonglor Bangkok Pet Hospital, DTM was used to identify two species of dermatophytes *Microsporum* spp. and *Trichophyton* spp. The exact species needed to be re-check with microscopes for the positive or negative results. The medium should be kept at room temperature for 21 days, and the colony appearred within 7 - 10 days (Diren et al., 2019) within a 15-year period, in the city of Istanbul, Turkey. Dermatological specimens were collected from 1504 dogs and 846 cats, which were presented clinical signs of ringworm. Direct microscopy and mycological cultures were performed. The fungal growth rate was detected at 8.2% and 22.8% from dogs and cats, respectively. Microsporum canis was the most frequently isolated species followed by *Trichophyton* spp., *M. gypseum*, *T. mentagrophytes*, *M. nanum*, other *Microsporum*

spp. moreover *T. tonsurans*. The cats less than two-year age and more than ten-year age showed a statistically significant higher isolation rate of infection ($P < 0.05$). There were four main steps in DTM culture diagnosis: (1) inoculate plates by plucking infected hair onto the surface in four or five areas, the infected hair can be collected through the assessment of Wood's lamp; (2) incubate the plates at 25°C to 30°C and store them in plastic bags to avoid dehydration; (3) monitor daily and assess the growth once weekly for contamination, Microsporum, or Trichophyton development; and (4) count the colonies on the plate when the pathogen was identified (Moriello, 2019) (Figure 2). The color of the DTM agar was changed from yellow to red, and the white or buff color colony grew on the agar when the result was positive (Jarjees & Issa, 2022) (Figure 3). However, the green or grey colony developing on the surface of the agar and changing the color of DTM to red would be due to contamination from other factors.

After observing the DTM agar daily, the colony growed on the agar after 7 to 10 days. Specific species of dermatophytes were identified by re-checking under the microscope through ATI method to collect the samples (Figure 4).

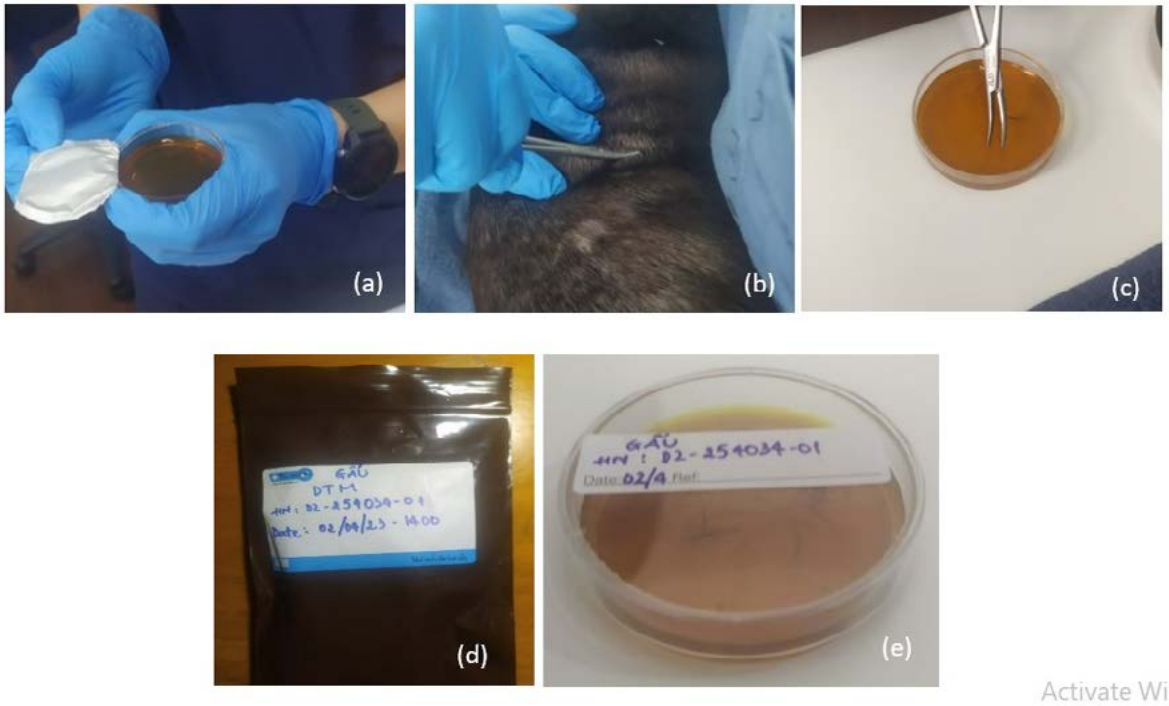

(a) DTM agar preparation, (b) Hair plucking, (c) Culture,
(d) Storage in dark plastic bag, (e) Observation from 7 to 10 days.

Figure 2. Procedure of Dermatophyte test media (DTM) culture.

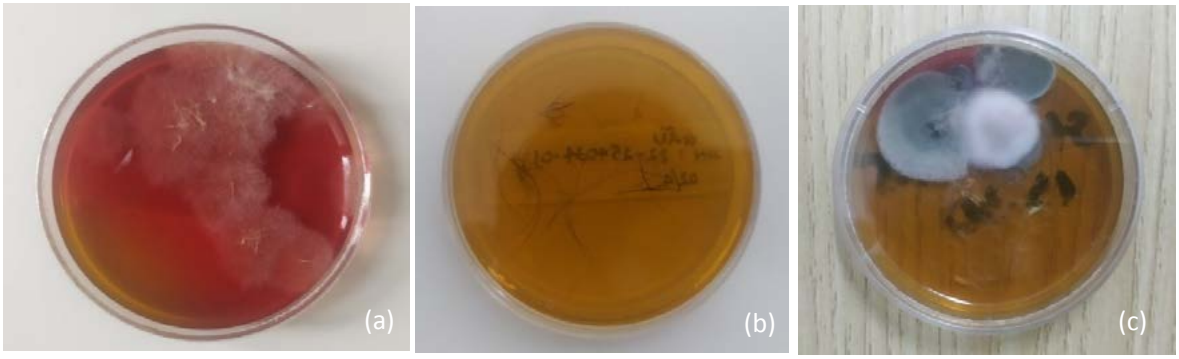

(a) Positive result: the agar will change from yellow to red color,
(b), (c) Negative result: no change or contaminated colony on the agar.
Figure 3. Results of Dermatophyte test media (DTM) agar after 7 - 10 days.

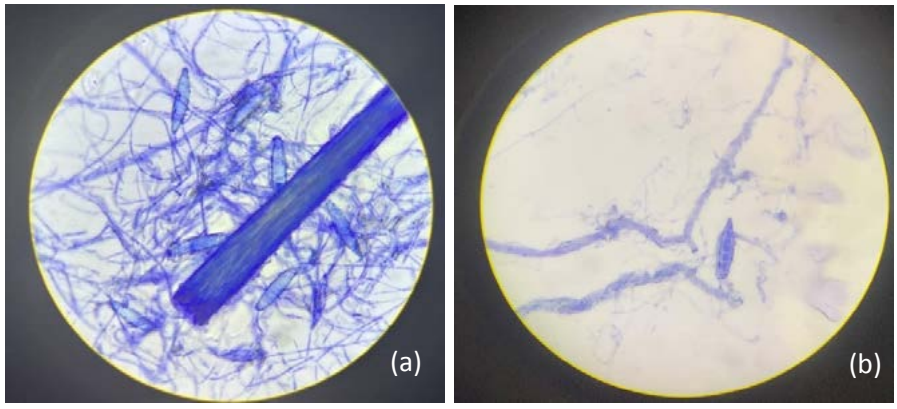

(a) *Microsporum Canis* in day 6th, (b) *Microsporum Canis* in day 10th
Figure 4. The morphology of dermatophytes identified under the microscope.

2.2. Predisposing factors of *Malassezia* infection and dermatophytosis between dogs and cats in groups of ages, breeds, and gender

After the evaluation of identification of *Malassezia* infection and dermatophytosis through clinical and subclinical examination, the data were analyzed the risk factors associated with the diseases, including types of animals, groups of ages, breeds, and gender. Dogs and cats were the primary animals that collected the information in the research. The ages of animals were divided into three groups, including groups of age under one year, from one to three years, and over three years. The age groups were divided due to the susceptibility of the immunity at different ages, with various predisposing factors easily affecting the hosts. The breeds of animals were analyzed based on two groups, including domestic and exotic groups, because some exotic breeds were considered to be more common with *Malassezia* infections (Sudipa et al., 2021) and dermatophytosis (Moriello et al., 2017). The differences between males and females in dogs and cats contribute to the influence of *Malassezia*

infection and dermatophytosis (Negre et al., 2009; Paryuni et al., 2020).

2.3. Effectiveness of treatment

All cases with *Malassezia* otitis, *Malassezia* dermatitis, and dermatophytosis were treated with some specific medicines combined with others for clinical treatment. With *Malassezia* otitis, Epiotic cleanser and Orydemyl ear drops were applied to control and treat *Malassezia* infection. Dermatological problems with *Malassezia* and dermatophytes were controlled by cleaning with chlorhexidine and treated with oral Itraconazole. For *Malassezia* otitis, the frequency of Epiotic and Orydemyl was different depending on the severity of the otitis. The low pH of the acid components in most ear cleansers helped inhibit bacterial growth (Swinney et al., 2008). The high population of *Malassezia* in the ears was controlled and treated with Epiotic and Orydemyl twice daily. Mild cases were applied once a day. With *Malassezia* dermatitis, topical and systemic therapy could improve the clinical signs. Therapy should be continued for 7 - 10 days. Follow-up examinations were necessary after 3 - 4 weeks for evaluation of clinical responses (Bajwa, 2019) and cytological examinations again. The treatment for dermatophytosis included topical antifungal shampoos or cleansers combined with systemic antifungal treatments (Moriello, 2019). Topical treatment could be used for the whole body or local lesions. In this research, systemic antifungals applied in dogs and cats were Itraconazole (5 mg/kg) orally once daily for one week.

3. Results and discussion

3.1. Determination of *Malassezia* infection and dermatophytosis cases in Thonglor Bangkok Pet Hospital

Total 208 cases were examined for treatment in Thonglor Bangkok Pet Hospital from December 2022 to May 2023. In which, fifty-three cases showed skin disease clinical signs, making up 25.48% (Table 1). Compared with the survey of the prevalence, diagnosis, and treatment of dermatological conditions in small animals in general practice in the United Kingdom, the percentage of dermatological problems was 21.4% (Hill et al., 2006), which was nearly the same as our rate in this study. Otherwise, 32 cases were identified with otitis externa, comprising 15.38% of the total cases in Thonglor Bangkok Pet Hospital (Table 1). In comparison with the study of the frequency and predisposing factors for canine otitis externa was conducted on 905,554 dogs in the UK during 2016, our rate was higher than 7.3% cases in this research (O'Neill et al., 2021). The difference in the rate depended on the predisposing factors affecting the statistical proportion. Our investigation was conducted in District 2, where the life conditions were better for pets and animals; however, the rate of otitis externa and dermatological problems was still higher than it in other surveys in foreign countries. This result showed the risk of otitis externa and dermatological problems in our local area.

According to Table 2, 24 cases (11.53%) were positive with *Malassezia* infection, while 61 cases were negative with *Malassezia* spp., and 123 cases were diagnosed with other diseases. Our *Malassezia* infected rate was 11.53% which was much lower than 48.26% in the research of *Malassezia* spp. in the external ear canal of the healthy and otitis dogs and cats performed by Carfachia et al. (2005). Tyler et al. (2020) evaluated 129 *Malassezia* cases in 341 total cats in the study of otoscopy and aural cytological findings in a population of rescue cats and cases

Table 1. The rate of dermatitis and otitis external cases in Thonglor Bangkok Pet Hospital (n = 208)

	Numbers of cases	Percentage (%)
Otitis externa	32	15.38
Dermatitis	53	25.48
Others	123	59.13
Total cases	208	100

Table 2. The rate of *Malassezia* infection in Thonglor Bangkok Pet Hospital (n_1 = 32, n_2 = 53, n_3 = 123, n = 208)

	Results	Otitis externa (%) n_1 = 32	Dermatitis (%) n_2 = 53	Total cases (%) n = 208
Malassezia infection	Positive	23 (71.8)	1 (1.9)	24 (11.53)
	Negative	9 (28.2)	52 (98.1)	
Other diseases (n_3 = 123)		-	-	184 (88.47)

n_1: total of otitis externa cases, n_2: total of dermatitis cases, n_3: total of other diseases, n: total cases came to the hospital.

Table 3. The rate of dermatophytosis in Thonglor Bangkok Pet Hospital (n_1 = n_2 = 53, n_3 = 155, n = 208)

	Results	ATI n_1 = 53 (%)	DTM culture n_2 = 53 (%)	Total cases n = 208 (%)
Dermatophytosis	Positive	3 (5.7)	1 (1.9)	1 (0.48)
	Negative	50 (94.3)	52 (98.1)	
Other diseases (n_3 = 155)		-	-	207 (99.52)

n_1, n_2: total of dermatitis cases, n_3: total of other diseases, n: total of cases came to the hospital; ATI: adhesive tape impression; DTM: dermatophyte test media.

in a referral small animal hospital in England and Wales, made up 37.8% which is higher than our ratie in Thonglor Bangkok Pet Hospital. Our results illustrated the low prevalence of *Malassezia* infections at Thonglor Bangkok Pet Hospital. This difference depended on the number of cases, the research methods, environmental conditions, and various predisposing factors at different places.

The results of the diagnostic tests of 53 animals with dermatological problems were presented in Table 3. In 53 animals, 3/53 animals were positive with the ATI method. All 53 dermatological cases were collected the sample and performed DTM culture. After 10 days, the colony in DTM agar grew, then it was collected and observed under the microscope to evaluate the species of dermatophyte. The results showed that 1/53 cases was positive with both ATI method and DTM culture, which detected species was *Microsporum canis*. Thus, in a total of 208 cases in Thonglor Bangkok Pet Hospital, dermatophytosis constituted 1/208 cases (0.48%) resulting in a low rate of dermatophytosis in our hospital.

3.2. Predisposing factors of *Malasssezia* infection and dermatophytosis at Thonglor Bangkok Pet Hospital

The study showed that dermatophytosis rate in dogs was 100% and in cats was 0% (Table 4). According to the observed data, dermatphytosis was detected in dogs more than in cats. This could be due to the small quantity of dermatophytosis in dogs and cats identified in hospital. The rate of *Malassezia* infection recorded in dogs is 91.7%, higher than 8.3% in cats. Some research papers studied that *Malassezia* mainly occurred in dogs more than cats, while others had higher results in cats than in dogs (Cafarchia et al., 2005). Our data were suitable with much research and dependent on two factors as (1) good hygiene and the life-being of dogs and cats in the local area, and (2) frequent ear cleaning for dogs and cats for *Malassezia* prevention.

Dermatophytosis occurred in 1 dog over three years old, while the high percentage of *Malassezia* infection rounded up the cases from 1 to 3 years, constituting 45.8% of *Malassezia* cases (Table 4). Based on the observed data, dermatophytosis occurred in old age, and *Malassezia* infection occurred primarily from 1 to 3 years old. Dhoot et al. (2021) carried out the study of prevalence of *Malassezia* infection in dogs of Nagpur City recorded that the percentage of Malassezia infection under one year was 0.39%, from 1 to 3 years was 3.92%, and gradually increased infection to 49.8% from 3 to 9 years old, then decreased to 2.7% at the age above 12 years old. Our data from 1 to 3 years old were 45.8%, higher than 3.92% compared with the study above. Otherwise, our data of cases over three years old is 33.3%, relatively analogous with the data from the study above (12.94 - 49.8%) and other study performed by Sudipa in Badung, Balo with 40% of *Malassezia* infection in dogs above three years (Sudipa et al., 2021).

The dermatophytic infection occurring in exotic animals was one case and there were no cases in domestic animals. The percentage of Malassezia infection in domestic breeds was 25.0%, lower than 75.0% in exotic animals (Table 4). Based on the observed data, dermatophytosis and Malassezia infection occurred mainly in exotic animals. However, in survey duration, we recorded two factors affecting the data results as (1) the number of exotic dogs and cats that came to Thonglor Bangkok Pet Hospital was much higher than domestic dogs and cats, and (2) genetic factors related to immunity and sensitivity were lower in exotic dogs and cats. Compared with other research about breed

Table 4. Dermatophytosis and *Malassezia* infection in Thonglor Bangkok Pet Hospital

Factors n		Dermatophytes (n_1 = 1)		*Malassezia* infection (n_2 = 24)	
		%	n	%	
Animal	Dogs	1	100	22	91.7
	Cats	0	0	2	8.3
Age	< 1 year	0	0	5	20.8
	1 - 3 years	0	0	11	45.8
	> 3 years	1	100	8	33.3
Breed	Domestic	0	0	6	25.0
	Exotic	1	100	18	75.0
Gender	Male	1	100	13	54.2
	Female	0	0	11	45.8

factors in dermatophytosis and *Malassezia*, Moriello et al. (2017) noted that 75.0% of Persian cats had just four cases diagnosed with dermatophytosis, and 23.6% of Yorkshire Terrier dogs were identified as being predisposing commonly to dermatophytosis. *Malassezia* infection could occur in dogs and cats of any age, breed, and sex. However, some dog breeds were identified to be predisposed, including American cocker spaniels, West Highland white terriers, basset hounds, poodles, and Australian silky terriers, while commonly in Sphynx and Devon Rex cats (Sykes et al., 2014). So our data were suitable with some studies that dermatophytosis and *Malassezia* could occur mainly in exotic breeds.

Both dermatophytosis and *Malassezia* infection occurred in males more than in females, which were 100% and 54.2% compared with 0% and 45.8%, respectively. Jarjees & Issa (2022) investigated the first study on molecular epidemiology of dermatophytosis in cats, dogs in the Kurdistan region of Iraq, the prevalence of dermatophytosis in male cats was higher than in female cats, 47.6% compared with 41.4% with no statistical significance, while this percentage was the same in male and female dogs. Dhoot et al. (2021) showed that *Malassezia* infection in males was 60% against 40% in females. Our data was relatively like the data collected in the study. However, Nardoni et al. (2004) in the study of occurrence of *Malassezia* species in healthy and dermatologically diseased dogs said that the prevalence of *Malassezia* infection between male and female were nearly the same. However, our data showed that dermatophytosis was only one case in males and zero in females, with a percentage of 100% compared with 0%. At the same time, the rate of *Malassezia* infection in males was also higher than in females.

3.3. Result of effectiveness in treatments

The effectiveness of Epitotic and Oridermyl ranged from good (1 - 2 weeks) to intermediate (2 - 4 weeks) response (Table 5). The efficacy of the treatment was recorded based on the recovery of clinical signs after 7 - 10 days and re-examination under the microscope. In 23 cases of *Malassezia* otitis, Epiotic played a significant role in improving all otitis cases. Compared to Swinney et al. (2008) in the study of the comparative in vitro antimicrobial efficiency of commercial ear cleaners, their results were recorded with the improvement of otitis in 16/31 dogs used Epiotic, which was effective in more than 50% of *Malassezia* otitis cases. Another study from Roy et al. (2012), they carried out with comparative short-term efficacy of Oridermyl auricular ointment and Revolution selamectin spot-on against feline otodectes cynotis and its associated secondary otitis externa, the results identified that 18/24 cases evaluated the number of *Malassezia* from day 0 to day 10 using Oridermyl. Our results were much better than these research.

Table 5. The effectiveness of treatments

Medication	Infection	The effectiveness of treatments	
		Time of treatment	n
Epiotic cleanser + Oridermyl	*Malassezia* otitis (n=23)	1 - 2 weeks	19
		2 - 4 weeks	4
		> 4 weeks	0
Itraconazole	*Malassezia* dermatitis	7 - 8 weeks	1
	Dermatophytosis	7 - 8 weeks	1

With *Malassezia* dermatitis and dermatophytosis, Itraconazole was used to treat fungal infections. The results illustrated the cases detected with *Malassezia* dermatitis and dermatophytosis. The effectiveness of these therapy was evaluated due to the improvement of the clinical signs after four weeks and recovered until 7 - 8 weeks (Table 5). According to Moriello (2019), the study of dermatophytosis in cats and dogs, and the practical diagnosis and treatment, the systemic therapy should follow during 8 weeks until clinical resolution of lesions.

4. Conclusions

During this study, the *Malassezia* infection occurred mainly in dogs rather than cats at every age. It was also found more in exotic animals than in domestic animals and usually in males than in females. The effectiveness of treatment illustrated the significant improvement in *Malassezia* otitis when using Epiotic solution combined with Oridemyl ear drop. Moreover, great improvement was evident in dermatophytosis therapy with Itraconazole. Due to low number cases of dermatophytosis, the predisposing factors of this fungus could not be evaluated.

Conflict of interest

The authors have no conflicts of interest to declare.

References

Bajwa, J. (2019). Canine otitis externa - Treatment and complications. *The Canadian Veterinary Journal* 60(1), 97-99.

Begum, J., & Kumar, R. (2021). Prevalence of dermatophytosis in animals and antifungal susceptibility testing of isolated *Trichophyton* and *Microsporum* species. *Tropical Animal Health and Production* 53(3), 1-8. https://doi.org/10.1007/s11250-020-02476-3.

Bouza-Rapti, P., Karafylia, A., Tamvakis, A., & Farmaki, R. (2023). Comparison of adhesive tape impression cytology, hair plucks, and fungal culture for the diagnosis of dermatophytosis in dogs and cats. *Veterinary Sciences* 10(183), 1-10. https://doi.org/10.3390/vetsci10030183.

Cafarchia, C., Gallo, S., Capelli, G., & Otranto, D. (2005). Occurrence and population size of *Malassezia* spp. in the external ear canal of dogs and cats both healthy and with otitis. *Mycopathologia* 160(2), 143-149. https://doi.org/10.1007/s11046-005-0151-x.

Dhoot, K. D., Panchbhai, G. R. B., Chaudhari, S. V. U., & Kolangath, S. (2021). Prevalence of *Malassezia* infection in dogs of Nagpur City. International *Journal of Current Microbiology and Applied Sciences* 10(2), 2269-2273.

Diren, S., B., Metiner, K., Çelik, B., Başaran Kahraman, B., İkiz, S., Bağcıgil, A. F., Özgür, N. Y., & Ak, S. (2019). Dermatophytes isolated from dogs and cats suspected dermatophytoses in Istanbul, Turkey within a 15-year-period: An updated report. *Kocatepe Veterinary Journal* 12(2), 116-121. https://doi.org/10.30607/kvj.495736.

Hill, P. B., Lo, A., Eden, C. a. N., Huntley, S., Morey, V., Ramsey, S., Richardson, C., Smith, D. J., Sutton, C., Taylor, M. D., Thorpe, E., Tidmarsh, R., & Williams, V. (2006). Survey of the prevalence, diagnosis and treatment of dermatological conditions in small animals in general practice. *Veterinary Record* 158(16), 533-539. https://doi.org/10.1136/vr.158.16.533.

Jarjees, K. I., & Issa, N. A. (2022). First study on molecular epidemiology of dermatophytosis in cats, dogs, and their companions in the Kurdistan region of Iraq. *Veterinary World* 15(12), 2971-2978. https://doi.org/10.14202/vetworld.2022.2971-2978.

Kaufmann, R., Blum, S. E., Elad, D., & Zur, G. (2016). Comparison between point-of-care dermatophyte test medium and mycology laboratory culture for diagnosis of dermatophytosis in dogs and cats. *Veterinary Dermatology* 27(4), 284-e68. https://doi.org/10.1111/vde.12322.

Moriello, K. (2019). Dermatophytosis in cats and dogs: A practical guide to diagnosis and treatment. *In Practice* 41(4), 138-147. https://doi.org/10.1136/inp.l1539.

Moriello, K. A., Coyner, K., Paterson, S., & Mignon, B. (2017). Diagnosis and treatment of dermatophytosis in dogs and cats: Clinical consensus guidelines of the world association for veterinary dermatology. *Veterinary Dermatology* 28(3), 266-268. https://doi.org/10.1111/vde.12440.

Nardoni, S., Mancianti, F., Corazza, M., & Rum, A. (2004). Occurrence of *Malassezia* species in healthy and dermatologically diseased dogs. *Mycopathologia* 157(4), 383-388. https://doi.org/10.1023/B:MYCO.0000030416.36743.dd.

Negre, A., Bensignor, E., & Guillot, J. (2009). Evidence-based veterinary dermatology: A systematic review of interventions for *Malassezia* dermatitis in dogs. *Veterinary Dermatology* 20(1), 1-12. https://doi.org/10.1111/j.1365-3164.2008.00721.x.

O'Neill, D. G., Volk, A. V., Soares, T., Church, D. B., Brodbelt, D. C., & Pegram, C. (2021). Frequency and predisposing factors for canine otitis externa in the UK - A primary veterinary care

epidemiological view. *Canine Medicine and Genetics* 8(1), 1-16. https://doi.org/10.1186/s40575-021-00106-1.

Paryuni, A. D., Indarjulianto, S., & Widyarini, S. (2020). Dermatophytosis in companion animals: A review. *Veterinary World* 13(6), 1174-1181. https://doi.org/10.14202/vetworld.2020.1174-1181.

Roy, J., Bédard, C., Moreau, M., & Sauvé, F. (2012). Comparative short-term efficacy of Oridermyl® auricular ointment and Revolution® selamectin spot-on against feline Otodectes cynotis and its associated secondary otitis externa. *The Canadian Veterinary Journal* 53(7), 762-766.

Sudipa, P. H., Gelgel, K. T. P., & Jayanti, P. D. (2021). Malassezia sp. infection prevalence in dermatitis dogs in Badung area. *Advances in Tropical Biodiversity and Environmental Sciences* 5(2), 45-49. https://doi.org/10.24843/ATBES.2021.v05.i02.p02.

Swinney, A., Fazakerley, J., McEwan, N., & Nuttall, T. (2008). Comparative in vitro antimicrobial efficacy of commercial ear cleaners. *Veterinary Dermatology* 19(6), 373-379. https://doi.org/10.1111/j.1365-3164.2008.00713.x.

Sykes, J. E., Nagle, T. M., & White, S. D. (2014). Malassezia infections. In Sykes, J. E. (Ed.). *Canine and feline infectious diseases* (570-573). Missouri, USA: Elsevier Saunders.

Tyler, S., Swales, N., Foster, A. P., Knowles, T. G., & Barnard, N. (2020). Otoscopy and aural cytological findings in a population of rescue cats and cases in a referral small animal hospital in England and Wales. *Journal of Feline Medicine and Surgery* 22(2), 161-167. https://doi.org/10.1177/1098612X19834969.

Optimization of essential oil extraction process from *Piper nigrum* L. by-products and investigation of its biological activities

Hanh T. Phan[1], Hang S. N. Vuong[1], Anh T. Ha[1], Anh V. T. Nguyen[1], Toan Q. Truong[2], Dong T. N. Le[2], Ly P. T. Trinh[1,2], & Biet V. Huynh[1,2*]

[1]Faculty of Biological Sciences, Nong Lam University, Ho Chi Minh City, Vietnam

[2]Research Institute for Biotechnology and Environment, Nong Lam University, Ho Chi Minh City, Vietnam

ARTICLE INFO

Research Paper

Received: April 29, 2023

Revised: May 24, 2023

Accepted: May 30, 2023

Keywords

Biological activity

Essential oil

Piper nigrum L. by-products

Response surface methodology

Steam distillation

***Corresponding author**

Huynh Van Biet

Email: hvbiet@hcmuaf.edu.vn

ABSTRACT

Black pepper (*Piper nigrum* L.) is an industrial crop commonly grown in Vietnam. Besides its economic value, its processing released large amounts of by-products into the environment including leaves, flatterned seeds, and seed-bearing branches. The objective of this study was to optimize the extraction of essential oil from the mixture of three black pepper by-products and evaluate its biological activities in order to exploit the potential value of the by-products. The essential oils were extracted by hydrodistillation in which the extraction conditions including extraction time, water to feed ratio, and ultrasonic pretreated time were optimized. The results showed that the highest essential oil yield was achieved after 4 h of extraction at a water to feed ratio of 10:1, and 10 min of ultrasonic pretreament. Isospathulenol, β-selinene, caryophyllene, α-pinene, and α-copaene were identified as the main components of the essential oil as a result of chemical composition analysis using gas chromatography mass spectrometry. The essential oils exhibited 2,2-Diphenyl-1-picrylhydrazyl radical scavenging capacity with an IC50 value of 4.205 mg/mL and antibacterial capacity against four strains of bacteria, including *Bacillus spizizenii, Bacillus cereus, Staphylococcus aureus* and *Salmonella enterica* with the diameters of inhibition zone of 11.37 mm, 4.12 mm, 7.75 mm, 5.37 mm, respectively.

Cited as: Phan, H. T., Vuong, H. S. N., Ha, A. T., Nguyen, A. V. T., Truong, T. Q., Le, D. T. N., Trinh, L. T. P., & Huynh, B. V. (2023). Optimization of essential oil extraction process from *Piper nigrum* L. by-products and investigation of its biological activities. *The Journal of Agriculture and Development* 22(6), 54-64.

1. Introduction

Piper nigrum L. belongs to the family Piperaceae and is a perennial industrial crop with high economic value. Black pepper contains 0.4 - 7% essential oil with main valuable components such as α- and β-pinene, limonene, myrcene, 3-carene, linalool, α-phellandrene, sabinene, and β-caryophyllene (Myszka et al., 2018). Besides providing nutritional and flavoring values, pepper essential oil has biological activities such as antioxidant, antibacterial, anti-inflammatory, anti-cancer, analgesic, and stress relief properties, which make it be widely used in cosmetics and pharmaceuticals (Ashokkumar et al., 2021). According to statistics from the General Statistics Office of the Ministry of Planning and Investment in 2018, the pepper cultivation area of Vietnam was 149,900 ha, the pepper output reached 255,400 tons and it kept the leading position with pepper export output of over 200,000 tons/year.

These figures not only show a positive sign of economic development but also bring out a concern about increasing amount of pepper by-products because they have the potential to carry diseases to young plants if not treated strictly. Black pepper by-products include leaves, flat seeds, and seed-bearing branches containing high organic matter that might cause environmental pollution. If these by-products are effectively utilized and recycled, they will bring high economic efficiency and create jobs for workers. The study was carried out to optimize the essential oil extraction from black pepper by-products and to investigate its biological properties that provide useful information for further application from inexpensive and environmentally friendly raw materials.

2. Material and Methods

2.1. Plant materials, chemicals, and reagents

A mixture of three by-products including pepper leaves, flat seeds and seed-bearing branches were collected in Gia Nghia city, Dak Nong province in May 2022 and preserved according to the regulations of Vietnam Pharmacopoeia V (MOH, 2018).

The antibacterial activity of the extracted essential oil was investigated on five strains of bacteria, including *Escherichia coli* (ATCC® 8739™), *Salmonella enterica* (ATCC®700623™), *Bacillus spizizenii* (ATCC® 6633™), *Bacillus cereus* (ATCC® 10876™), and *Staphylococus aureus* (ATCC® 6538™). These strains were provided by the Research Institute for Biotechnology and Environment, Nong Lam University, Ho Chi Minh City, Vietnam.

The 2,2-diphenyl-1-picrylhydrazyl (DPPH) was purchased from Merck. Other chemicals, including petroleum ether, Na2SO4, and dimethyl sulfoxide (DMSO) were obtained from Sinochem Group.

2.2. Optimization of essential oil extraction conditions from mixture of three by-products by response surface method (RSM - CCD)

2.2.1. Experimental design and statistical analysis

Optimization of extraction conditions for total essential oil content was carried out using a central composite design (CCD) of response surface methodology (RSM). Experimental design included five levels of the three independent variables including extraction time (X1), ultrasonic time (X2), water to feed ratio (X3). The design model consists of 16 experiments with 2 runs at the central point (000).

Table 1. Experimental design-matrix encoding the independent variables

Variable name	Unit	Code variable	Levels of evidence				
			- α	- 1	0	+ 1	+ α
Extraction time	h	X_1	0	2	4	6	8
Ultrasonic time	min	X_2	0	5	10	15	20
Water to feed ratio		X_3	6	8	10	12	14

α =2; The maximum and minimum points of each interval are equal to the levels +α and –α. The maximum or minimum levels are equal to the levels +1 and -1. The center points of each interval are equal to the levels 0.

The experimental data were analyzed using the statistical software JMP 10.

2.2.2. Determination of essential oil content

Essential oils in the mixture of three by-products were extracted by hydrodistillation using Clevenger apparatus system. The essential oil was isolated from the obtained mixture by extracting with 50 mL of petroleum ether (3 times) before dried on anhydrous sodium sulfate. Finally, the essential oil was obtained by removing water using a rotary vacuum evaporator.

2.3. Compositional analysis of essential oils from mixture of three by-products by GC-MS

The components of essential oils obtained from the by-product mixture were analyzed using gas chromatography-mass spectrometry (GC-MS). The essential oil was dissolved in n-hexane (1:50, v/v), mixed well and filtered through a PTFE syringe filter with a 0.22 µM pore size. The GC-MS was performed with an Agilent 6890 gas chromatography instrument coupled with an Agilent 5973 mass spectrometer. A capillary column (30 m x 0.25 mm i.d.) coated with 0.25 mM film of 5% phenyl methyl siloxane was used for separation. High purity helium was used as carrier gas with a flow-rate of 1.0 mL/min.The mass spectrometer was operated using electron-impact (EI) mode with the ionization energy of 70 eV and the scan rate was 0.34 s per scan. The quadrupole and ionization source temperature were 150 and 230°C. The experiment was performed once.

The components of essential oils were identified based on a comparison with data in NIST 14 (National Institute of Standards and Technologies, Mass Spectra Libraries).

2.4. Determination of biological activities of the essential oils from mixture of three by-products

2.4.1. DPPH radical scavenging assay

Antioxidant activity of the essential oils was estimated by DPPH assay (Kedare & Singh, 2011). Each 1.0 mL of sample was added to 1 mL of 0.2 mM DPPH. The mixture was incubated in darkness at room temperature for 30 min. The absorbance was measured at 517 nM. A control experiment was performed by adding 1.0 mL of water to 1 mL of the DPPH solution. Ascorbic acid was used as a reference.

The antioxidant activity was determined according to the following equation:

$$\text{The antioxidant activity (\%)} = \frac{Abs_{control} - Abs_{sample}}{Abs_{control}} \times 100$$

A correlation between sample concentration and antioxidant capacity was established, from which the IC50 value (the concentration of essential oil at which 50% of free radicals is captured) was determined to serve as a basis for comparing the antioxidant capacity between experiments. The lower the IC50 value, the higher the antioxidant activity.

2.5 Antibacterial activity

Antibacterial activity of the essential oil was determined by Kirby-Bauer method (Bauer et al., 1966) at different ratios of essential oil to dimethyl sulfoxide (DMSO) of 1:1, 2:1, and 4:1. The antibacterial activity was tested on five strains of bacteria, including *Staphylococcus aureus* (ATCC® 6538™), *Escherichia coli* (ATCC® 8739™), *Salmonella enterica* (ATCC®700623™), *Bacillus spizizenii* (ATCC® 6633™) and *Bacillus cereus* (ATCC® 10876™). One hundred µL of the bacterial suspensions (10^8 CFU/mL) was spread over the Luria Bertani agar plate. Sterile filter paper discs impregnated with essential oils with one DMSO negative control and tetracycline positive control were placed on the surface of the agar plate in a triangular pattern and the samples were incubated at 37°C. Inhibition zones were measured after 24 h for *E. coli* and *S. enterica*, 48 - 72 h for *S. aureus*, *B. spizizenii*, and *B. cereus*. All experiments were conducted in triplicate.

2.6. Data analysis

All data are presented as mean ± standard deviation. The results were statistically processed using Microsoft Excel 2016 and Pearson's correlation coefficient (r) with the level of significance ($P \leq 0.05$).

3. Results and discussion

3.1. Effect of extraction conditions on the essential oil content from mixture of three by-products

The results of empirical experiments are shown in Table 2.

The relationship between the essential oil content and the independent variables is shown in the following function:

$$Y = (4.231 \times 10^{10}) - 5.59 \times 10^{10} X_2 X_3$$

The *P*-value of testing the model's incompatibility (lack of fit) of 0.094 indicated the above regression model was compatible with the experiments. The R-square value of 0.98 demonstrated high correlation between the experimental data and the predicted values. Essential oil contents obtained from the empirical experiments and predicted value on the model are shown in Figure 1.

The pretreatment of raw materials with ultrasonic strongly affected the essential oil yield. Ultrasound is able to disrupt the cell wall structure that might enhance essential oil extraction and shorten extraction time (Kumar et al., 2021).

Table 2. Experimental results of essential oil yield

No.	X_1 (h)	X_2 (min)	X_3	Y (%)
1	4	10	6	0.85
2	4	10	10	1.35
3	2	15	12	0.84
4	4	20	10	1.24
5	2	5	12	0.64
6	6	5	12	1.59
7	6	5	8	1.01
8	4	10	14	1.40
9	8	10	10	1.16
10	6	15	8	1.34
11	6	15	12	2.23
12	0	10	10	0
13	4	0	10	0.82
14	2	15	8	0.79
15	4	10	10	1.28
16	2	5	8	1.09

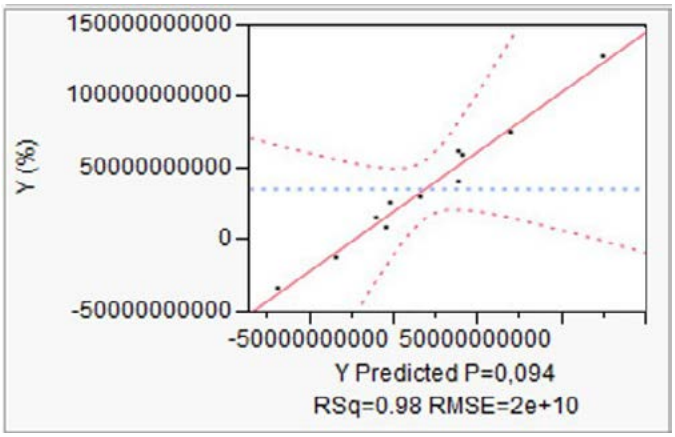

Figure 1. Essential oil contents obtained from the experimental data and the model.

In the extraction process, the steam penetrates the cell layers, breaking the essential oil bags and releasing the oil into the water. However, when the steam becomes saturated with essential oils, it doesn't give effectiveness to release more essential oils. Thus the water to feed ratio is an important factor. In addition, too much water reduces the economic efficiency of the distillation process by consuming heat and time. In this study the highest essential oil yield obtained from the by-

product mixture extract process of 3.9% was obtained by applying 10 min of pretreament with ultrasonic, followed by 4 h of extraction at a water to feed ratio of 10:1 (Figure 2).

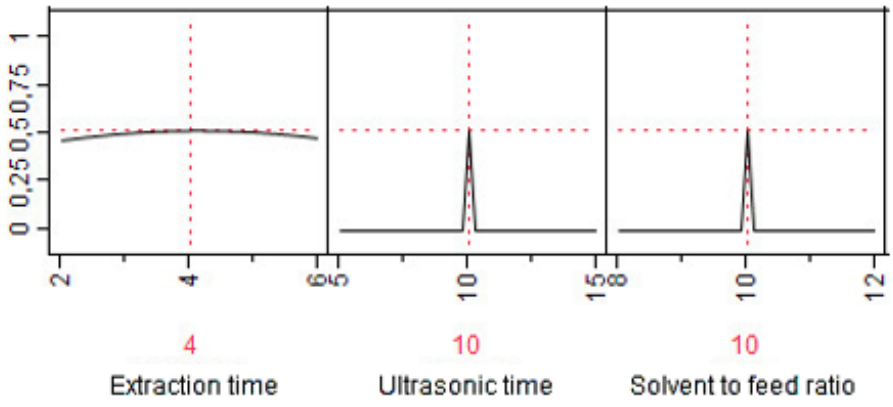

Figure 2. Optimized conditions for the highest response level.

3.2. Chemical compositions of essential oils

There were 16 main compounds found in the essential oil extracted from a mixture of three by-products pepper and the majority belongs to the monoterpenes and sesquiterpenes (Table 2 and Figure 3). These compounds are responsible for the aroma and spicy taste and important biological properties of essential oils (Salzer & Furia, 1977).

The main component of the essential oil is isospathulenol (20.87%) calculated based on the ratio of the peak area of the substance to the total peak area and does not accurately reflect the content present in the essential oil, which has antioxidant activity by decreasing MDA, which is a toxic product due to the degradation of cell membranes due to lipid peroxidation, causing cell rupture and inhibiting inflammatory parameters such as leukocyte migration and

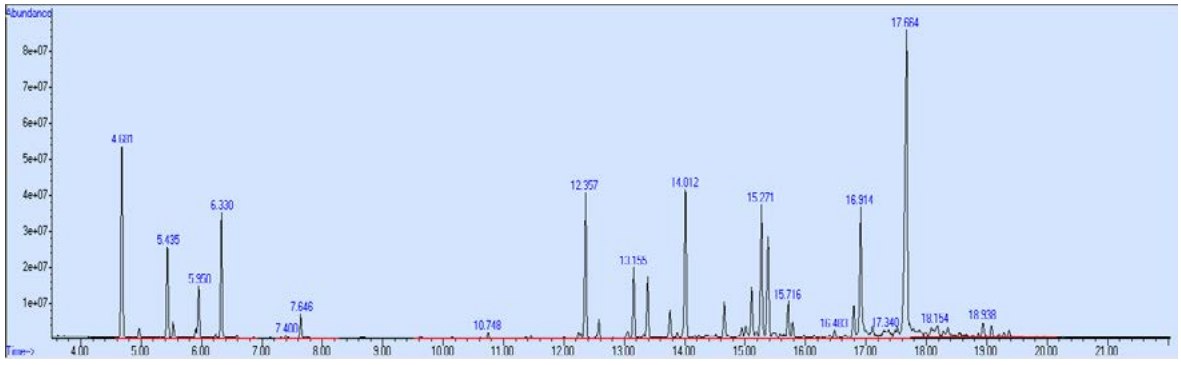

Figure 3. Gas chromatography-mass spectrometry chromatograms of the essential oil.

Table 3. Chemical compositions of mixture pepper by-products essential oil

Number	Chemical composition	Retention time (min)	% Area
1	-Pinene	4.683	7.70
2	-Pinene	5.438	4.80
3	3-Carene	5.952	2.18
4	D-Limonene	6.329	4.72
5	Terpinolene	7.398	0.12
6	-Myrcene	7.644	0.99
7	.delta.-Elemene	12.359	6.02
8	-Copaene	13.153	6.67
9	Caryophyllene	14.011	10.16
10	β-Selinene	15.274	14.25
11	Cadinene	15.714	3.08
12	Germacrene B	16.485	0.86
13	Unknown	16.914	8.84
14	Isospathulenol	17.663	20.87
15	Alloaromadendrene	18.154	3.87
16	-Bisabolene	18.937	3.04

protein extravasation (Nascimento et al., 2018). Other major compounds included β-selinene (14.25%) and caryophyllene (10.16%). These were demonstrated to show pharmacological activities, such as immunoinhibitory, anti-inflammatory, anti-cancer, apoptosis inducer, and highly repellent to insect (Mohammed et al., 2016).

3.3. Antioxidant activity of the essential oil

The essential oil was extracted at optimized conditions and diluted at 5 concentrations of 4 mg/mL, 13 mg/mL, 22 mg/mL, 31 mg/mL, and 40 mg/mL. In the DPPH assay, the purple color

Figure 4. The 2,2-Diphenyl-1-picrylhydrazyl scavenging capacity of the essential oil with increasing concentrations.

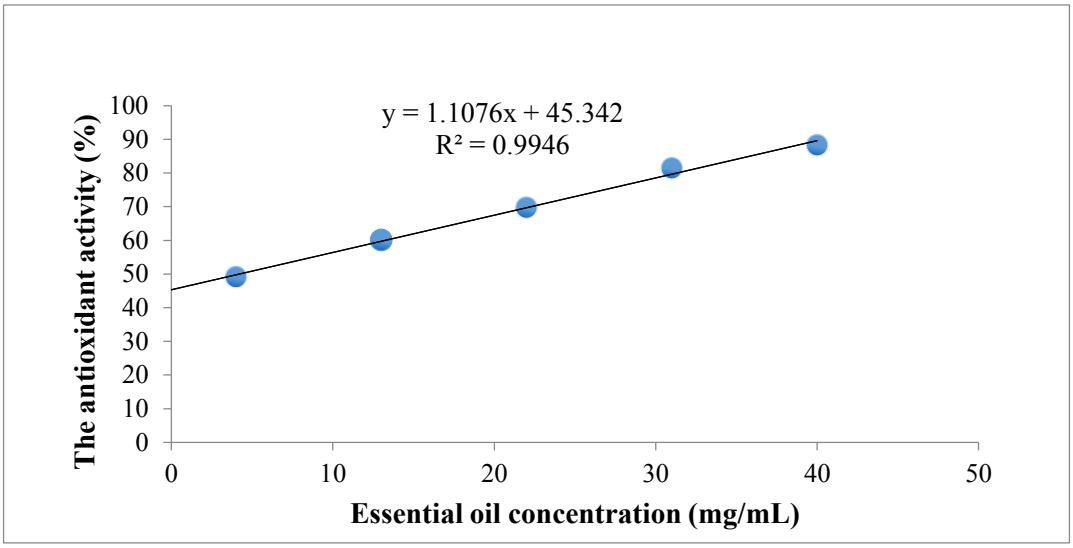

Figure 5. The 2,2-Diphenyl-1-picrylhydrazyl scavenging activity of the essential oil.

intensity gradually decreased with increasing essential oil concentrations (Figure 4). This proves that in the optimal extract, there are groups of substances with antioxidant activity combined with free radicals of DPPH leading to this phenomenon. As shown in Figure 5, IC50 value of the essential oil from the mixture of three black pepper by-products was approximately 4.205 mg/mL, which was much higher than the IC50 of ascorbic acid (0.024 mg/mL). As a result, the essential oils have lower antioxidant capacity. Its antioxidant properties are attributed to main components such as isospathulenol (Nascimento et al., 2018) and D-limonene (Yu et al., 2017).

3.4. Antibacterial activity of the essential oil

The essential oil was extracted at optimized conditions prior to evaluating its antibacterial activity against five strains of bacteria, including *Escherichia coli, Salmonella enterica, Bacillus spizizenii, Bacillus cereus*, and *Staphylococcus aureus*. The bacterial optical density at 600 nM was measured and the suspension turbidity was adjusted according to McFarland turbidity standards by adding distilled water to 10 times the dilutions of the bacterial suspension so that OD600 of 0.5 was achieved, which was equivalent to a colony density of 108 CFU/mL. The agar plates were incubated from 24 to 72 h depending on the bacterial species at room temperature and the results are shown in Figure 6. The essential oil extracted from mixture of three by-products pepper showed good activities against *Salmonella enterica* (D = 5.37 mm), *Bacillus spizizenii* (D = 11.37 mm), *Bacillus cereus* (D = 4.12 mm), and *Staphylococcus aureus* (D = 7.75 mm) but didn't affect the growth of *Escherichia coli*. However, diameters of inhibition zone were smaller than those of the reported data due to different raw material source and extraction conditions such as, techniques, time, temperature, and also bacterial proliferation conditions.

Diameters of inhibition zones were significantly affected by essential oil concentrations (Table 4). Larger inhibition zones were obtained at higher essential oil

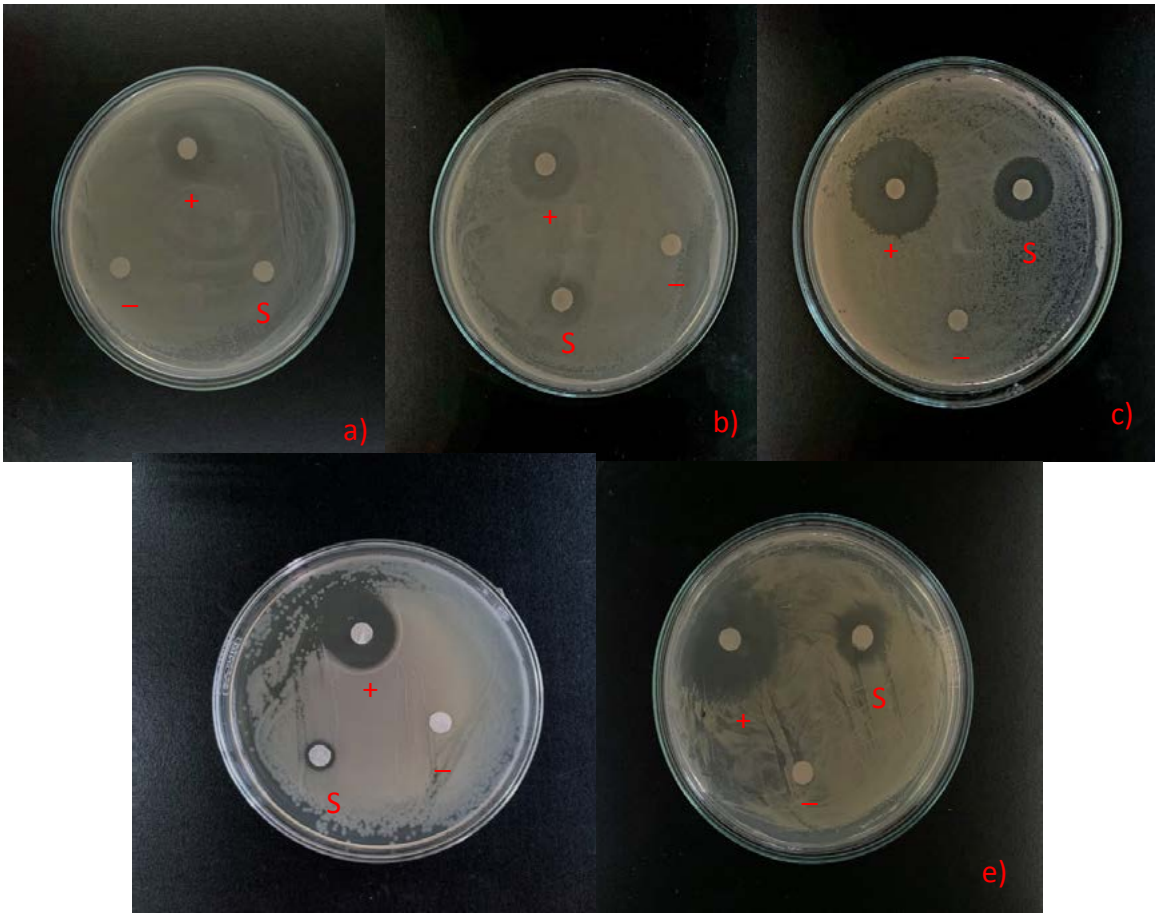

Figure 6. The antibacterial ability of the essential oil against (a) *Escherichia coli*; (b) *Salmonella enterica*; (c) *Bacillus spizizenii*; (d) *Bacillus cereus*; (e) *Staphylococus aureus*; (S) Ratio of essential oil to dimethyl sulfoxide (DMSO) was 4:1; (+) Positive control is Tetracylin; (-) Negative control is DMSO.

concentrations. *B. spizizennii* was the most susceptible strain to the essential oil, followed by S. aureus and S. enterica. The *E. coli* was the most resistant strain to the essential oil. Gram-positive bacteria have a cell membrane structure without lipopolysaccharide molecules. The hydrophilic components of essential oils can directly combine with the phospholipid bilayer of the cell membrane, disrupting the metabolism on both sides of the membrane bacterial cells.

Antibacterial capacity was commonly attributed to the terpenoids representing in the essential oil. Terpenoids are able to inhibit two crucial processes which are essential to microbial survival including oxygen uptake and oxidative phosphorylation. Aerobic microbes require oxygen in order to yield energy for their growth. Previously, it was proven that low oxygen levels caused limited respiration rates in bacteria. In addition, oxidative phosphorylation is a crucial biochemical process responsible for cellular respiration that takes place in the cytoplasmic membrane. Thus, terpenoids interfere cellular respiration, which later causes uncoupling of oxidative phosphorylation in the microbe (Mahizan et al., 2019).

Table 4. Diameter of the inhibition zones (mm)

Species	The ratio of essential oil to dimethyl sulfoxide		
	1:1	2:1	4:1
Escherichia coli	0	0.25 ± 0.10	0.31 ± 0.01
Salmonella enterica	3.00 ± 0.12	3.62 ± 0,14	5.37 ± 0.13
Bacillus spizizenii	2.87 ± 0.14	3.50 ± 0.26	11.37 ± 0.17
Bacillus cereus	1.12 ± 0.11	2.00 ± 0.16	4.12 ± 0.21
Staphylococus aureus	2.25 ± 0.13	2.62 ± 0.23	7.75 ± 0.24

4. Conclusions

The optimized conditions for extracting essential oil from three type by-products of black pepper were found to be 4 h of extraction time, water to feed ratio of 10:1 (v/w), and an ultrasonic time of 10 min. The main chemical compositions of the essential oil included isospathulenol, β-selinene, caryophyllene, α-pinene, and α-copaene. The essential oil obtained from the optimization process showed an antioxidant capacity with an IC50 of 4.205 mg/mL and antibacterial activity against four bacterial strains including *Bacillus spizizenii*, *Bacillus cereus*, *Staphylococcus aureus*, and *Salmonella enterica* with the diameter of inhibition zone of 11.37 mm, 4.12 mm, 7.75 mm, 5.37 mm, respectively. The results provide an understanding of the exploitation, development, and application of black pepper by-products in various areas such as foods, healthcare, and pharmaceuticals.

Conflict of interest

The authors have no conflicts of interest to declare.

Acknowledgements

This research was funded by a research grant (CS-SV21-KHSH-02) from Nong Lam University Ho Chi Minh City, Vietnam.

References

Ashokkumar, K., Murugan, M., Dhanya, M. K., Pandian, A., & Warkentin, T. D. (2021). Phytochemistry and therapeutic potential of black pepper *Piper nigrum* L. essential oil and piperine: a review. *Clinical Phytoscience* 7(52), 1-11. https://doi.org/10.1186/s40816-021-00292-2.

Bauer, A. W., Kirby, W. M. M., Sherris, J. C., & Turck, M. (1966). Antibiotic susceptibility testing by a standardized single disk method. *American Journal of Clinical Pathology* 45(4), 493-496. https://doi.org/10.1093/ajcp/45.4_ts.493.

Kedare, S. B., & Singh, R. P. (2011). Genesis and development of DPPH method of antioxidant assay. *Journal of Food Science and Technology* 48(4), 412-422. https://doi.org/10.1007/s13197-011-0251-1.

Kumar, K., Srivastav, S., & Sharanagat, V. S. (2021). Ultrasound assisted extraction (UAE) of bioactive compounds from fruit and vegetable processing by-products: A review. *Ultrasonics Sonochemistry* 70, 105325. https://doi.org/10.1016/j.ultsonch.2020.105325.

Mahizan, N. A., Yang, S. K., Moo, C. L., Song, A. A. L., Chong, C. M., Chong, C. W., Abushelaibi, A., Lim, S. H. E., & Lai, K. S. (2019). Terpene Derivatives as a potential agent against antimicrobial resistance (AMR) pathogens.

Molecules 24(14), 1-21. https://dx.doi.org/10.3390/molecules24142631.

MOH (Vietnam Ministry of Health). (2018). *Vietnamese pharmacopoeia* V. Vietnam. Ha Noi, Vietnam: Vietnam Government Publishing Service.

Mohammed, G. J., Omran, A. M., & Hussein, H. M. (2016). Antibacterial and phytochemical analysis of *Piper nigrum* using gas chromatography - Mass spectrum and fourier-transform infrared spectroscopy. *International Journal of Pharmacognosy and Phytochemical Research* 8(6), 977-996.

Myszka, K., Leja, K., & Majcher, M. (2018). A current opinion on the antimicrobial importance of popular pepper essential oil and its application in food industry. *Journal of Essential Oil Research* 31(1), 1-18. https://doi.org/10.1080/10412905.2018.1511482.

Nascimento, K. F. D., Moreira, F. M. F., Santos, J. A., Kassuya, C. A. L., Croda, J. H. R., Cardoso, C. A. L., Vieira, M. D. C., Ruiz, A. L. T. G., Foglio, M. A., Carvalho, J. E. D., & Formagio, A. S. N. (2018). Antioxidant, anti-inflammatory, antiproliferative and antimycobacterial activities of the essential oil of *Psidium guineense* Sw. and spathulenol. *Journal of Ethnopharmacology* 210(1), 351-358. https://doi.org/10.1016/j.jep.2017.08.030.

Salzer, U. J., & Furia, T. E. (1977).The analysis of essential oils and extracts (oleoresins) from seasonings - A critical review. *Critical Reviews in Food Science and Nutrition* 9, 345-373.

Yu, L., Yan, J., & Sun, Z. (2017). D-limonene exhibits anti-inflammatory and antioxidant properties in an ulcerative colitis rat model via regulation of iNOS, COX-2, PGE2 and ERK signaling pathways. *Molecular Medicine Reports* 15(4), 2339-2346. https://doi.org/10.3892/mmr.2017.6241.

Optimization of ultrasound-assisted enzymatic extraction of betalains from red beetroot (*Beta vulgaris* L.)

Dat T. Huynh*, Thien H. Nguyen, Ngan K. T. Nguyen, Anh N. T. Dang, Thuy T. Le, Dan T. N. Duong, & Huan T. Phan

Faculty of Chemical Engineering and Food Technology, Nong Lam University, Ho Chi Minh City, Vietnam

ARTICLE INFO

Research Paper

Received: May 01, 2023

Revised: May 30, 2023

Accepted: May 31, 2023

Keywords

Betalains

Red beetroot

Response surface method

Ultrasound-assisted enzymatic extraction

***Corresponding author**

Huynh Tien Dat
Email:
dat.huynhtien@hcmuaf.edu.vn

ABSTRACT

Betalains in red beetroot (*Beta vulgaris* L.) offer health benefits and are commonly used as a food colorant. This study aimed to investigate betalains extraction using ultrasound-assisted enzymatic extraction (UAEE). The most significant factors involved in UAEE such as enzyme concentration, extraction temperature, and extraction time were studied and optimized using the response surface method (RSM) to achieve the highest betalains yield. The results showed that the optimal extraction conditions were as follows: enzyme concentration (32.1 U/mL), extraction temperature (40°C), and extraction time (117 min) gave the highest yield of betalains at the level of 550.51 ± 25.76 mg/L. The findings are promising for the industrial scale of extraction betalains for food applications.

Cited as: Huynh, D. T., Nguyen, T. H., Nguyen, N. K. T., Dang, A. N. T., Le, T. T., Duong, D. T. N., & Phan, H. T. (2023). Optimization of ultrasound-assisted enzymatic extraction of betalains from red beetroot (*Beta vulgaris* L.). *The Journal of Agriculture and Development* 22(6), 65-78.

1. Introduction

Betalains are a class of nitrogen-containing compounds that are highly soluble in water and derived from betalamic acid. They are typically categorized into two subgroups: betacyanins, which produce red to purple pigments, and betaxanthins, which produce yellow to orange pigments. Currently, scientists have identified and isolated approximately 75 betalain compounds, including 42 betacyanins and 33 betaxanthins (Carreón-Hidalgo et al., 2022). One of the most well-known betalains is betanin, which is a red pigment compound classified as a food coloring additive with the code E162. In the food industry, betalains are often used as natural colorants, antioxidants, and functional food ingredients. However, they also have a wide range of other potential applications, such as in biological packaging (Yao et al., 2020), fabric dyes (Guesmi et al., 2012), and metal coatings (Fares & Bani-Domi, 2021).

Unlike anthocyanins, which are widely distributed in different plant orders, betalains can only be found in plants of the Caryophyllales order, such as Amaranthaceae, Basellaceae, Cactaceae, Portulacaceae, Nyctaginaceae, and a few other families (Carreón-Hidalgo et al., 2022). Some notable examples of betalains-containing plants include red beetroot (*Beta vulgaris* L.), the fruit of Malabar spinach (*Basella alba* L.), peels of red-fleshed dragon fruit (*H. polyrhizus*), rose moss flower (*Portulaca grandiflora*), and flowers of the bougainvillea plant (*Bougainvillea* spp.) (Carreón-Hidalgo et al., 2022). Among these plants, red beetroot is the most extensively studied and cultivated source of betalains. It is highly valued for its significant content of betalains and its wide cultivation area, making it the main raw material used for betalains research and commercial applications (Carreón-Hidalgo et al., 2022).

Betalains extracted from red beetroot are gaining significant attention from the scientific community due to their potential applications. To optimize the extraction process, researchers have focused on using the response surface method (RSM) or principal component analysis (PCA) to increase extraction efficiency and ensure betalains stability during extraction (Calva-Estrada et al., 2022). Traditional extraction methods for betalains from red beetroot include pickling extraction using water:ethanol (85:15) (Neagu & Barbu, 2014), water:ethanol (50:50) (Pandey et al., 2023), and continuous diffusion extraction (Wiley & Lee, 1978). However, these methods have drawbacks such as long extraction time, use of organic solvents, high temperatures causing betalains loss, and low extraction efficiency (Tiwari & Cullen, 2012). Currently, modern extraction methods are being increasingly employed for extracting betalains from beetroot, including enzymatic-assisted extraction (Lombardelli et al., 2021), ultrasound-assisted extraction (Silva et al., 2018), and microwave-assisted extraction (Cardoso-Ugarte et al., 2014). These methods offer several advantages such as short extraction time, precise temperature control, reduced use of organic solvents, and improved extraction efficiency, making them more environmentally friendly.

In recent years, there has been an increasing interest in developing new extraction methods for natural compounds. Among these methods, ultrasound-assisted enzymatic extraction (UAEE) stands out due to its numerous advantages. This method combines enzyme-assisted extraction (EAE) and ultrasound-assisted extraction (UAE), where enzymes act as biological catalysts to rapidly hydrolyze the plant cell wall components, while ultrasound waves create high-frequency vibrations and tiny

air bubbles that further disrupt the material's matrix system, allowing for better solvent penetration and component dissolution. The UAEE method has many advantages over using each method individually, as shown by studies on polysaccharide extraction from freshwater mussels (*Corbicula fluminea*) (Liao et al., 2015) and protein extraction from sesame seed husks (Görgüç et al., 2019), which demonstrated significantly higher extraction efficiencies compared to using EAE or UAE alone.

Given that betalains compounds share similarities with highly polar and hydrophilic polysaccharides and proteins, due to their numerous hydroxyl and carboxyl groups, the UAEE method has great potential for the extraction of betalains from beetroot. By optimizing extraction processes through the UAEE method, extraction efficiency, and betalains stability could be improved, making this method an eco-friendly and efficient alternative to traditional extraction methods. Therefore, in this study, the UAEE was applied to the extraction of betalains from red beetroot. Various synergistic modes of UAEE were investigated and multiple UAEE parameters, such as enzyme concentration, enzyme composition, extraction temperature, and extraction time were studied and optimized using the response surface method (RSM).

2. Materials and Methods

2.1. Beetroot powder

Ripe red beetroot (*Beta vulgaris* L.) was provided by a local producer in Ho Chi Minh City, Vietnam. After being thoroughly washed, the peels were removed. The red beetroot fleshes were sliced into pieces of 5 mm thickness, before being dried by hot air at 60°C, until moisture content reached under 5%. The dried red beetroot pieces were then ground and stored in an airtight bag at in the freezer (-20°C) in the dark until used.

2.2. Enzymes and chemicals

Cellulase from Aspergillus niger (2000 IU/g) was provided by Antozyme Biotech Pvt. Ltd. (Vadodara, Gujara, India), pectinase from *Aspergillus niger* (60,000 IU/g) was provided by ICFOOD Co., Ltd. (Yuseong-gu, Daejeon, Korea). Ethanol, acetic acid, sodium hydroxide (NaOH), and sodium acetate were obtained from Sigma Aldrich (St. Louis, MO, USA).

2.3. Selection of synergistic modes in UAEE procedure

Ultrasound-assisted enzymatic extraction (UAEE) can significantly increase in extraction yield compared to techniques using single treatment such as enzyme or ultrasound (Liao et al., 2015; Görgüç et al., 2019). In addition, different synergistic modes of UAEE have different effects on extraction yield (Wu et al., 2014). Thus, various synergistic modes of ultrasound and enzymatic extraction, and conventional extraction methods were studied and an optimal mode was selected. These modes included: (I) C (conventional extraction): 1 g of red beetroot powder was extracted with water:ethanol (75:25), at 25°C for 90 min; (II) EAE (enzymatic-assisted extraction): 1 g of red beetroot was mixed with a buffer solution having cellulase:pectinase (6:4) mixture at 25 U/g concentration, pH 5.5, extraction temperature of 25°C for 120 min before enzyme inactivation; (III) UAE (ultrasound-assisted extraction): 1 g of red beetroot powder was extracted in water:ethanol (75:25), extraction temperature 45°C, ultrasound powder 250 W, frequency of 40 kHz for 90 min; (IV) Eu (enzymatic hydrolyzation first,

followed by ultrasound extraction): 1 g of red beetroot powder was mix buffer solution having cellulase:pectinase (3:2) mixture at 25 U/g concentration, pH 5.5, the mixture was incubated at 25°C with constant stirring for 120 min followed by enzyme inactivation and sonication for 90 min (V) Ue (ultrasound treatment first, followed by EAE) 1 g of red beetroot powder was sonicated for 90 min, followed by EAE (cellulase:pectinase (3:2) mixture at 25 U/g, pH 5.5, extraction temperature of 25°C for 120 min); (VI) UE (ultrasound treatment and enzymatic hydrolyzation happened simultaneously): 1 g of red beetroot powder was mixed with enzyme mixture (cellulase:pectinase (3:2), the concentration of 25 U/g, pH 5.5) when immediately treated with ultrasound (250W, 40 kHz) for 90 min, the enzyme was then inactivated.

2.4. UAEE procedure

After selecting the synergistic UAEE mode, the UAEE was performed as described by Liu et al. (2014)an efficient ultrasound-assisted enzymatic extraction procedure for the water-soluble polysaccharides from the fruit of Lycium barbarum was investigated and optimized. Response surface methodology (RSM with minor modifications. The enzyme mixture solution was prepared by mixing cellulase and pectinase with pH 5.5 acetate buffer at given enzyme concentrations and enzyme compositions. Red beetroot powder (1 g) was mixed with 15 mL of enzyme mixture solution in a 50 mL falcon tube. This mixture was ultrasound treated at the designed temperature and time in an ultrasound cleaning bath (Elma P60H, Singen, Germany) with fixed ultrasound frequency and power at 40 kHz and 250 W, respectively. The extracting solution was centrifuged at 2,500 g for 15 min and the supernatant was collected.

2.5. Determination of total betalains (TB) content

The total betalains (TB) content of red beetroot extract was determined using a spectrometric method as described by Wruss et al. (2015) with slight modifications. The absorbance was measured at two different wavelengths, 485 nm for betaxanthins and 536 for betacyanins, respectively.

The total betalains (TB) content was expressed in mg/L and was the sum of betacyanins (BC) and betaxanthins (BX) content according to formula (1).

$$BC\ or\ BX\left(\frac{mg}{L}\right) = \frac{A \times DF \times M_w \times 1000}{\varepsilon \times L} \quad (1)$$

Whereas, A is the maximum absorbance value at 536 nm for BC and 485 nm for BX; DF is the dilution factor; Mw is the molecular weight of BC (Mw = 550 g/mol) and BX (Mw = 339 g/mol), ε is the extinction coefficient of BC (ε = 60,000 L/mol.cm) and BX (ε = 48,000 L/mol.cm), L is the path length (1 cm).

2.6. Preliminary experiments design

A series of single-factor, completely randomized experiments was conducted before the optimization experiment to identify significant factors and narrow the condition ranges. The independent variables studied were: enzyme concentration (20 U/mL, 25 U/mL, 30 U/mL, 35 U/mL), enzyme ratio (cellulase/pectinase 1/0, 3/2, 2/3 & 0/1), extraction temperature (30°C, 40°C, 50°C & 60°C), and extraction time (60 min, 90 min, 120 min, & 150 min). Total betalains (TB) was the response variable. After each experiment, the condition level resulting in the highest TB was chosen as the control variable for the next experiments.

2.7. Central Composite Design and statistical analysis

Based on single-factor preliminary experiments, central composite design (CCD) was used to optimize the UAEE procedure of betalains from red beetroot. An experimental factorial model with three independent variables (X_1, enzyme concentration; X_2, extraction temperature; X_3, extraction time) at three levels was performed. To ensure the data reproducibility and determine the experimental error, 4 replicated central points were used. The levels and ranges of independent variables were presented in Table 1. The dependent variable studied was total betalains (TB) content (mg/L) and was related to the coded variables by a second-degree polynomial using Equation 2:

$$Y = b_o + b_1X_1 + b_2X_2 + b_3X_3 + b_{12}X_1X_2 + b_{13}X_1X_3 + b_{23}X_2X_3 + b_{11}x_1^2 + b_{22}x_2^2 + b_{33}x_3^2 \quad (2)$$

Where is the dependent response while the coefficients of the polynomial are represented by b_o (constant term); b_1, b_2, b_3 (linear effects); b_{11}, b_{22}, b_{33} (quadratic effects); and b_{12}, b_{13}, b_{23} (interaction effect).

Table 1. Levels of the independent variables used in the central composite design

Independent variables	Levels		
	-1	0	1
Enzyme concentration (U/mL)	25	30	35
Extraction temperature (°C)	40	50	60
Extraction time (min)	90	120	150

2.8. Statistical analysis

All the experiments and analyses were done in triplicates except for the optimization experiment, which had 4 replicated center points. The data analysis was conducted using Excel and JMP Pro statistical software (version 17.0, SAS Institute, Cary, NC, USA). All data are presented as mean values ± SD except for the optimization experiment. In preliminary experiments, one-way analysis of variance (ANOVA) and Tukey's HSD were used to analyze the mean values at $P < 0.05$ (Wilkinson, 1989) to detect significant differences among levels of treatment. In the RSM-CCD experiment, ANOVA tables were developed to determine the effect and regression coefficients of individual linear, quadratic, and interaction terms.

3. Results and Discussion

3.1. Selection of synergistic modes

The betalains extraction yields of conventional (C), enzyme-assisted extraction (EAE), ultrasound-assisted extraction (UAE) methods, and different synergistic modes of UAEE (Eu, Ue, UE) are shown in Figure 1. The EAE and UAE enhanced the betalains extraction yield in comparison with the conventional (C) method ($P < 0.05$) because EAE using cellulase and pectinase to hydrolyze and break down plant cell wall constituents which led to the release of intracellular contents (Karki et al., 2011) and UAE employs ultrasound cavitation to break

down plant tissues, agitate the mixture and enhance extraction yield (Chen et al., 2012).

Moreover, the effects of synergistic modes on betalains extraction yield are shown by the comparison among Eu mode (enzymatic hydrolyzation first, followed by ultrasound extraction), Ue (ultrasound treatment first, followed by enzymatic-assisted extraction), UE (ultrasound treatment and enzymatic hydrolyzation happened simultaneously). In which, UE mode showed the highest betalains extraction yield ($P < 0.05$). This was in line with other reports on UAEE application on polysaccharides and polyphenols (Wu et al., 2014; Li et al., 2017), where the extraction yield was significantly improved by applying both treatments simultaneously. The presence of ultrasound cavitation was found to cause an increase in the contact area between phases and subsequently decreased mass transfer limitations within the enzyme-substrate system. High-intensity focused ultrasound led to a decrease in size, thereby increasing the amount of substrate in contact with the enzyme. Furthermore, the boost in reaction rates observed after ultrasound treatment was believed to be due to a greater number of collisions between the enzyme and substrate (Capelo et al., 2005). Therefore, the synergistic mode UE (ultrasound treatment and enzymatic hydrolyzation happened simultaneously) was selected and used in subsequent UAEE experiments.

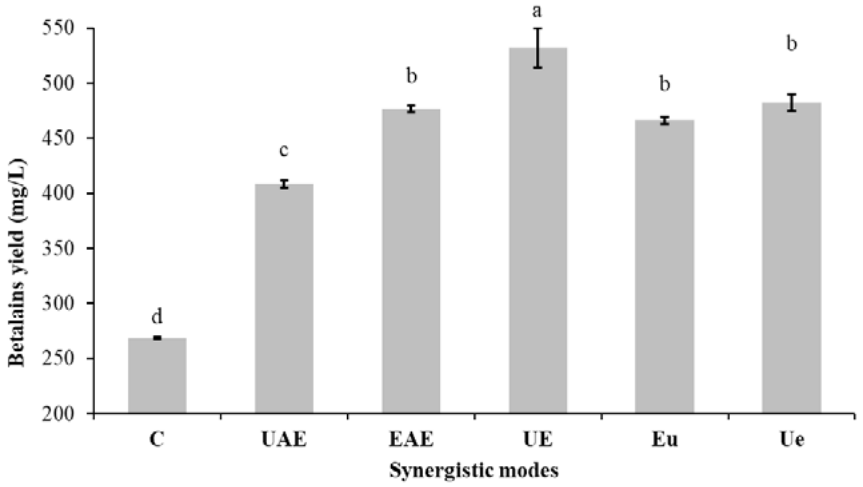

Figure 1. Effect of different synergistic modes on extraction yield of betalains from red beetroot. The models are: C, conventional solvent extraction; UAE, ultrasound-assisted extraction; EAE, enzyme-assisted extraction; Eu, enzymatic hydrolyzation first, followed by ultrasound extraction); Ue, ultrasound treatment first, followed by enzymatic-assisted extraction; UE, ultrasound treatment and enzymatic hydrolyzation happened simultaneously. Values marked by the same letter are not significantly different ($P < 0.05$).

3.2. Effect of enzyme concentration on betalains extraction yield

The effect of enzyme concentration on betalains extraction yield is shown in Figure 2a. The enzyme concentration was studied at different levels while other extraction conditions were fixed as follows: enzyme mixture composition, C:P (3:2); extraction temperature, 40°C; extraction time, 90 min. A significant increase in betalains yield was observed by increasing the enzyme concentration from 20 U/mL to 30 U/mL because higher enzyme concentration can enhance the hydrolyzation of the plant cell wall. The peak yield (516.83 ± 23.44 mg/L) was achieved at an enzyme concentration of 30 U/mL. When higher dosage of the enzyme mix (35 U/mL) were employed, the extraction yields decreased compared to the 30 U/mL dosage. This reduction in yield can be attributed by an end-production inhibition causing by a too fast hydrolysis as proposed in literature (Çinar, 2005; Ranveer et al., 2013). The enzyme concentration was selected as 30 U/mL for subsequent experiments.

3.3. Effect of enzyme mixture composition on betalains extraction yield

To study the effect of enzyme mixture composition on betalains extraction yield, the UAEE process was conducted using different enzyme mixture compositions (C:P). Other extraction conditions were fixed as follows: enzyme concentration, 30 U/mL; extraction temperature, 40°C; extraction time, 90 min. As shown in Figure 2b, when the compositions of C:P were set at 3:2, the betalains yield reached its peak value (513.43 ± 24.28 mg/L). The result indicated that this enzyme composition matches well with the cell wall composition of red beetroot, thus maximizing the hydrolyzation effect. This is in agreement with the cell wall composition of red beetroot determine in another study (Wu et al., 2014), where cellulose was 37% and pectin was 28%. The composition of C:P (3:2) was selected for subsequent experiments.

3.4. Effect of extraction temperature on betalains yield

The impact of extraction temperature on betalains yield is depicted in Figure 2c. Keeping other extraction condition constant (enzyme concentration 30 U/mL; enzyme composition, C:P (3:2); extraction time, 90 min), while various extraction temperatures were employed. An increase in extraction temperature from 30°C to 50°C led to a significant rise in betalains yield due to the enzyme-catalyzed activities that favor the release of betalains. The maximum yield (533.64 ± 14.46 mg/L) was achieved at 50°C, after which the yield decreased significantly ($P < 0.05$) upon further temperature increase. Higher temperatures resulted in a decrease in the number of cavitation bubbles and reduced the impact of cavity collapse on homogenized samples, leading to a decrease in enzyme activity (Palma & Barroso, 2002). As a result, the temperature was chosen to be 50°C for subsequent experiments.

3.5. Effect of extraction time on betalains yield

The UAEE method was conducted at different extraction times while fixing other extraction parameters as follows: enzyme concentration 30 U/mL; enzyme composition, C:P (3:2); extraction temperature, 50°C. As shown in Figure 2d, betalains yield was increased with the increase of extraction time up to 120 min ($P < 0.05$). This was since in the early stages of extraction, the ultrasound-induced damage to cell structures resulted in low diffusion resistance for intracellular matters, which facilitated their extraction (Linares & Rojas 2022). However, a notable decline in the yield of betalains in red

beetroot was observed when the extraction time exceeded 120 min ($P < 0.05$). This suggests that excessive extraction time (beyond 120 min) under ultrasound conditions caused oxidative degradation of betalains, thus resulting in reduced yield (Maran et al., 2015).

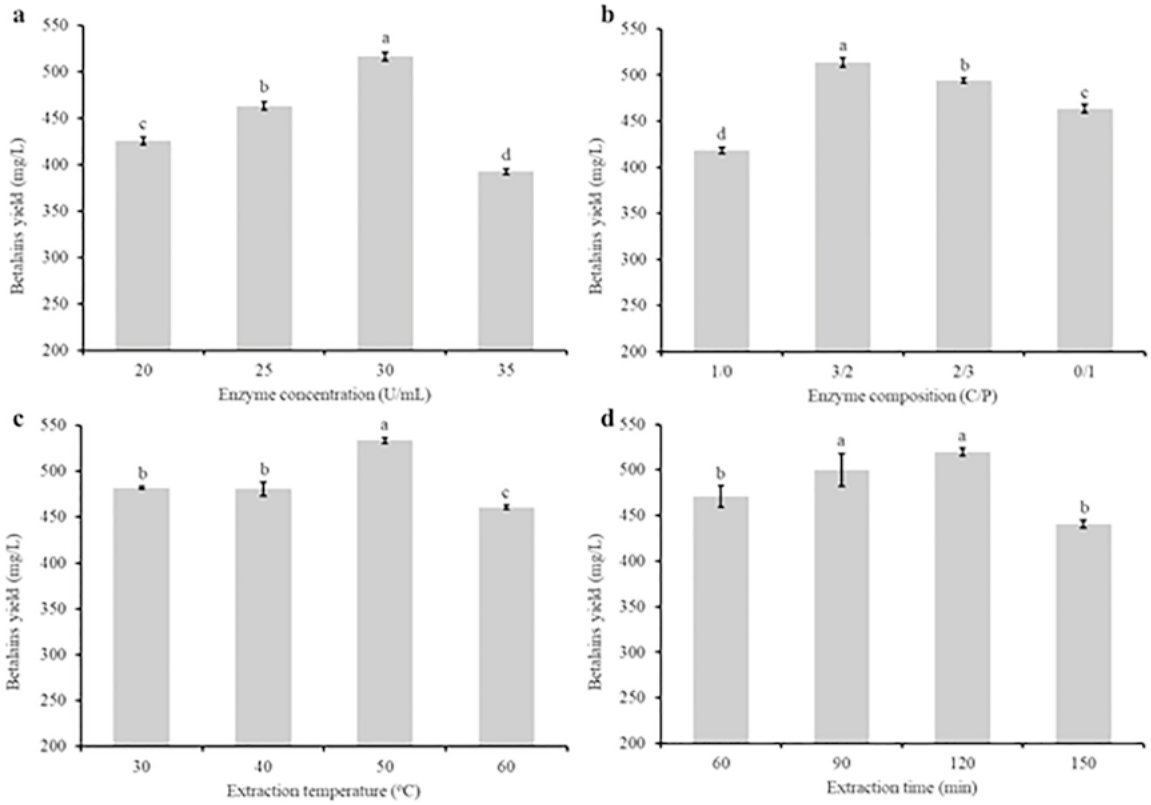

Figure 2. Effect of dependent variables on the extraction yield of betalains from red beetroot: (a) enzyme concentration; (b) enzyme composition; (c) extraction temperature; (d) extraction time. Values marked by the same letter are not significantly different ($P < 0.05$).

3.6. Optimization experiment

All 18 random sequential experiments under different extraction conditions were performed to study the reciprocal influence of independent variables (enzyme concentration, extraction temperature, and extraction time) on betalains extraction yield and to optimize the operating parameters. The actual and predicted values according to the factorial design are presented in Table 2. The experimental results showed that the linear coefficient of extraction temperature (X_2) and extraction time (X_3) were considerable ($P < 0.05$). In addition, enzyme concentration (X_1) and extraction temperature (X_3) had a significant quadratic effect on the yield of betalains ($P < 0.05$). The interaction terms of X_1X_2 was an extremely prominent effect for the betalains yield ($P < 0.01$). The unaffected factors ($P > 0.05$) are excluded from the quadratic equation. By applying multiple regression analysis to the experimental data, the final quadratic equation obtained in terms of actual actors is given below (3):

$$Y=517.75- 20.23X_2-12.51X_3-20.75X_1X_2-27.26X_1^2-41.91X_3^2$$

where, X_1, X_2, and X_3 are enzyme concentration, extraction temperature and extraction time, respectively.

Table 2. Response surface central composite design and results for extraction yield of betalains

Run	X_1 (U/mL)	X_2 (°C)	X_3 (min)	Betalains extraction yield (mg/L)	
				Predicted	Experimental
1	25	40	90	464.64	470.98
2	25	40	150	427.81	432.20
3	25	60	90	468.11	463.90
4	25	60	150	426.42	427.00
5	35	40	90	497.59	500.27
6	35	40	150	489.25	496.72
7	35	60	90	418.06	416.94
8	35	60	150	404.86	401.79
9	25	50	120	487.64	480.53
10	35	50	120	493.34	487.37
11	30	40	120	539.00	518.11
12	30	60	120	498.54	506.36
13	30	50	90	488.34	484.64
14	30	50	150	463.33	453.96
15	30	50	120	517.75	527.88
16	30	50	120	517.75	550.51
17	30	50	120	517.75	509.27
18	30	50	120	517.75	509.50

Enzyme concentration (U/mL).
Extraction temperature (°C).
Extraction time (min).

The prediction models for the yield of betalains was significant ($P < 0.01$) with a coefficient of determination (R2) of 0.923, indicating that there are 92.3% of the corresponding response variations could be explained as a function of three UAEE parameters (Myers et al., 2016) (Figure 3). An R^2 value of at least 0.75 recommended that the model fitted the experimental values well (Wang et al., 2019). In addition, the adjusted determination coefficient R^2_{Adj} value was used to check the overestimation of the R^2. The R^2_{Adj} value was calculated to be 0.837, also demonstrating a good correlation between experimental and predicted values. The results presented in Figure 3 also supported the adequacy of the model, where the points were very close to the fitted line.

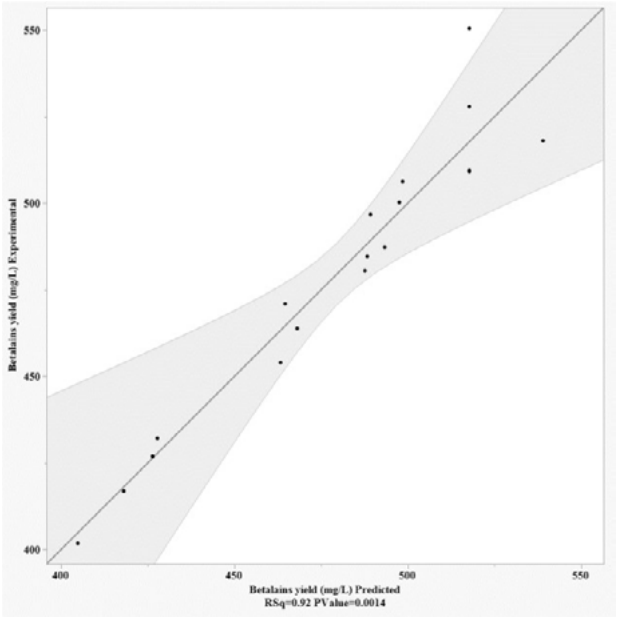

Figure 3. Predicted versus Experimental betalains yield.

To observe the effects of two UAEE parameters on betalains yield, the response surface plots were generated (Figure 4). One variable was kept constant at its respective zero level while two variables varied within their experimental ranges to understand their main and interactive effects on the dependent variable. The results show that increasing enzyme concentration and extraction time up to a threshold limit led to an increase in the betalains yield. However, when those parameters were increased above the threshold, the yield decreased. On the other hand, when increasing the temperature from 40°C to 60°C, the betalains yield decreased. These findings showed that better betalains yield could be obtained when the appropriate enzyme concentration and extraction time were applied. In addition, when the temperature was increased above the optimum level, the surface tension and viscosity of the solvent might be decreased, which altered the ultrasound cavitation and mass transfer intensity, thus reducing the extraction yield (Maran et al., 2015).

The response surface method was employed to predict the optimal conditions of betalains extraction and calculate the maximum betalains content. In this study, the desirability function was used as a tool to find the parameter settings that maximize overall desirability. According to the obtained model, the optimal conditions were determined as enzyme concentration of 32.1 U/mL, extraction temperature of 40°C and extraction time of 117 min with a desirability value of 0.91. Under these conditions, the predicted betalains yield was 544.5 mg/L. The validation experiment was performed, and experimental results showed an optimum betalains extraction yield of 550.51 ± 25.76 mg/L that was not statistically different compared to the predicted model ($P > 0.05$) suggesting that the model was adequate to reflect the expected optimization.

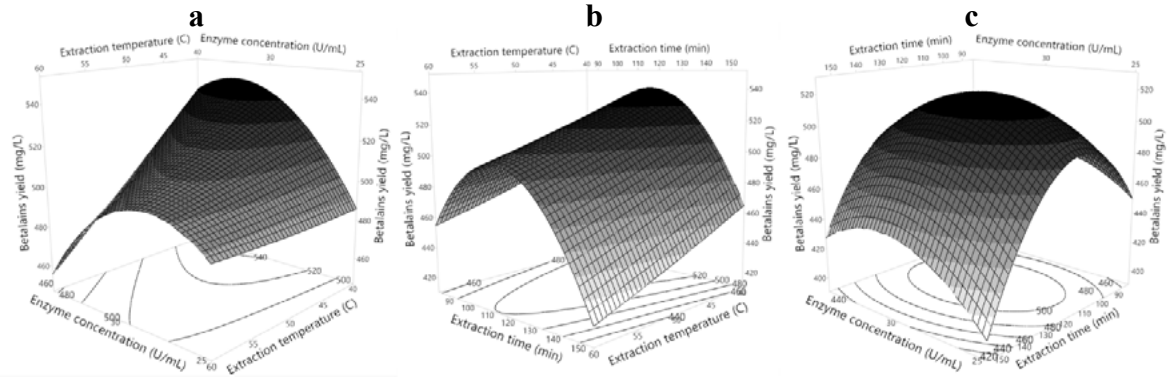

Figure 4. Response surface showing the effects of four variables (enzyme concentration, extraction temperature, extraction time) on extraction yield of betalains from red beetroot.

Conclusions

Ultrasound-assisted enzymatic extraction were employed for betalains extraction from red beetroot. The synergistic mode of simultaneous enzymatic hydrolyzation and ultrasound treatment was chosen for the UAEE process. The response surface methodology optimization of enzyme concentration, extraction temperature and temperature were performed. At the optimum conditions of enzyme concentration (32.1 U/mL), temperature (117°C) and time (117 min) yielded the highest betalains at the level of 550.51 ± 25.76 mg/L. Ultrasound-assisted enzymatic extraction is promissing for extracting betalains from red beetroot. The physicochemical and biological properties of obtained betalains should be further studied to elucidate the potentials of food applications.

Conflict of interest

The authors declare that they have no conflict of interest.

Acknowledgements

This study was funded by Nong Lam University Lecturer Scientific Research Grant (CS-CB22-HHTP-03).

References

Calva-Estrada, S. J., Jiménez-Fernández, M., & Lugo-Cervantes, E. (2022). Betalains and their applications in food: The current state of processing, stability and future opportunities in the industry. *Food Chemistry: Molecular Sciences 4*, 100089. https://doi.org/https://doi.org/10.1016/j.fochms.2022.100089.

Capelo, J. L., Maduro, C., & Vilhena, C. (2005). Discussion of parameters associated with the ultrasound solid–liquid extraction for elemental analysis (total content) by electrothermal atomic absorption spectrometry. An overview. *Ultrasounds Sonochemistry* 12(3), 225-232. https://doi.org/https://doi.org/10.1016/j.ultsonch.2003.10.010.

Cardoso-Ugarte, G. A., Sosa-Morales, M. E., Ballard, T., Liceaga, A., & Martín-González, M. F. S. (2014). Microwave-assisted extraction of betalains from red beet (Beta vulgaris). *LWT - Food Science and Technology* 59(1), 276-282. https://doi.org/https://doi.org/10.1016/j.lwt.2014.05.025.

Carreón-Hidalgo, J. P., Franco-Vásquez, D. C., Gómez-Linton, D. R., & Pérez-Flores, L. J. (2022). Betalain plant sources, biosynthesis, extraction, stability enhancement methods, bioactivity, and applications. *Food Research*

International 151, 110821. https://doi.org/https://doi.org/10.1016/j.foodres.2021.110821.

Chen, R. Z., Li, S. Z., Liu, C. M., Yang, S. M., & Li, X. L. (2012). Ultrasound complex enzymes assisted extraction and biochemical activities of polysaccharides from Epimedium leaves. *Process Biochemistry* 47(12), 2040-2050. https://doi.org/10.1016/j.procbio.2012.07.022.

Çinar, I. (2005). Effects of cellulase and pectinase concentrations on the colour yield of enzyme extracted plant carotenoids. *Process Biochemistry* 40(2), 945-949. https://doi.org/10.1016/j.procbio.2004.02.022.

Fares, M. M., & Bani-Domi, A. (2021). Sustainable betalain pigments as eco-friendly film coating over aluminium surface. *Journal of Materials Science* 56(24), 13556-13567. https://doi.org/doi:10.1007/s10853-021-06179-4.

Görgüç, A., Bircan, C., & Yılmaz, F. M. (2019). Sesame bran as an unexploited by-product: Effect of enzyme and ultrasound-assisted extraction on the recovery of protein and antioxidant compounds. *Food Chemistry* 283, 637-645. https://doi.org/10.1016/j.foodchem.2019.01.077.

Guesmi, A., Ladhari, N., Hamadi, N. B., & Sakli, F. (2012). Isolation, identification and dyeing studies of betanin on modified acrylic fabrics. *Industrial Crops and Products* 37(1), 342-346. https://doi.org/https://doi.org/10.1016/j.indcrop.2011.12.034.

Karki, B., Maurer, D., Kim, T. H., & Jung, S. (2011). Comparison and optimization of enzymatic saccharification of soybean fibers recovered from aqueous extractions. *Bioresource Technology* 102(2), 1228-1233. https://doi.org/10.1016/j.biortech.2010.08.004.

Li, F., Mao, Y. D., Wang, Y. F., Raza, A., Qiu, L. P., & Xu, X. Q. (2017). Optimization of ultrasound-assisted enzymatic extraction conditions for improving total phenolic content, antioxidant and antitumor activities in vitro from *Trapa quadrispinosa* Roxb. residues. *Molecules* 22(3), 396. https://doi.org/10.3390/molecules22030396.

Liao, N. B., Zhong, J. J., Ye, X. Q., Lu, S., Wang, W. J., Zhang, R. H., Xu, J., Chen, S. G., & Liu, D. H. (2015). Ultrasound-assisted enzymatic extraction of polysaccharide from Corbicula fluminea: Characterization and antioxidant activity. *LWT - Food Science and Technology* 60(2)2, 1113-1121. https://doi.org/10.1016/j.lwt.2014.10.009.

Linares, G., & Rojas, M. L. (2022). Ultrasound-assisted extraction of natural pigments from food processing by-products: A review. *Frontiers in Nutrition* 9. https://doi.org/10.3389/fnut.2022.891462.

Liu, Y., Gong, G., Zhang, J., Jia, S., Li, F., Wang, Y., & Wu, S. (2014). Response surface optimization of ultrasound-assisted enzymatic extraction polysaccharides from *Lycium barbarum*. *Carbohydrate Polymers* 110, 278-284. https://doi.org/10.1016/j.carbpol.2014.03.040.

Lombardelli, C., Benucci, I., Mazzocchi, C., & Esti, M. (2021). A Novel process for the recovery of betalains from unsold red beets by low-temperature enzyme-assisted extraction. *Foods* 10(2), 236. https://doi.org/10.3390/foods10020236.

Maran, J. P., Priya, B., & Nivetha, C. V. (2015). Optimization of ultrasound-assisted extraction of natural pigments from *Bougainvillea glabra* flowers. *Industrial Crops and Products* 63, 182-189. https://doi.org/https://doi.org/10.1016/j.indcrop.2014.09.059.

Myers, R. H., Montgomery, D. C., & Anderson-Cook, C. M. (2016). Response surface methodology: process and product optimization using designed experiments. In Wiley, J. (Ed.). *Wiley series in probability and statistics* (4th ed.). Retrieved April 1, 2023, from https://www.wiley.com/en-us/s.+and+Product+Optimization+Using+Designed+Experiments%2C+4th+Ed

ition-p-9781118916018.

Neagu, C., & Barbu, V. (2014). Principal component analysis of the factors involved in the extraction of beetroot betalains. *Journal of Agroalimentary Processes and Technologies* 20(4), 311-318.

Palma, M., & Barroso, C. G. (2002). Ultrasound-assisted extraction and determination of tartaric and malic acids from grapes and winemaking by-products. *Analytica Chimica Acta* 458(1), 119-130. https://doi.org/https://doi.org/10.1016/S0003-2670(01)01527-6.

Pandey, G., Pandey, V., Pandey, P. R., & Thomas, G. (2018). Effect of extraction solvent temperature on betalain content, phenolic content, antioxidant activity and stability of beetroot (*Beta vulgaris* L.) powder under different storage conditions. *Plant Archives* 18(2), 1623-1627.

Ranveer, R. C., Patil, S. N., & Sahoo, A. K. (2013). Effect of different parameters on enzyme-assisted extraction of lycopene from tomato processing waste. *Food and Bioproducts Processing* 91(4), 370-375. https://doi.org/10.1016/j.fbp.2013.01.006.

Silva, H. R. P. D., Silva, C. D., & Bolanho, B. C. (2018). Ultrasound-assisted extraction of betalains from red beet (*Beta vulgaris* L.). *Journal of Food Process Engineering* 41(6). https://doi.org/10.1111/jfpe.12833.

Tiwari, B. K., & Cullen, P. J. (2012). Extraction of red beet pigments. In Neelwarne, B. (Ed.). *Red beet biotechnology: Food and pharmaceutical applications* (373-391). Massachusetts, USA: Springer Publishing. https://doi.org/10.1007/978-1-4614-3458-0_14.

Wang, F., Wang, F., Zhang, Y., Hu, J., Huang, J., & Xie, J. (2019). Rice yield estimation using parcel-level relative spectral variables from UAV-based hyperspectral imagery. *Frontiers in Plant Science* 10, 453. https://doi.org/10.3389/fpls.2019.00453.

Wiley, R. C., & Lee, Y. N. (1978). Recovery of betalaines from red beets by a diffusion-extraction procedure. *Journal of Food Science* 43(4), 1056-1058. https://doi.org/10.1111/j.1365-2621.1978.tb15231.x.

Wilkinson, L. (1989). *SYSTAT: The system for statistics*. Illinois, USA: SYSTAT.

Wruss, J., Waldenberger, G., Huemer, S., Uygun, P., Lanzerstorfer, P., Müller, U., Höglinger, O., & Weghuber, J. (2015). Compositional characteristics of commercial beetroot products and beetroot juice prepared from seven beetroot varieties grown in Upper Austria. *Journal of Food Composition and Analysis* 42, 46-55. https://doi.org/10.1016/j.jfca.2015.03.005.

Wu, H., Zhu, J. X., Diao, W. C., & Wang, C. R. (2014). Ultrasound-assisted enzymatic extraction and antioxidant activity of polysaccharides from pumpkin (*Cucurbita moschata*). *Carbohydrate Polymers* 113(113), 314-324. https://doi.org/10.1016/j.carbpol.2014.07.025.

Yao, X., Hu, H., Qin, Y., & Liu, J. (2020). Development of antioxidant, antimicrobial and ammonia-sensitive films based on quaternary ammonium chitosan, polyvinyl alcohol and betalains-rich cactus pears (Opuntia ficus-indica) extract. *Food Hydrocolloids* 106, 105896. https://doi.org/https://doi.org/10.1016/j.foodhyd.2020.105896.

Friedel-Crafts sulfonylation catalyzed by chloroaluminate ionic liquid immobilized on magnetic nanoparticles: Optimization by response surface methodology

Lan N. T. Nguyen[1*], Ngan T. T. Luu[1], Huy H. Le[1], Ha T. T. Phan[2], Viet B. Nguyen[1], & Thi X. T. Luu[2]

[1]Faculty of Chemical Engineering and Food Technology, Nong Lam University, Ho Chi Minh City, Vietnam

[2]Faculty of Chemistry, University of Science, Vietnam National University of Ho Chi Minh City, Ho Chi Minh City, Vietnam

ARTICLE INFO

Research Paper

Received: May 16, 2022

Revised: June 16, 2022

Accepted: July 11, 2022

Keywords

Ionic liquid

Magnetic nanoparticles

Response surface methodology

Sulfone

Sulfonylation

***Corresponding author**

Nguyen Thi Ngoc Lan

Email:

ntngoclan@hcmuaf.edu.vn

ABSTRACT

This study focused on optimizing the Friedel-Crafts sulfonylation reaction between 1,3-dimethoxybenzene and p-toluenesulfonic anhydride using chloroaluminate ionic liquid immobilized on magnetic nanoparticles as the catalyst. Various reaction conditions including the ratio between reagents (0.9:1.0 - 1.1:1.0), the catalyst amount (0.1 - 0.3 g), reaction temperature (100 - 120°C), and time (1 - 3 h) were optimized using response surface methodology based on a central composite design model. The results showed that the optimal reaction conditions were achieved at 115°C for 2.3 h, using 0.24 g of catalyst with a reagent ratio of 1.0:1.0, resulting in the highest sulfones yield of 82%.

Cited as: Nguyen, L. N. T., Luu, N. T., Le, H. H., Phan, H. T. T., Nguyen, V. B., & Luu, T. X. T. (2023). Friedel-Crafts sulfonylation catalyzed by chloroaluminate ionic liquid immobilized on magnetic nanoparticles: Optimization by response surface methodology. *The Journal of Agriculture and Development* 22(6), 78-91.

1. Introduction

Sulfones are organosulfur compounds with structural formula R-S(O)2-R', where R and R' are organic groups. Under different reaction conditions, the carbon bearing sulfonyl group can be converted to a cation, an anion or a radical (Trost & Kalnmals, 2019). Therefore, sulfones were used as intermediates in many organic synthesis processes (Leusen et al., 1977; Swenson et al., 2002; Li & Corey, 2005). Among them, aryl sulfones have wide applications such as agrochemicals (Michaely et al., 1988), polymers (Robello et al., 1993; MacKinnon & Wang, 1998). For aryl sulfones preparation, Friedel-Crafts sulfonylation is one of the most common methods (Figure 1). The electrophilic substitution reaction of arenes and sulfonylating reagents is catalysed by various Lewis acid such as metal salts (Marquié et al., 2001; Fleck et al., 2006), metals with or without solvent (Bandgar & Kasture, 2001; Jang et al., 2006), solid acids (Choudary et al., 2000), ionic liquids (Nara et al., 2001; Bahrami et al., 2008). Although aryl sulfones can be obtained with moderate to high yield (50 - 90%), the catalysts are difficult to recover and reuse.

With the development of green chemistry, various alternative methods were introduced for chemical processes. Recent studies mainly focused on applying eco-friendly catalysts for organic syntheses. For example, our group successfully synthesized chloroaluminate ionic liquid immobilized on magnetic nanoparticles and then applying this catalyst for Friedel-Crafts sulfonylation (Nguyen et al., 2022). The material overcomes the disadvantages of homogeneous and heterogeneous catalysts in terms of dispersion, reuse and can be recovered easily after the reaction by external magnets.

As most organic synthesis reactions, the yield of Friedel-Crafts sulfonylation also strongly depends on the reaction conditions such as the molar ratio, the time, temperature of reaction and of course, the amount of catalyst. These factors are often correlated with each other, so it is necessary to investigate their interaction effects. Response surface methodology (RSM) is a useful statistical tool which is widely applied for optimization in many fields such as extraction (Zhang et al., 2018; Yu et al., 2019; Andres et al., 2020), organic synthesis (Hamsaveni et al., 2001; García-Cabeza et al., 2015; He et al.,

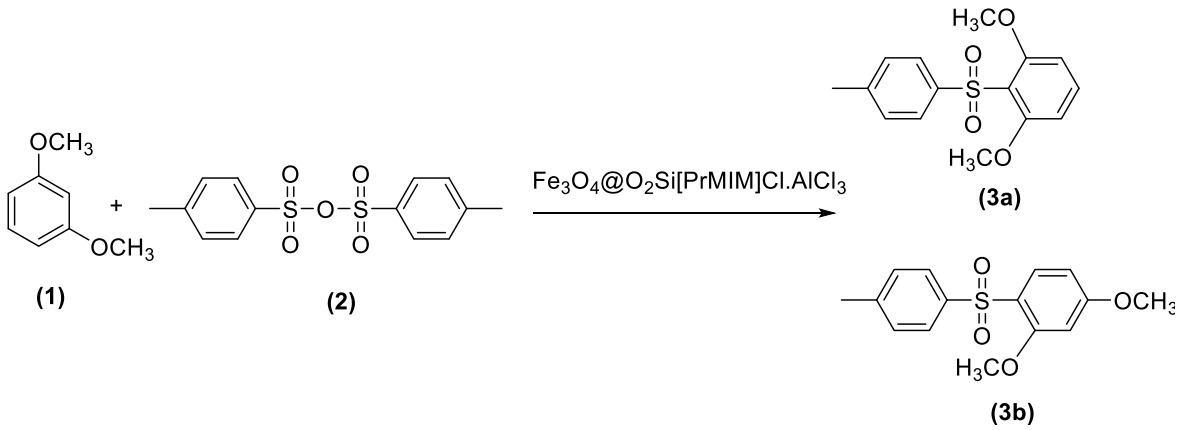

Figure 1. The Friedel-Crafts sulfonylation between 1,3-dimethoxybenzene and p-toluenesulfonic anhydride catalyzed by $Fe_3O_4@O_2Si.[PrMIM]Cl.AlCl_3$.

2017), nanomaterial synthesis (Perez et al., 2017; Abdulhameed et al., 2019; Sarsfield et al., 2021). This study, therefore, aimed to apply RSM to optimize a Friedel-Crafts sulfonylation between 1,3-dimethoxybenzene and p-toluenesulfonic anhydride using chloroaluminate ionic liquid immobilized on magnetic nanoparticles as the catalyst.

2. Materials and Methods

2.1. Materials

1,3-dimethoxybenzene, 1-methylimidazole, (3-chloropropyl) trimethoxysilane, anhydrous aluminum chloride were purchased from Sigma-Aldrich (Germany) while n-hexane, ethyl acetate, diethyl ether, ammonia solution, sodium sulphate, sodium hydroxide, iron (II) sulphate heptahydrate, iron (III) nitrate nonahydrate were provided by Xilong (China). Other chemical compounds including p-toluenesulfonic anhydride and ethanol absolute were from Acros (Belgium) and Prolabo (France), respectively.

2.2. Methods

2.2.1. Preparation of catalyst

Magnetic Fe_3O_4 nanoparticles (MNPs) were prepared by the modified chemical coprecipitation method (Safari & Zarnegar, 2013). Typically, $FeSO_4.7H_2O$ (6.0 mmol) and $Fe(NO_3)_3.9H_2O$ (12.0 mmol) were dissolved in 100 mL distilled water. Under mechanical stirring at 500 rpm, the mixture were dropped slowly into a 500 mL beaker containing 200 mL NaOH 0.25 M solution within 1 h at 80°C. The black precipitated particles were washed with distilled water (2 x 100 mL) until pH 7 and dried at 150°C for 4 h.

For Fe_3O_4@O_2Si[PrMIM]Cl.$AlCl_3$, a mixture of (3-chloropropyl) trimethoxysilane (20 mmol) and 1-methylimidazole (20 mmol) in a round-bottom 25 mL flask were stirred at 80°C for 3 days. After reaction completion, the mixture of products was washed with diethyl ether (3 × 5 mL) and the solvent was remove under vacuum pressure (Safari & Zarnegar, 2013). Then, MNPs (1.0 mmol), 3-methyl-1-(3-trimethoxysilylpropyl)-1H-imidazole-3-ium chloride (2.0 mmol), absolute ethanol (5.0 mL), and 28% ammonia solution (0.2 mL) were added into a round-bottom 25 mL flask and stirred at room temperature for 24 h. After reaction completion, Fe_3O_4@O_2Si[PrMIM]Cl was separated by an external magnet, washed with ethanol (2 x 5 mL) and left to dry in a desiccator. In the next step, anhydrous aluminum chloride $AlCl_3$ (4.0 mmol), was added slowly into a 25 mL round-bottom flask containing Fe_3O_4@O_2Si[PrMIM]Cl dispersed in 5 mL of absolute ethanol. The mixture was stirred at room temperature for 12 h. Finally, the catalyst Fe_3O_4@O_2Si[PrMIM]Cl.$AlCl_3$ was washed with ethanol (2 x 5 mL) and put into a desiccator overnight.

2.2.2. Typical procedure for the Friedel-Crafts sulfonylation

1,3-dimethoxybenzene, p-toluenesulfonic anhydride and catalyst were added into a 5 mL round-bottom flask assembled with the condenser. The reaction mixture was heated for a specific period of time. After completion of the reaction, the mixture of products was cooled and extracted with ethyl acetate (4 × 5 mL) and the solid catalyst was separated by using a magnetic bar. The organics were washed with water (2 × 10 mL), dried with anhydrous Na_2SO_4 and the solvent was removed using a rotary evaporator (Heidolph, Germany). Sulfones were purified by column chromatography using eluent as a mixture of n-hexane and ethyl acetate (8:2 v/v) and identified by 1H and 13C NMR spectroscopy.

2.2.3. Expermental design

Four important parameters of the reaction were studied, including temperature (X_1), reaction time (X_2), amount of catalyst (X_3), and molar ratio of 1,3-dimethoxybenzene to p-toluenesulfonic anhydride (X4). Screening experiments were conducted to evaluate the effects of each factor. The temperature was investigated in a range of 80 - 110°C while reaction time was kept from 0.5 - 2.0 h. The mixture of 1,3-dimethoxybenzene and p-toluenesulfonic anhydride were investigated at different ratios of 0.9:1.0 - 1.2:1.0 and the amount of catalyst was in a range of 0.1 - 0.2 g. Then the reaction conditions of sulfone synthesis were optimized by RSM combined with a central composite design (CCD). The range and levels of the factors used in the experiment design were list in Table 1.

Table 1. Experimental range and levels of the factors

Factors	Level		
	-1	0	+1
X_1 (Temperature/°C)	100	110	120
X_2 (Reaction time/h)	1	2	3
X_3 (Amount of catalyst/g)	0.1	0.2	0.3
X_4 (Molar ratio)	0.9:1.0	1.0:1.0	1.1:1.0

2.2.4. Analytical method

Gas chromatography system (Agilent, USA) with a capillary column (30 m x 0.25 mm x 0.25 μM) was used for analyzing sulfone yields. The carrier gas flow rate is 21.6 mL of hydrogen/min. The GC oven temperature program was 60°C (1 min hold), 20°C/min to 300°C (10 min hold) for a total runtime of 23 min. Aryl sulfones yield and conversion were determined by the following formula:

$$\text{Yield} = \frac{m_1 . b}{m_2} \text{x} 100\%$$

$$\text{Conversion} = \frac{m_3}{m_4} \text{x} 100\%$$

Where

m_1: mass of the crude product after the reaction (g)

b: percent composition of the product based on the *gas chromatography/flame ionization detector analyses*

m_2: mass of the product in theory (g)

m_3: mass of 1,3-dimethoxybenzene after the reaction (g)

m_4: mass of 1,3-dimethoxybenzene before the reaction (g)

2.2.5. Statistical analysis

All experiments were carried out 2 times. Optimal data were designed and analysed using a software JMP (v.14, SAS Institute, USA). The effects of reaction time, reaction temperature, the reagent ratio and the amount of catalyst were evaluated by ANOVA at 95% confident interval using a software Statgraphics Centurion (v.XVI, Statgraphics Technologies, USA).

3. Results and Discussion

3.1. Screening experiments

The effect of reaction time on the sulfone yield was depicted on the Figure 2. The conditions were fixed at the ratio of 1,3-dimethoxybenzene and p-toluenesulfonic anhydride as 1.0:1.0, temperature of 110°C with 0.2 g Fe_3O_4@O_2Si.[PrMIM]Cl.$AlCl_3$ as catalyst. For a chemical reaction, it takes a certain time for the substrate and reagent to react with each other, so as the reaction time is increased from 0.5 to 2 h, the yield also increases gradually. When the reaction time increases to 2 h, the conversion reaches 100% and the yield reaches its maximum value of 83%. Therefore, 2 h was chosen as the appropriate time for the sulfonylation and fixed for further experiments.

Figure 3 shows the change of reaction yield when increasing the temperature from 80 to 110°C. The sulfonylation was carried out at ratio of 1,3-dimethoxybenzene and *p*-toluenesulfonic anhydride as 1.0:1.0 with 0.2 g of catalyst for 2 h. At 80°C, the yield of sulfone reached 41% and gradually increased, the highest reaction yield was 83% at 110°C. The possible reason was that the Friedel-Crafts sulfonylation is an endothermic reaction, so a higher temperature can make the substrate convert completely and obtain a higher yield. Then, the suitable temperature for the reaction was chosen as 110°C and fixed for next experiments.

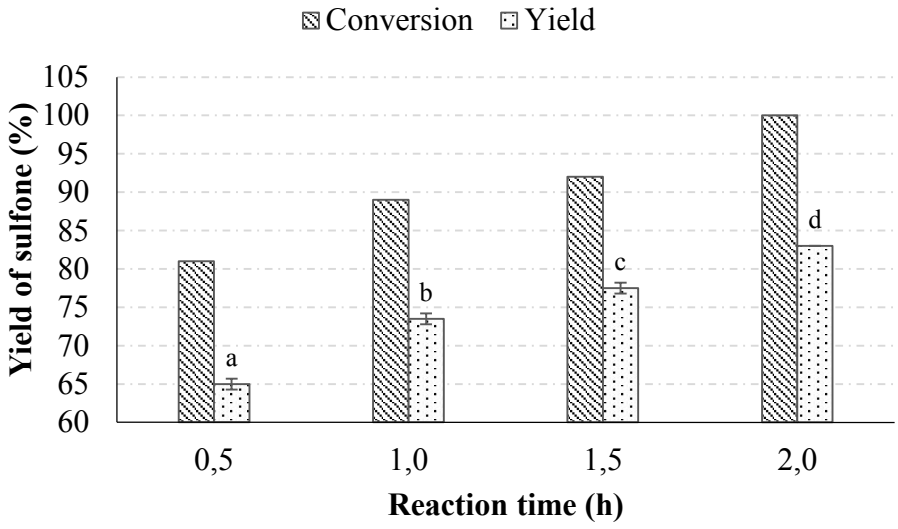

Figure 2. Effect of reaction time on the yield of sulfone. *The letters a,b,c,d represent the difference of the treatments; ***Yields were calculated based on the gas chromatography/flame ionization detector analyses.*

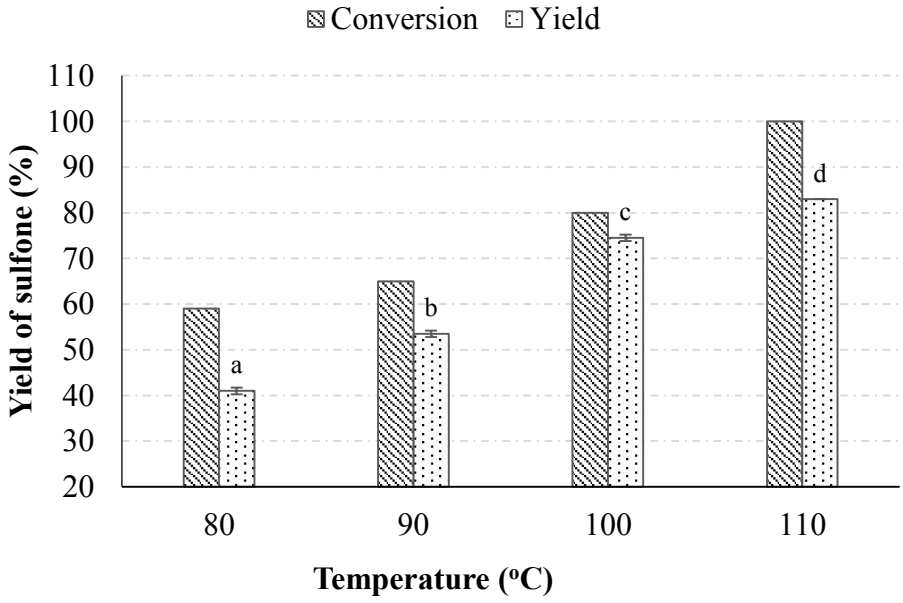

Figure 3. Effect of temperature on the yield of sulfone. *The letters a,b,c,d represent the difference of the treatments; ***Yields were calculated based on the gas chromatography/flame ionization detector analyses.*

To investigate the effect of catalyst amount, sulfone was synthesized at fixed ratio of 1,3-dimethoxybenzene and *p*-toluenesulfonic acid anhydride as 1.0:1.0, temperature of 110°C and reaction time of 2 h. The amount of Fe_3O_4@ O_2Si.[PrMIM]Cl.$AlCl_3$ used for the reaction was investigated from 0.1 to 0.2 g. Friedel-Crafts sulfonylation is an electrophilic substitution, it requires the presence of Lewis acid as a catalyst. That means the yield and conversion of the reaction will be higher when the catalytic amount is increased. As seen in Figure 4, when the amount of catalyst was increased to 0.2 g, sulfone was obtained with the highest yield. Therefore, the catalyst used for the following experiments is 0.2 g.

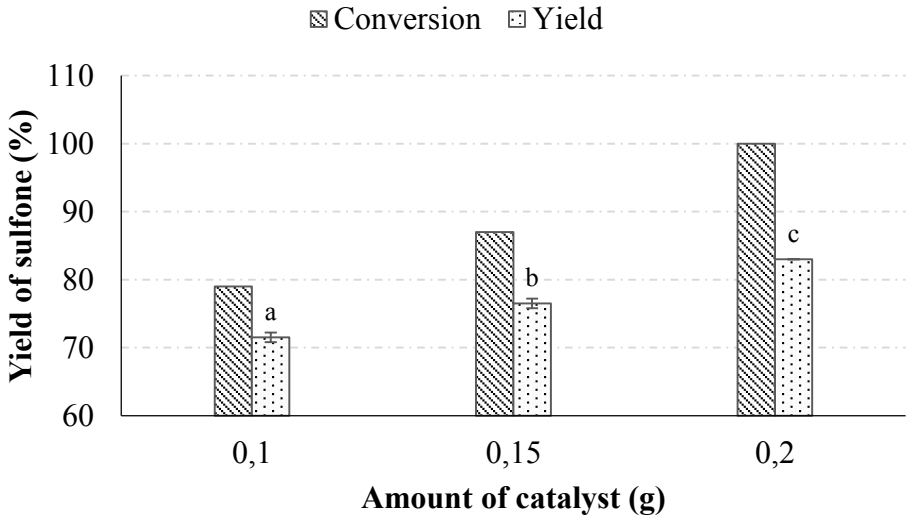

Figure 4. Effect of catalyst amount on the yield of sulfone. *The letters a,b,c represent the difference of the treatments; ***Yields were calculated based on the gas chromatography/flame ionization detector analyses.*

After the reaction, *p*-toluenesulfonic anhydride was converted to acid and removed in the aqueous phase. So, in order to evaluate the appropriate molar ratio of reagents, the reaction was carried out at 110°C for 2 h with 0.2 g of catalyst and the moles of 1,3-dimethoxybenzene was varied from 0.9 to 1.2 mmol. When the substrate:reagent ratio increases to 1.0:1.0, the yield of sulfone reaches the maximum value and the reaction is converted completely. While the molarity of 1,3-dimethoxybenzene exceeds 1.0 mmol, the reduced product content leads to a decrease in sulfone yield. This shows that the suitable ratio between 1,3-dimethoxybenzene and *p*-toluenesulfonic anhydride for the reaction should be 1.0:1.0 (Figure 5).

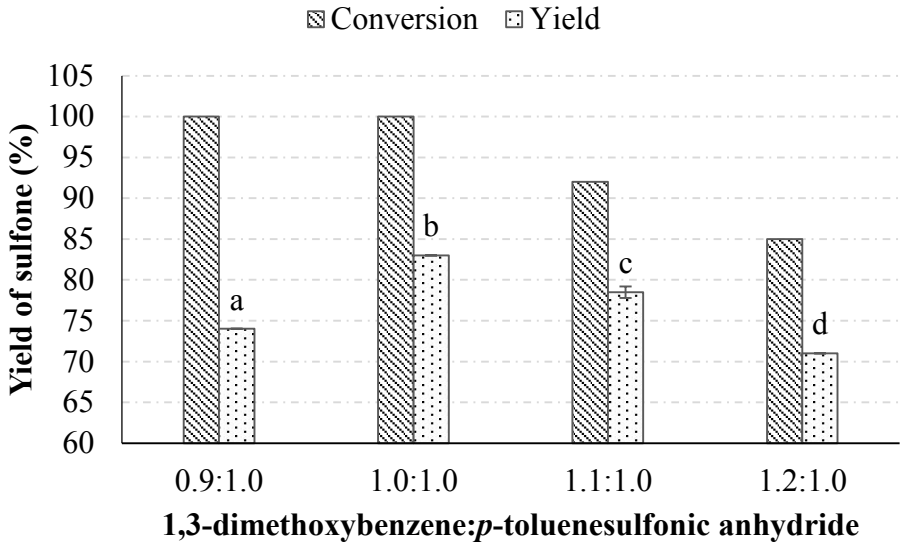

Figure 5. Effect of substrate:reagent ratio on the yield of sulfone. *The letters a,b,c,d represent the difference of the treatments; ***Yields were calculated based on the gas chromatography/flame ionization detector analyses.*

3.2. Optimization of reaction conditions by RSM

Based on the results of the single-factor experiments, reaction conditions including temperature (X_1), reaction time (X_2), amount of catalyst (X_3) and molar ratio (X_4) were selected as independent variables for the optimization process. The CCD design and reaction yield results are presented in Table 2.

It can be seen that the reaction yield is varied from 65 to 83%. Besides, the RSM model describing the relationship between the reaction yield and the reaction conditions was determined as follows:

$$Y = 80.5 + 1.2778X_1 + 1.1667X_2 + 2.9444X_3 + 1.3333X_4 - 1.3125X_2X_3 + 1.3125X_3X_4 - 3.6667X_3^2 - 3.1667X_4^2$$

Table 2. Design model and results of response surface experiments

Entry[a]	Temperature (°C) X_1	Time (h) X_2	Amount of catalyst (g) X_3	Molar ratio[b] X_4	Yield[c] (%) (3a:3b)
1	120	3	0.1	1.1:1.0	70 (10:90)
2	110	2	0.1	1.0:1.0	72 (9:91)
3	100	3	0.3	0.9:1.0	68 (17:83)
4	100	2	0.2	1.0:1.0	75 (9:91)
5	100	1	0.1	0.9:1.0	65 (11:89)
6	120	1	0.1	1.1:1.0	66 (14:86)
7	100	3	0.1	1.1:1.0	68 (11:89)
8	100	3	0.3	1.1:1.0	73 (15:85)
9	120	3	0.3	0.9:1.0	72 (14:86)
10	110	2	0.3	1.0:1.0	80 (16:84)
11	110	1	0.2	1.0:1.0	74 (9:91)
12	120	1	0.3	1.1:1.0	76 (2:98)
13	110	2	0.2	1.0:1.0	83 (17:83)
14	110	3	0.2	1.0:1.0	82 (16:84)
15	110	2	0.2	1.0:1.0	83 (15:85)
16	120	3	0.1	0.9:1.0	73 (12:88)
17	120	2	0.2	1.0:1.0	81 (13:87)
18	100	3	0.1	0.9:1.0	68 (10:90)
19	120	1	0.3	0.9:1.0	72 (8:92)
20	100	1	0.1	1.1:1.0	66 (14:86)
21	110	2	0.2	1.1:1.0	79 (13:87)
22	100	1	0.3	1.1:1.0	76 (9:91)
23	120	3	0.3	1.1:1.0	78 (9:91)
24	120	1	0.1	0.9:1.0	65 (9:91)
25	100	1	0.3	0.9:1.0	71 (2:98)
26	110	2	0.2	0.9:1.0	74 (15:85)

[a] Experiments are conducted at random. [b] 1,3-dimethoxybenzene : *p*-toluenesulfonic anhydride.

[c] Yields were calculated based on the GC/FID analyses.

The analysis results show that the regression model has R2 value of 0.93 with *P-value* is less than 5%. Therefore, this RSM model is appropriate to predict the reaction yield for the Friedel-Crafts sulfonylation reaction between 1,3-dimethoxybenzene and p-toluenesulfonic anhydride using chloroaluminate ionic liquid immobilized on magnetic nanoparticles as the catalyst.

According to the effect summary results (Table 3), it can be seen that the reaction yield is influenced by the linear effects of all 4 factors: temperature (X_1), reaction time (X_2), amount of catalyst (X_3), molar ratio (X_4); the quadratic effects of X_3, X_4 and the interaction effects between X_2 and X_3, X_3 and X_4. The influence of these factors on the reaction yield is depicted by three-dimensional surface response and 2D contour plots in Figure 6 with the red area representing the highest yield, while the blue area representing the lower results. The reaction yield began to increase to the central value, and then tend to decrease or approach the horizontal line with increasing reaction time, temperature, catalyst amount and molarity of 1,3-dimethoxybenzene. In which, the amount of catalyst (X_3) is the most influential factor. Besides, the isomer selectivity between para and ortho does not change significantly when investigating the influence of four factors.

Table 3. Coefficients in the regression equation

Sources	Variables	Coefficient value	*P*-value	
Linear effects	Constant	80.5	<0.0001	Significant
	X_1	1.2778	0.0322	Significant
	X_2	1.1667	0.0469	Significant
	X_3	2.9444	0.0001	Significant
	X_4	1.3333	0.0267	Significant
Quadratic effects	X_1^2	-1.6667	0.2533	
	X_2^2	-1.6667	0.2533	
	X_3^2	-3.6667	0.0225	Significant
	X_4^2	-3.1667	0.0427	Significant
Interaction effects	X_1X_2	0.9375	0.1182	
	X_1X_3	0.1875	0.7410	
	X_2X_3	-1.3125	0.0370	Significant
	X_1X_4	-0.1875	0.7410	
	X_2X_4	-0.1875	0.7410	
	X_3X_4	1.3125	0.0370	Significant

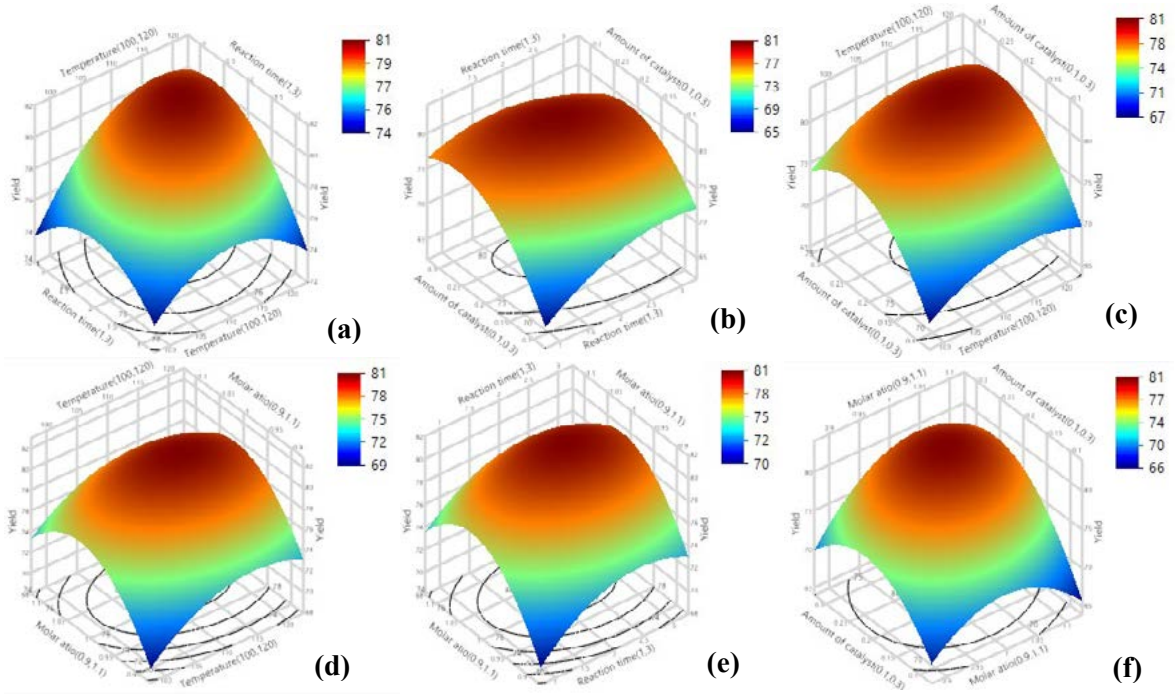

Figure 6. Response surface (3D) show the effect of the temperature and reactione time (**a**), reaction time and amount of catalyst (**b**), temperature and amount of catalyst (**c**), temperature and molar ratio (**d**), reaction time and molar ratio (**e**), amount of catalyst and molar ratio (**f**) on the reaction yield.

Numerical optimization was performed to predict the reaction yield and the profile was summarized in Figure 7. The optimal conditions for Friedel-Crafts sulfonylation are the temperature 115°C, the reaction time 2.3 h, the catalyst amount 0.24 g and the molar ratio 1.0:1.0. The predicted yield under the optimal conditions is 82%. To evaluate the compatibility of the results obtained from the regression equation by RSM with the experiment, the sulfonylation was carried out at the selected optimal conditions. Compared with the model results, the actual yield obtained from verification experiment is 81 ± 0.7%. With an error of less than 5%, that means the measured yield is suitable for the predicted value of the quadratic regression equation.

4. Conclusions

This study applied response surface methodology combined with CCD to investigate the effect of reaction temperature, reaction time, amount of catalyst, molar ratio on the yield of Friedel-Crafts sulfonylation between 1,3-dimethoxybenzene and p-toluenesulfonic anhydride using chloroaluminate inonic liquid immobilized on magnetic nanoparticles as the catalyst. The results showed that all investigated factors have significant effects on the sulfone yield and the predicted optimal values for this reaction are determined as follows: temperature 115°C, reaction time 2.3 h, amount of catalyst 0.24 g and ratio of 1,3-dimethoxybenzene and p-toluenesulfonic anhydride 1.0:1.0. At the

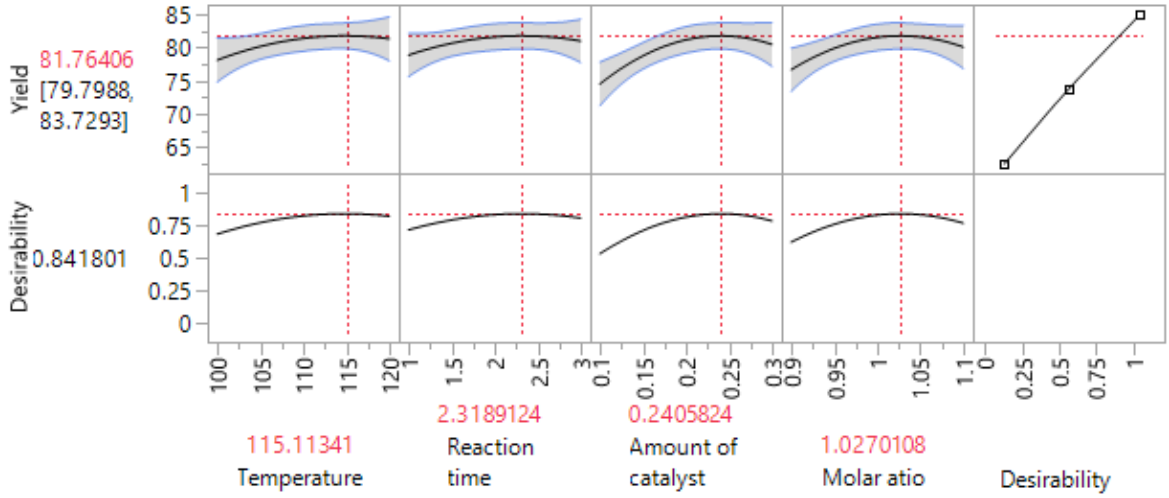

Figure 7. Optimal condition prediction model.

optimal reaction conditions, the reaction yield of the Friedel-Crafts sulfonylation could achieve 82%.

Conflict of interest

The authors declare no conflict of interest.

Acknowledgements

The authors would like to thank Nong Lam University, Ho Chi Minh City for sponsoring our research (project number: CS-CB21-CNHH-02).

References

Abdulhameed, A. S., Mohammad, A. T., & Jawad, A. H. (2019). Application of response surface methodology for enhanced synthesis of chitosan tripolyphosphate/TiO_2 nanocomposite and adsorption of reactive orange 16 dye. *Journal of Cleaner Production* 232, 43-56. https://doi.org/10.1016/j.jclepro.2019.05.291.

Andres, A. I., Petron, M. J., Lopez, A. M., & Timon, M. L. (2020). Optimization of extraction conditions to improve phenolic content and in vitro antioxidant activity in craft brewers' spent grain using response surface methodology (RSM). *Foods* 9(10), 1398. https://doi.org/10.3390/foods9101398.

Bahrami, K., Khodei, M. M., & Shahbazi, F. (2008). Highly selective catalytic Friedel–Crafts sulfonylation of aromatic compounds using a $FeCl_3$-based ionic liquid. *Tetrahedron Letters* 49(24), 3931-3934. https://doi.org/10.1016/j.tetlet.2008.04.051.

Bandgar, B. P., & Kasture, S. P. (2001). Zinc-mediated fast sulfonylation of aromatics. *Synthetic Communications* 31(7), 1065-1068. https://doi.org/10.1081/scc-100103538.

Choudary, B. M., Chowdari, N. S., & Kantam, M. L. (2000). Friedel–Crafts sulfonylation of aromatics catalysed by solid acids: An eco-friendly route for sulfone synthesis. *Journal of the Chemical Society, Perkin Transactions* 1 16, 2689-2693. https://doi.org/10.1039/b002931i.

Fleck, T. J., Chen, J. J., Lu, C. V., & Hanson, K. J. (2006). Isomerization-free Sulfonylation and its application in the synthesis of PHA-565272A.

Organic Process Research & Development 10(2), 334-338. https://doi.org/10.1021/op050208a.

García-Cabeza, A. L., Ray, L. P., Marín-Barrios, R., Ortega, M. J., Moreno-Dorado, F. J., Guerra, F. M., & Massanet, G. M. (2015). Optimization by response surface methodology (RSM) of the Kharasch–Sosnovsky oxidation of valencene. *Organic Process Research & Development* 19(11), 1662-1666. https://doi.org/10.1021/op5002462.

Hamsaveni, D. R., Prapulla, S. G., & Divakar, S. (2001). Response surface methodological approach for the synthesis of isobutyl isobutyrate. *Process Biochemistry* 36(11), 1103-1109. https://doi.org/10.1016/S0032-9592(01)00142-X.

Jang, D. O., Moon, K. S., Cho, D. H., & Kim, J. G. (2006). Highly selective catalytic Friedel–Crafts acylation and sulfonylation of activated aromatic compounds using indium metal. *Tetrahedron Letters* 47(34), 6063-6066. https://doi.org/10.1016/j.tetlet.2006.06.099.

Leusen, A. M. V., Wildeman, J., & Oldenziel, O. H. (1977). Chemistry of sulfonylmethyl isocyanides. 12. Base-induced cycloaddition of sulfonylmethyl isocyanides to carbon,nitrogen double bonds. Synthesis of 1,5-disubstituted and 1,4,5-trisubstituted imidazoles from aldimines and imidoyl chlorides. *The Journal of Organic Chemistry* 42(7), 1153-1159. https://doi.org/10.1021/jo00427a012.

Li, J. J., & Corey, E. J. (2005). *Name reactions in heterocyclic chemistry*. New Jersey, USA: John Wiley & Sons. https://doi.org/10.1002/0471704156.

MacKinnon, S. M., & Wang, Z. Y. (1998). Anhydride-containing polysulfones derived from a novel A2X-type monomer. *Macromolecules* 31(22), 7970-7972. https://doi.org/10.1021/ma9803640.

Marquié, J., Salmoria, G., Poux, M., Laporterie, A., Dubac, J., & Roques, N. (2001). Acylation and related reactions under microwaves. 5. Development to large laboratory scale with a continuous-flow process. *Industrial and Engineering Chemistry Research* 40(21), 4485-4490. https://doi.org/10.1021/ie0103299.

Michaely, W. J., & Kraatz, G. W. (1988). *Certain 2-(substituted benzoyl)-1,3-cyclohexanediones and ther use as herbicdes*. Virginia, USA: Zeneca Inc, Syngenta Crop Protection LLC.

Nara, S. J., Harjani, J. R., & Salunkhe, M. M. (2001). Friedel-Crafts sulfonylation in 1-Butyl-3-methylimidazolium chloroaluminate ionic liquids. *The Journal of Organic Chemistry* 66(25), 8616-8620. https://doi.org/10.1021/jo016126b.

Nguyen, L. T. N., Nguyen, A. Q., Le, K. T., Luu, T. T. X., Tran, N. T. K., & Pham, B. P. (2022). Chloroaluminate ionic liquid immobilized on magnetic nanoparticles as a heterogeneous lewis acidic catalyst for the friedel-crafts sulfonylation of aromatic compounds. *Molecules* 27(5). https://doi.org/10.3390/molecules27051644.

Perez, J. V. D., Nadres, E. T., Nguyen, H. N., Dalida, M. L. P., & Rodrigues, D. F. (2017). Response surface methodology as a powerful tool to optimize the synthesis of polymer-based graphene oxide nanocomposites for simultaneous removal of cationic and anionic heavy metal contaminants. *RSC Advances* 7(30), 18480-18490. https://doi.org/10.1039/c7ra00750g.

Robello, D. R., Ulman, A., & Urankar, E. J. (1993). Poly(p-phenylene sulfone). *Macromolecules* 26(25), 6718-6721. https://doi.org/10.1021/ma00077a004.

Safari, J., & Zarnegar, Z. (2013). Immobilized ionic liquid on superparamagnetic nanoparticles as an effective catalyst for the synthesis of tetrasubstituted imidazoles under solvent-free conditions and microwave irradiation. *Comptes Rendus Chimie* 16(10), 920-928. https://doi.org/10.1016/j.crci.2013.01.019.

Sarsfield, M., Roberts, A., Streletzky, K. A., Fodor, P. S., & Kothapalli, C. R. (2021). Optimization of gold nanoparticle synthesis in continuous-flow micromixers using response surface methodology. *Chemical Engineering and Technology* 44(4), 622-630. https://doi.org/10.1002/ceat.202000314.

Swenson, R. E., Sowin, T. J., & Zhang, H. Q. (2002). Synthesis of substituted quinolines using the dianion addition of N-Boc-anilines and α-Tolylsulfonyl-α,β-unsaturated ketones. *The Journal of Organic Chemistry* 67(26), 9182-9185. https://doi.org/ 10.1021/jo0203387.

Trost, B. M., & Kalnmals, C. A. (2019). Sulfones as chemical chameleons: versatile synthetic equivalents of small-molecule synthons. *Chemistry* 25(48), 11193-11213. https://doi.org/10.1002/chem.201902019.

Yu, M., Wang, B., Qi, Z., Xin, G., & Li, W. (2019). Response surface method was used to optimize the ultrasonic assisted extraction of flavonoids from Crinum asiaticum. *Saudi Journal of Biological Sciences* 26(8), 2079-2084. https://doi.org/10.1016/j.sjbs.2019.09.018.

Zhang, X., Han, C., Chen, S., Li, L., Zong, J., Zeng, J., & Mei, G. (2018). Response surface methodology for the optimization of ultrasound-assisted extraction of tetrodotoxin from the liver of *Takifugu pseudommus*. *Toxins* 10(12). https://doi.org/10.3390/toxins10120529.